UNIVERSITÄT SIEGEN

Naturwissenschaftlich Technische Fakultät

Measurement-based models of friction and dissipative collapse

Masterarbeit
zur Erlangung des akademischen Grades
Master of Science

Department Physik

Michael Gaida
1076406

Gutachter:
Jun. Prof. Dr. Stefan Nimmrichter
Prof. Dr. Otfried Gühne

Abgabedatum: 6. März 2022

TQO Theoretical Quantum Optics

Ich erkläre hiermit an Eides statt, dass ich die vorliegende Arbeit ohne Hilfe Dritter und ohne Benutzung anderer als der angegebenen Hilfsmittel angefertigt habe; die aus fremden Quellen direkt oder indirekt übernommenen Gedanken sind als solche kenntlich gemacht. Die Arbeit wurde bisher in gleicher oder ähnlicher Form in keiner anderen Prüfungsbehörde vorgelegt und auch noch nicht veröffentlicht.

Ort, Datum Unterschrift

Für meine Eltern, die mich auf meinem Weg immer unterstützen. Einfach mal DANKE !

"No matter how bad you wanna just fall flat on your face and collapse"

Eminem, "Till I collapse"

Abstract

Collapse models are objective modifications of quantum theory that aim to solve the measurement problem [1]. One of the most studied models is the Continuous Spontaneous Localisation (CSL) model [2] and its dissipative extension [3]. We present a protocol based on randomly occurring Gaussian position measurements and unitary feedback operations that reproduces the single particle dynamics of dissipative CSL. Inspired by this protocol, we introduce a class of measurement-based models, implementing classical friction forces. We find that the specific model for linear Stokes friction, reproduces the single-particle dissipative CSL master equation, as well.

We examine how a single-particle state evolves and equilibrates under the Stokes friction model in the characteristic function representation in phase space. The main result is that, in general, the model does not lead to a thermal Gibbs state, except for the singular case of free motion without spatial confinement.

In order to better understand the equilibration process under Stokes friction, we then focus our view on the special case of harmonic motion. We obtain a closed set of linear equations of motion for the first and second moments of position and momentum and find that the system relaxes to a finite energy for wide range of model parameters.

Finally, we extent the Stokes friction model to a many-particle theory using symmetry and consistency arguments that should apply to arbitrary mass scales. The mass dependence of our model differs notably from the proposed dissipative CSL model.

Contents

Introduction

The measurement problem is a flaw at the core of quantum mechanics that has not been settled for decades being discussed to this day [1, 4]. In a nutshell the problem is that quantum theory postulates two fundamentally incompatible ways for a system to change its state: The linear and continuous time evolution described by the Schrödinger equation and the discontinuous reduction, or collapse, of the state when a measurement occurs [5].

Since the advent of quantum mechanics in the early 20th century, several resolutions of the problem were proposed. Some see it as a feature rather than a problem of the theory, which emphasizes that the state of knowledge about a quantum system, the wave function, be updated upon observation, just like in classical statistical inference. Others circumvent the problem by assuming there is only the Schrödinger equation, which applies to small quantum systems and measurement devices alike. Upon measurement, the system and the measurement device evolve into an entangled state consisting of definite system states and measurement outcomes, and each such branch corresponds to one of many worlds in a multiverse of possible realities [6].

Finally, a third group postulates an objective modification to the Schrödinger equation that causes a spontaneous collapse of the wave function of macroscopic systems. The modification leaves small quantum systems on the atomic scale largely unaffected, but it prevents a large measurement apparatus from ever exhibiting quantum behavior. Specific realizations of such a modification are called collapse models. Contrary to the two former resolution of the measurement problem, collapse models make explicit predictions that deviate from quantum theory and can thus be tested in experiments.

The most widely studied examples of collapse models are the Ghirardi–Rimini–Weber (GRW) model [7], the Continuous Spontaneous Localisation (CSL) model [2] ,and the Diosi model [8] . In fact, each of the three represent a whole class of models due to free parameters. While describing the collapse correctly, the models lead to a steady increase of energy, heating every considered system up to an infinite temperature [9]. Although this effect is small for the typical choice of parameters, it makes problems with energy conservation evident. A modification of the GRW and CSL models, introducing a dependence on the momentum of the particle, was proven to introduce dissipation that leads to a relaxation to finite energies [3, 10]. Here we focus on the CSL model, which has stood the test of time so far and continues to motivate efforts towards ever more accurate experimental tests, even in a future space mission [11].

In this work, we examine the mathematical structure and predictions of the dissipative CSL model. We provide a measurement feedback-based Interpretation that is later generalized to a wider class of models. Focusing on the equilibration, we derive the time evolution of the characteristic function and various statistical moments. Finally, we consider the mass scaling of the parameters in a many particle theory.

We set the stage with the survey sections 1 and 2 on the theoretical basics and on the CSL model. In section 3, starting with our own results, we show how the one particle dynamics of dissipative CSL model can emerge from randomly occurring position measurements followed by a unitary conditioned on the measurement result. On the one

hand, this introduces an operational interpretation of dissipative CSL as a measurement feedback protocol.

On the other hand, this motivates a straight forward construction of more general models: In section 4, the centerpiece of the thesis, we will formulate a generic measurement feedback model of friction, both for single quantum particles and for many particle systems. Contrary to the microscopic description of friction arising from uncontrolled scattering processes with environmental degrees of freedom [12], the dissipation model developed here is more closely related to feedback cooling techniques in optomechanics [13] or stochastic cooling in particle accelerators [14]. We will show the impact of the models on the motional degrees of freedom and present explicit models implementing a constant Coulomb-like and a linear Stokes-like friction force. Suprisingly, the model for Stokes friction is found to reproduce the one particle dynamics of dissipative CSL, yielding a second operational interpretation of this model.

In the succeeding sections, we will investigate the implications of our model for the motional state of a single particle, focusing our view mostly on the more tractable linear friction force. In order to understand the equilibration under Stokes friction, we derive the time evolution of a quantum characteristic function in 5. This presents a compact, algebraic condition for the equilibrium state to be the corresponding Gibbs state. Based on this condition, we provide an argument that excludes any Gibbs state with an unsingular characteristic function. In contrast to this actual functions, the Gibbs state of a free particle fulfills this condition due to its distibutional nature.

The fact that most results in the literature, like [3], only consider the special case of a free particle, questions the general validity of such results. To this end, we investigate on the equilibration of a harmonic oscillator under stokes friction in section 6. We find that the first and second statistical moments of the oscillator, and by that energy as well, equilibrate for a wide range of parameters.

Finally, in section 7, we will study how the single-particle friction model can be consistently extended to a scale-invariant many particle theory of dissipative wavefunction collapse. We will find that the mass scaling does not coincide with dissipative CSL.

1. Preliminaries

The purpose of this section is to revisit basic concepts used throughout the entire thesis and to establish a standard notations. We start with the quantum mechanical description of motion in subsection 1.1, which introduces the operators and states that are frequently used. In subsection 1.2 we introduce generalized measurements that are later used in our models. In subsection 1.3 we learn about the characteristic function of the Wigner function, which is a representation of quantum mechanical states in terms of space coordinates and will be of great use to investigate equilibrium properties later. In subsection 1.4 we introduce the formalism of second quantization that is used in the models of interest. Master equations, which is our typical form of time evolution, are introduced in subsection 1.5. Finally, we find the link between master equations and stochastic Schrödinger equations in subsection 1.6.

1.1. Description of motional degrees of freedom

The quantum mechanical description of a physical system requires the choice of a (complex) Hilbertspace $\mathcal{H}$ and an algebra of self-adjoint operators acting on that space [15]. We start with a one dimensional description of motion, the generalization to three dimension follows in a straight forward manner. The two most important operators, when dealing with the (one dimensional) motion of a particle, are the position operator $\hat{x}$ and the momentum operator $\hat{p}$.

Commutation relation and consequences Since operators do not necessarily commute, it is important to know the effect of changing their order. In case of $\hat{x}$ and $\hat{p}$ we get the canonical commutation relation

$$[\hat{x}, \hat{p}] := \hat{x}\hat{p} - \hat{p}\hat{x} = i\hbar\mathbb{1} \ . \tag{1.1}$$

Where i is the imaginary unit, $\hbar$ is the reduced Planck constant and $\mathbb{1}$ is the identity operator. The meaning of this commutator becomes clear when considering the unitary transformation

$$\mathrm{e}^{\frac{i}{\hbar}y\hat{p}}\ \hat{x}\ \mathrm{e}^{-\frac{i}{\hbar}y\hat{p}} = \hat{x} + y \quad \forall y \in \mathbb{R}, \tag{1.2}$$

which is derived in Appendix A.1. It shows that the momentum operator generates translations. Therefore the exponential in (1.2) is called translation operator. Analogously we can generate kicks (boosts) with the position operator by

$$\mathrm{e}^{\frac{i}{\hbar}q\hat{x}}\ \hat{p}\ \mathrm{e}^{-\frac{i}{\hbar}q\hat{x}} = \hat{p} - q \quad \forall q \in \mathbb{R} \ . \tag{1.3}$$

States Up to now we have only considered properties that follow immediately from the canonical commutation relation without considering the underlying Hilbert space $\mathcal{H}$. In fact there are many possible choices for the explicite form of $\mathcal{H}$, $\hat{x}$, $\hat{p}$, which are called representations. The two most frequently used representations are defined on the space

of square integrable functions $\mathcal{H} = L^2(\mathbb{R})$ where either $\hat{x}$ (position representation) or $\hat{p}$ (momentum representation) is a multiplication operator while the other one becomes a derivative.

The more physical approach is to choose a basis of $\mathcal{H}$, in which the operator of choice is diagonal. Unfortunately, $\hat{x}$ and $\hat{p}$ have a continuous spectrum and no eigenvectors in a proper sense. We circumvent the problem by introducing a complete orthonormal basis of improper eigenvectors that fulfill

$$\hat{x}\,|x\rangle = x\,|x\rangle\,, \quad \langle x|y\rangle = \delta(x-y), \quad \int_{\mathbb{R}} \mathrm{d}x\,|x\rangle\,\langle x| = \mathbb{1}, \quad \forall x, y \in \mathbb{R} \tag{1.4}$$

where δ is the Dirac delta function and the second and third equation in (1.4). The spectral decomposition of $\hat{x}$ can then be written as

$$\hat{x} = \int_{\mathbb{R}} \mathrm{d}x\; x\,|x\rangle\,\langle x|\;. \tag{1.5}$$

In the basis $(|x\rangle)_x$ we can now expand a pure state $|\psi\rangle$ as

$$|\psi\rangle = \int_{\mathbb{R}} \mathrm{d}x\; \psi(x)\,|x\rangle \tag{1.6}$$

with a square integrable function $\psi \in L^2(\mathbb{R})$ representing the expansion coefficients. The big advantage of this approach lies in the straightforward basis transformations: We can use the completeness of the momentum eigenstates to expand $|\psi\rangle$ from equation 1.6 in this basis

$$|\psi\rangle = \int_{\mathbb{R}} \mathrm{d}x\; \psi(x) \left(\int_{\mathbb{R}} \mathrm{d}p\,|p\rangle\,\langle p| \right) |x\rangle = \int_{\mathbb{R}} \mathrm{d}p \left(\int_{\mathbb{R}} \mathrm{d}x\,\langle p|x\rangle\,\psi(x) \right) |p\rangle = \int_{\mathbb{R}} \mathrm{d}p\;\phi(p)\,|p\rangle\;. \tag{1.7}$$

Given the momentum eigenstates $|p\rangle$ in position representation

$$|p\rangle = \int_{\mathbb{R}} \frac{\mathrm{d}x}{\sqrt{2\pi\hbar}} \mathrm{e}^{i\frac{p\cdot x}{\hbar}}\,|x\rangle\;, \tag{1.8}$$

we see that

$$\langle x|p\rangle = \frac{1}{\sqrt{2\pi\hbar}} \mathrm{e}^{i\frac{p\cdot x}{\hbar}} \tag{1.9}$$

and can conclude that the coefficients in momentum representation $\phi(p)$ are connected to the coefficients in position representation $\psi(x)$ via fourier transform.

The scaling transformation In equations (1.2), (1.3) we have seen how translations and boosts are generated by forming the exponential of $\hat{x}$ or $\hat{p}$. We find another unitary operator, that will occur at different points of this thesis, by considering the exponential

of the anti-commutator $\{\hat{x},\hat{p}\} := \hat{x}\hat{p} + \hat{p}\hat{x}$. We define

$$\hat{S}_K := \exp\left(\frac{i \ln K}{\hbar}\frac{\{\hat{x},\hat{p}\}}{2}\right) \tag{1.10}$$

for a $K > 0$. In order to understand the effect of this operator, consider a state in position representation $\psi(x) := \langle x|\psi\rangle$ and define the family of transformed states $\psi_K(x) := \langle x|\,\hat{S}_K\,|\psi\rangle$. Differentiating with respect to K yields the differential equation

$$\frac{\mathrm{d}}{\mathrm{d}K}\psi_K(x) = \langle x|\,\frac{i}{\hbar K}\frac{\{\hat{x},\hat{p}\}}{2}\hat{S}_K\,|\psi\rangle = \frac{1}{2K}\left(\psi_K(x) + 2x\frac{\mathrm{d}}{\mathrm{d}x}\psi_K(x)\right)\ . \tag{1.11}$$

It is easy to check that under the initial condition $\hat{S}_1 = \mathbb{1}$ equation 1.11 has the solution

$$\psi_K(x) = \sqrt{K}\psi_1(Kx)\ , \tag{1.12}$$

which is a scaling transformation by the factor K. Applying the transformation to the expansion in equation 1.6 and using the substitution rule for integrals we get the effect on position eigenstates

$$\hat{S}_K\,|x\rangle = \frac{1}{\sqrt{K}}\,|K^{-1}x\rangle\ . \tag{1.13}$$

This in turn can be used to find the transformation rule for the position operator by using the spectral decomposition of $\hat{x}$,

$$\hat{S}_K\hat{x}\hat{S}_K^\dagger = \int_{\mathbb{R}}\mathrm{d}x\ x\ \hat{S}_K\,|x\rangle\,\langle x|\,\hat{S}_K^\dagger = \int_{\mathbb{R}}\frac{\mathrm{d}x}{K}\ x\,|K^{-1}x\rangle\,\langle K^{-1}x| = K\int_{\mathbb{R}}\mathrm{d}y\ y\ \ |y\rangle\,\langle y| = K\hat{x}\ . \tag{1.14}$$

Note that $\hat{p}\hat{x} = \frac{1}{2}\left(\{\hat{x},\hat{p}\} - i\hbar\mathbb{1}\right)$ commutes with the generator of $\hat{S}_K$ and is therefore unaffected by the transformation. We find

$$\hat{p}\hat{x} = \hat{S}_K\hat{p}\hat{S}_K^\dagger\hat{S}_K\hat{x}\hat{S}_K^\dagger = \hat{S}_K\hat{p}\hat{S}_K^\dagger(K\hat{x}). \tag{1.15}$$

From this we can infer that

$$\hat{S}_K\hat{p}\hat{S}_K^\dagger = \frac{1}{K}\hat{p}\ . \tag{1.16}$$

Concluding, we note that the unitary $\hat{S}_K$ rescales $\hat{x}$ and $\hat{p}$ with the factor $K^{\pm}$. This means that, depending on K, the coordinate systems get stretched or compressed.

Higher dimensions We conclude this subsection by explaining the treatment of three-dimensional movement: We can start with the introduction of vector-operators with two or three components $\hat{\mathbf{x}} = (\hat{x}_1,\hat{x}_2,\hat{x}_3)$, $\hat{\mathbf{p}} = (\hat{p}_1,\hat{p}_2,\hat{p}_3)$, where we demand the commutation relations

$$[\hat{x}_i,\hat{p}_j] := i\hbar\mathbb{1}\delta_{ij}\ . \tag{1.17}$$

As basis states we can now choose the three-fold tensor product of the one dimensional states

$$|\mathbf{x}\rangle := |x_1, x_2, x_3\rangle := |x_1\rangle \otimes |x_2\rangle \otimes |x_3\rangle \ . \tag{1.18}$$

Thanks to the commutation relations, operators belonging to one spatial dimension do not act on the other coordinates. Therefore we can use everything we have just developed component-wise. For example, the expansion of a state $|\psi\rangle$ can now be done with a square-integrable function $\psi(x) \in L^2(\mathbb{R}^3)$ as

$$|\psi\rangle = \int_{\mathbb{R}^3} \mathrm{d}\lambda^3(\mathbf{x})\psi(\mathbf{x})\,|\mathbf{x}\rangle = \int \mathrm{d}\lambda(\mathbf{x})\psi(\mathbf{x})\,|\mathbf{x}\rangle\,. \tag{1.19}$$

Here, we choose a notation with the n-dimensional Lebesgue measure λ^n.

1.2. Measurements and POVMs

In the course of this thesis we will explore the possibilities of modelling dynamics based on measurement-feedback protocols. Generally, the statistics of possible outcomes for any quantum mechanical measurement are described by so-called positive operator-valued measures (POVMs).

Discrete POVMs We start with the standard notion of POVMs on a finite-dimensional space and with discrete outcomes. Suppose we have a quantum system prepared in a state $\hat{\rho}$ and a measurement apparatus that produces one of n possible outcomes. The corresponding POVM can be seen as a family of positve-semi-definite operators $(\hat{E}_j)_{j=1}^n$ that obey

$$\sum_{j=1}^{n} \hat{E}_j = \mathbb{1} \ . \tag{1.20}$$

This defines a valid probability distribution on the n possible outcomes with

$$p_j = \mathrm{Tr}(\hat{\rho}\hat{E}_j) \tag{1.21}$$

being the probability to measure outcome j.

General POVMs To construct a physically realistic POVM for the position of a particle we start with the abstract notion of a POVM: Mathematically speaking a POVM is a map $\hat{E}$ from the set of possible locations $\mathcal{A}$ of the particle, which are subsets of the real line to the positive-semi-definite operators such that

$$\hat{E}(\{\}) = 0 \ , \quad \hat{E}(\mathbb{R}) = \mathbb{1} \tag{1.22}$$

and

$$\hat{E}\left(\dot{\bigcup_j} A_j\right) = \sum_j \hat{E}(A_j) \tag{1.23}$$

for a disjoint family of sets $(A_j)_j \subset \mathcal{A}$ [16]. The connection to the former discrete point of view lies in the definition of $\hat{E}_j := \hat{E}(\{j\})$. Note that $\mathcal{A}$ does not contain all subsets of $\mathbb{R}$, but since it is of no practical use to go into detail of this so-called Borel σ-Algebra we just think of intervals and everything we can construct geometrically from them.

As a first example we can consider a special case of a POVM called a projector valued measure (PVM), that can be obtained from the completeness of our position eigenstates given in equation (1.4). For $A \in \mathcal{A}$ we define

$$\hat{E}(A) := \int_A \mathrm{d}x \, |x\rangle \langle x| \ . \tag{1.24}$$

It is straight forward to check that this map fulfills all conditions to be a POVM. We see that $|x\rangle \langle x|$ relates to $\hat{E}(A)$ in the same fashion as classical continuous probability

densities relate to classical probabilities. We take this as a motivation to call an object like $|x\rangle\langle x|$ a continuous POVM. If there is no ambiguity, we will call it just a POVM. The downside of this POVM is that it allows an exact determination of the position. Therefore it can just be seen as the idealized version of an actual measurement apparatus, which always has a finite resolution.

The Gaussian POVM A (continuous) POVM for the position of a particle with a realistic finite resolution is given by

$$\hat{g}(y) := \frac{1}{\sqrt{2\pi}\sigma} \exp\left(-\frac{(\hat{x}-y)^2}{2\sigma^2}\right), \tag{1.25}$$

which is a Gaussian probability distribution centered at y with variance σ^2 evaluated at the position operator. With help of the spectral decomposition of the position operator we can confirm that this defines a POVM: Given wavefunctions $\psi(x) = \langle x|\psi\rangle$ and $\phi(x) = \langle x|\phi\rangle$ we get

$$\langle\psi|\,\hat{g}(y)\,|\psi\rangle = \frac{1}{\sqrt{2\pi}\sigma}\int_{\mathbb{R}} \mathrm{d}x\ \mathrm{e}^{-\frac{(x-y)^2}{2\sigma^2}}|\psi(x)|^2 \geq 0 \tag{1.26}$$

and therefore any integral with respect to y is positive as well. For the normalization we see

$$\langle\phi|\left(\int_{\mathbb{R}} \mathrm{d}y\ \hat{g}(y)\right)|\psi\rangle = \frac{1}{\sqrt{2\pi}\sigma}\int_{\mathbb{R}^2} \mathrm{d}\lambda^2(x,y)\ \mathrm{e}^{-\frac{(x-y)^2}{2\sigma^2}}\phi^*(x)\psi(x) \tag{1.27}$$

$$= \int_{\mathbb{R}} \mathrm{d}x\ \phi^*(x)\psi(x)\int_{\mathbb{R}}\frac{\mathrm{d}y}{\sqrt{2\pi}\sigma}\mathrm{e}^{-\frac{(x-y)^2}{2\sigma^2}} \tag{1.28}$$

$$= \int_{\mathbb{R}} \mathrm{d}x\ \phi^*(x)\psi(x) = \langle\phi|\psi\rangle \tag{1.29}$$

where we first changed the order of integration and then used that the integral with respect to y is just the area under a normalized Gaussian probability density. Since this holds for all states $|\psi\rangle$, $|\phi\rangle$ we can conclude

$$\int_{\mathbb{R}} \mathrm{d}y\ \hat{g}(y) = \mathbb{1}\ . \tag{1.30}$$

We will call this now well defined POVM Gaussian POVM.

Post-measurement state In practice we are often not only interested in the measurement statistics but also want to have a description of the state after the measurement. In the discrete case it is a practical choice to set the conditional post-measurement state

given outcome j as

$$\hat{\rho}_j = \frac{\sqrt{\hat{E}_j}\hat{\rho}\sqrt{\hat{E}_j}^\dagger}{p_j}, \tag{1.31}$$

which is normalized by the outcome probability p_j from (1.21) [16]. In the case that the measurement result is unknown, one must average over all possible outcomes weighted by their probabilities. The unconditional post-measurement $\hat{\rho}_{\text{p.m.}}$ state becomes

$$\hat{\rho}_{\text{p.m.}} = \sum_j p_j \frac{\sqrt{\hat{E}_j}\hat{\rho}\sqrt{\hat{E}_j}^\dagger}{p_j} = \sum_j \sqrt{\hat{E}_j}\hat{\rho}\sqrt{\hat{E}_j}^\dagger \ . \tag{1.32}$$

Analogously we define for the continuous case

$$p(y) = \text{Tr}(\hat{g}(y)\hat{\rho}) \ , \tag{1.33}$$

$$\hat{\rho}_y = \frac{\sqrt{\hat{g}(y)}\hat{\rho}\sqrt{\hat{g}(y)}^\dagger}{p(y)} \ , \tag{1.34}$$

$$\hat{\rho}_{\text{p.m.}} = \int_{\mathbb{R}} \mathrm{d}y \sqrt{\hat{g}(y)}\hat{\rho}\sqrt{\hat{g}(y)}^\dagger \ . \tag{1.35}$$

Note that a conditional state (1.34) exists only for actual outcomes with $p(y) > 0$.

Fourier transform of the Gaussian POVM In the following we will introduce notion of a Fourier transformed operator and especially how it looks for the Gaussian POVM. This is a mathematical tool, simplifying later calculations significantly. The operator $\sqrt{\hat{g}(y)}$ can be thought of as plugging the operator $\hat{x} - y$ into the function

$$f(x) := \left(\sqrt{2\pi}\sigma\right)^{-\frac{1}{2}} \mathrm{e}^{-\frac{x^2}{4\sigma^2}} \ . \tag{1.36}$$

Instead of plugging $\hat{x} - y$ in this function directly, we first express it by its Fourier-transform

$$f(x) = \int_{\mathbb{R}} \mathrm{d}p \ F(p)\mathrm{e}^{i\frac{px}{\hbar}} \tag{1.37}$$

where

$$F(p) := \int_{\mathbb{R}} \frac{\mathrm{d}x}{2\pi\hbar} \ \mathrm{e}^{-i\frac{px}{\hbar}} f(x) \tag{1.38}$$

$$= \frac{\sqrt{\sigma}}{(2\pi)^{\frac{1}{4}}\sqrt{\pi}\hbar} \mathrm{e}^{-\frac{\sigma^2}{\hbar^2}p^2} \ . \tag{1.39}$$

So the Fourier-transform of the operator becomes

$$\sqrt{\hat{g}(y)} = \frac{\sqrt{\sigma}}{(2\pi)^{\frac{1}{4}}\sqrt{\pi}\hbar}\int_{\mathbb{R}} \mathrm{d}p\ \mathrm{e}^{-\frac{\sigma^2}{\hbar^2}p^2}\mathrm{e}^{i\frac{p(\hat{x}-y)}{\hbar}} \tag{1.40}$$

The advantage of this representation can be seen when we use it in equation 1.35 to rephrase it by

$$\begin{aligned}
\hat{\rho}_{p.m.} &= \int_{\mathbb{R}} \mathrm{d}y \sqrt{\hat{g}(y)}\hat{\rho}\sqrt{\hat{g}(y)}^{\dagger} && (1.41)\\
&= \frac{\sigma}{\sqrt{2\pi}\pi\hbar^2}\int_{\mathbb{R}} \mathrm{d}y \left(\int_{\mathbb{R}} \mathrm{d}q\ \mathrm{e}^{-\frac{\sigma^2}{\hbar^2}q^2}\mathrm{e}^{i\frac{q(\hat{x}-y)}{\hbar}}\right)\hat{\rho}\left(\int_{\mathbb{R}} \mathrm{d}p\ \mathrm{e}^{-\frac{\sigma^2}{\hbar^2}p^2}\mathrm{e}^{-i\frac{p(\hat{x}-y)}{\hbar}}\right) && (1.42)\\
&= \frac{\sigma}{\sqrt{2\pi}\pi\hbar^2}\int_{\mathbb{R}^2} \mathrm{d}\lambda^2(q,p)\mathrm{e}^{-\frac{\sigma^2}{\hbar^2}\left(q^2+p^2\right)}\ \mathrm{e}^{i\frac{q\hat{x}}{\hbar}}\ \hat{\rho}\ \mathrm{e}^{-i\frac{p\hat{x}}{\hbar}}\int_{\mathbb{R}} \mathrm{d}y\ \mathrm{e}^{i\frac{(q-p)y}{\hbar}} && (1.43)\\
&= \sqrt{\frac{2\sigma^2}{\pi\hbar^2}}\int_{\mathbb{R}} \mathrm{d}p\ \mathrm{e}^{-\frac{2\sigma^2}{\hbar^2}p^2}\mathrm{e}^{i\frac{p\hat{x}}{\hbar}}\ \hat{\rho}\ \mathrm{e}^{-i\frac{p\hat{x}}{\hbar}}\ . && (1.44)
\end{aligned}$$

Here we made use of the integral representation of the delta function,

$$\int_{\mathbb{R}} \mathrm{d}y\ \mathrm{e}^{i\frac{(q-p)y}{\hbar}} = 2\pi\hbar\delta(q-p). \tag{1.45}$$

With this Fourier transform, the post measurement state becomes a linear combination of momentum-kicked states. It can easily be checked that this is a trace-preserving convex combination of unitaries, since the prefactor in equation (1.44) is the right normalization for the gaussian in p

$$\mu(p) := \sqrt{\frac{2\sigma^2}{\pi\hbar^2}}\mathrm{e}^{-\frac{2\sigma^2}{\hbar^2}p^2}\ . \tag{1.46}$$

Hence, we see that a Gaussian position measurement with unknown outcome and resolution σ is equivalent to the state transformation after random Gaussian-distributed momentum kicks with standard deviation $\hbar/(2\sigma)$. This shows explicitly how measurements in position disturb the momentum, which is an immediate consequence of the uncertainty principle.

1.3. The Wigner function and its characteristic function

In this subsection we introduce a different representation of a motional quantum state. In classical probability theory the Fourier-transform of a random variable with respect to a probability measure can be a helpful tool. It is called characteristic function because it characterizes the probability distribution of the random variable. In quantum theory we can try to mimic the classical characteristic function by the expectation value

$$G(\mathbf{k}_1, \mathbf{k}_2) := \mathrm{Tr}\left(\mathrm{e}^{i(\mathbf{k}_1\cdot\hat{\mathbf{x}}+\mathbf{k}_2\cdot\hat{\mathbf{p}})}\hat{\rho}\right) \ . \tag{1.47}$$

Other definitions of the characteristic function exist in the literature [17], based on the different possibilities to order a product of operators. Since we focus on G defined as above, ambiguity is not a problem and we call it just characteristic function. This function is convenient when the symmetrical moments of $\hat{\mathbf{x}}$ and $\hat{\mathbf{p}}$ are needed, as we can see from the Taylor expansion of the exponential before calculating the trace. For better overview we start with the one dimensional case, where k_1 and k_2 are just numbers,

$$G(k_1, k_2) = 1 + ik_1\langle\hat{x}\rangle + ik_2\langle\hat{p}\rangle - \frac{k_1^2}{2}\langle\hat{x}^2\rangle - \frac{k_2^2}{2}\langle\hat{p}^2\rangle - \frac{1}{2}k_1k_2\langle\{\hat{x},\hat{p}\}\rangle + \mathcal{O}(k^3) \ . \tag{1.48}$$

So the moments can be generated as partial derivatives evaluated at zero e.g.

$$\langle\hat{x}\rangle = \frac{1}{i}\frac{\partial}{\partial k_1}G(k_1, k_2)\big|_{k_1=0,k_2=0} \ . \tag{1.49}$$

In the three dimensional case this works in the same way. A Fourier-transform as in [18] yields the Wigner quasi probability distribution

$$W(\mathbf{x}, \mathbf{p}) := \frac{1}{(\pi\hbar)^3}\int_{\mathbb{R}^3} \mathrm{d}\lambda^3(\mathbf{y})\,\langle\mathbf{x}+\mathbf{y}|\,\hat{\rho}\,|\mathbf{x}-\mathbf{y}\rangle\,\mathrm{e}^{-2i\frac{\mathbf{p}\cdot\mathbf{y}}{\hbar}} \ . \tag{1.50}$$

It is not an actual probability distribution as it is not positive but integrating out one variable yields the correct marginal distribution of the other variable. Considering the pure state $\hat{\rho} = |\psi\rangle\langle\psi|$ we have i.e.

$$\int_{\mathbb{R}^3} \mathrm{d}\lambda^3(\mathbf{p})W(\mathbf{x}, \mathbf{p}) = |\psi(\mathbf{x})|^2 \ . \tag{1.51}$$

This is helpful for intuitive insight and is the starting point of quantum mechanics in phase space [19].

1.4. Many particles and field operators

Universal models for the wave function collapse require a consistent many-body formulation. Therefore the treatment of many-particle quantum physics is presented here. Although our investigation takes place in situations where the particle number can be assumed to be constant, the formalism of second quantization is a convenient tool.

States Following the ideas of [20] we start with a single-particle Hilbert space $\mathcal{H}$ and an operator whose eigenstates we will use as a basis. Choosing the position (vector-) operator $\hat{\mathbf{x}}$ and by that the improper position eigenstates $(|\mathbf{x}\rangle)_{\mathbf{x}}$ as a basis of $\mathcal{H}$, we can build up the N-particle Hilbert space as the N-fold tensor product $\mathcal{H}^{\otimes N} =: \mathcal{H}_N$ and can expand states $|\Psi_N\rangle \in \mathcal{H}_N$ as

$$|\Psi_N\rangle = \int_{\mathbb{R}^N} \mathrm{d}\lambda^{3N}(\mathbf{x}_1, \ldots, \mathbf{x}_N)\ \psi(\mathbf{x}_1, \ldots, \mathbf{x}_N)\, |\mathbf{x}_1, \ldots, \mathbf{x}_N\rangle \ . \tag{1.52}$$

Unfortunately, quantum states of identical particles fulfill additional symmetries when the particles are permuted. To define these symmetries, we introduce the transposition operator $\hat{P}_{ij}$, that exchanges the position of two particles like

$$\hat{P}_{1,2}\, |\psi_1\rangle\, |\psi_2\rangle = |\psi_2\rangle\, |\psi_1\rangle \ . \tag{1.53}$$

The spin-statistics theorem from relativistic quantum theory argues that states of systems of identical particles will either stay unchanged [21], or flip their sign under $\hat{P}_{ij}$. Particles of the first kind are called bosons and particles of the second kind fermions. From this we can see that a product state of the $|\psi_1\rangle\, |\psi_2\rangle$ can not be either of them. In contrast to that, the following (unnormalized) states carry symmetries we are looking for

$$|\psi_1\rangle\, |\psi_1\rangle \tag{1.54}$$
$$|\psi_2\rangle\, |\psi_2\rangle \tag{1.55}$$
$$|\psi_1\rangle\, |\psi_2\rangle + |\psi_2\rangle\, |\psi_1\rangle \tag{1.56}$$
$$|\psi_1\rangle\, |\psi_2\rangle - |\psi_2\rangle\, |\psi_1\rangle \ , \tag{1.57}$$

where the first three belong to the symmetric boson subspace and the fourth one to the anti-symmetric fermion subspace. Especially from the two last states we can take the motivation for a (anti-)symmetrizing operator $\hat{S}_\pm$

$$\hat{S}_\pm := \sum_{\hat{\mathcal{P}}} (\pm 1)^p\, \hat{\mathcal{P}} \ , \tag{1.58}$$

where the sum goes over all permutation operators $\hat{\mathcal{P}}$ and p is the number of transpositions the permutation is made of. The positive and negative signs represent bosons and fermions, respectively. With this operator we can construct the (anti-)symmetrized

states as

$$|\mathbf{x}_1, \dots \mathbf{x}_N\rangle^{(\pm)} := \frac{1}{N!} \hat{S}_\pm \, |\mathbf{x}_1, \dots \mathbf{x}_N\rangle \ , \tag{1.59}$$

which make up the subspaces $\mathcal{H}_N^{(\epsilon)}$ and fulfill a completeness relation

$$\int_{\mathbb{R}^N} \mathrm{d}\lambda^{3N}(\mathbf{x}_1, \dots \mathbf{x}_N) \ |\mathbf{x}_1, \dots \mathbf{x}_N\rangle^{(\pm)} \langle \mathbf{x}_1, \dots \mathbf{x}_N|^{(\pm)} = \mathbb{1} \tag{1.60}$$

on $\mathcal{H}_N^{(\epsilon)}$.

Operators In practice the construction of states with the desired symmetry is tedious. We can circumvent this problem by introducing operators that build up the states from vacuum $|\mathrm{vac}\rangle^{\pm}$ and fulfill the symmetries automatically. For our position eigenstates we obtain the so-called field operator $\hat{\psi}^\dagger(\mathbf{x})$ that maps from the N-particle Hilbert space to the $N+1$-particle Hilbert space by adding one particle at position $\mathbf{x}$

$$\hat{\psi}^\dagger(\mathbf{x}_1) \, |\mathrm{vac}\rangle^{(\pm)} = \sqrt{1} \, |\mathbf{x}_1\rangle^{(\pm)} \tag{1.61}$$

$$\hat{\psi}^\dagger(\mathbf{x}_2) \, |\mathbf{x}_1\rangle^{(\pm)} = \sqrt{2} \, |\mathbf{x}_2, \mathbf{x}_1\rangle^{(\pm)} \tag{1.62}$$

$$\dots \tag{1.63}$$

$$\hat{\psi}^\dagger(\mathbf{x}) \, |\mathbf{x}_N, \dots, \mathbf{x}_1\rangle^{(\pm)} = \sqrt{N+1} \, |\mathbf{x}, \mathbf{x}_N, \dots, \mathbf{x}_1\rangle^{(\pm)} \ . \tag{1.64}$$

For this property we call $\hat{\psi}^\dagger(\mathbf{x})$ a creation operator. The counterpart of the creation operator is the annihilation operator with the property

$$\sqrt{N} \cdot \hat{\psi}(\mathbf{y}) \, |\mathbf{x}_1, \dots, \mathbf{x}_N\rangle^{(\pm)} = \tag{1.65}$$

$$(\pm 1)^0 \, \delta^{(3)}(\mathbf{y} - \mathbf{x_1}) \, |\mathbf{x}_2, \dots, \mathbf{x}_N\rangle^{(\pm)} \tag{1.66}$$

$$+ (\pm 1)^1 \, \delta^{(3)}(\mathbf{y} - \mathbf{x_2}) \, |\mathbf{x}_1, \mathbf{x}_3, \dots, \mathbf{x}_N\rangle^{(\pm)} \tag{1.67}$$

$$\dots \tag{1.68}$$

$$+ (\pm 1)^{N-1} \, \delta^{(3)}(\mathbf{y} - \mathbf{x_N}) \, |\mathbf{x}_1, \dots, \mathbf{x}_{N-1}\rangle^{(\pm)} \ . \tag{1.69}$$

It removes a particle from the position state at position $\mathbf{y}$, if there is any.

We can try to express all properties of interest by our field operators. Since $\hat{\psi}(\mathbf{x})$ can be seen as an operator valued wave function, this formalism is referred to as second quantization. The consecutive application of both operators yields

$$\hat{\psi}^\dagger(\mathbf{y})\hat{\psi}(\mathbf{y}) \, |\mathbf{x}_1, \dots, \mathbf{x}_N\rangle^{(\pm)} = \left(\sum_{k=1}^{N} \delta^{(3)}(\mathbf{y} - \mathbf{x}_k) \right) |\mathbf{x}_1, \dots, \mathbf{x}_N\rangle^{(\pm)} \tag{1.70}$$

$$= \left(\sum_{k=1}^{N} \delta^{(3)}(\mathbf{y} - \hat{\mathbf{x}}_k) \right) |\mathbf{x}_1, \dots, \mathbf{x}_N\rangle^{(\pm)} \tag{1.71}$$

Integrating this expression with respect to $\mathbf{y}$, the prefactor simply reduces to the number

of particles. This motivates the definition of the number operator $\hat{N}$

$$\hat{N} = \int_{\mathbb{R}^3} \mathrm{d}\lambda^3(\mathbf{y})\ \hat{\psi}^\dagger(\mathbf{y})\hat{\psi}(\mathbf{y})\ , \tag{1.72}$$

with $\hat{\psi}^\dagger(\mathbf{y})\hat{\psi}(\mathbf{y})$ being the particle number density operator at position $\mathbf{y}$. A comparison with the operator product of opposite order, $\hat{\psi}(\mathbf{y})\hat{\psi}^\dagger(\mathbf{y})$, yields the important (anti-)commutation relation for our field operators. Together with the convention

$$\left[\hat{A}, \hat{B}\right]_\mp := \hat{A}\hat{B} \mp \hat{B}\hat{A} \tag{1.73}$$

we obtain

$$\left[\hat{\psi}^\dagger(\mathbf{x}), \hat{\psi}^\dagger(\mathbf{y})\right]_\mp = \left[\hat{\psi}(\mathbf{x}), \hat{\psi}(\mathbf{y})\right]_\mp = 0 \tag{1.74}$$

$$\left[\hat{\psi}(\mathbf{x}), \hat{\psi}^\dagger(\mathbf{y})\right]_\mp = \delta^{(3)}(\mathbf{x}-\mathbf{y})\ . \tag{1.75}$$

This builds the foundation for calculations with the field operators.

Translation from first to second quantization A simple correspondence rule between first and second quantization exists for one-or two-particle operators, i.e. sums of identical terms acting only on the Hilbert space of each individual particle pair,

$$\sum_{k=1}^{N} \hat{A}_k \longmapsto \int_{\mathbb{R}^6} \mathrm{d}\lambda^6(\mathbf{x},\mathbf{y})\, \langle \mathbf{y}|\, \hat{A}_1\, |\mathbf{x}\rangle\, \hat{\psi}^\dagger(\mathbf{y})\hat{\psi}(\mathbf{x}) \tag{1.76}$$

$$\frac{1}{2}\sum_{j,k}^{j\neq k} \hat{B}_{j,k} \longmapsto \int_{\mathbb{R}^{12}} \mathrm{d}\lambda^{12}(\mathbf{x}_1,\mathbf{x}_2,\mathbf{y}_1,\mathbf{y}_2)\, \langle \mathbf{y}_1,\mathbf{y}_2|\, \hat{B}_{1,2}\, |\mathbf{x}_1,\mathbf{x}_2\rangle\, \hat{\psi}^\dagger(\mathbf{y}_1)\hat{\psi}^\dagger(\mathbf{y}_2)\hat{\psi}(\mathbf{x}_1)\hat{\psi}(\mathbf{x}_2)\ . \tag{1.77}$$

So the one-particle transition rate $\langle \mathbf{y}|\, \hat{A}_1\, |\mathbf{x}\rangle$ links the creation of a particle at position $\mathbf{y}$ and the annihilation of a particle at position $\mathbf{x}$. Note how in both cases the left hand side and right hand side are not equal, since the former acts on N-particle states, the latter acts on states of arbitrary particle number.

Basis transformations The above second quantization framework is based on field operators defined with respect to position eigenstates. Alternatively, consider the basis of momentum eigenstates $(|\mathbf{p}\rangle)_\mathbf{p}$, for which we can define the corresponding creation and annihilation operators $\hat{a}^\dagger(\mathbf{p})$ and $\hat{a}(\mathbf{p})$ in the same manner, with the (anti-)commutation relation

$$\left[\hat{a}(\mathbf{p}), \hat{a}^\dagger(\mathbf{q})\right]_\mp = \delta^{(3)}(\mathbf{p}-\mathbf{q})\ . \tag{1.78}$$

A change of basis can be performed in full analogy to the basis vector for single-particle states

$$\hat{a}^\dagger(\mathbf{p})\,|\mathrm{vac}\rangle^\pm = |\mathbf{p}\rangle = \int_{\mathbb{R}^3} \frac{\mathrm{d}\lambda^3(\mathbf{x})}{\sqrt{2\pi\hbar}^3} \mathrm{e}^{i\frac{\mathbf{p}\cdot\mathbf{x}}{\hbar}}\,|\mathbf{x}\rangle = \int_{\mathbb{R}^3} \frac{\mathrm{d}\lambda^3(\mathbf{x})}{\sqrt{2\pi\hbar}^3} \mathrm{e}^{i\frac{\mathbf{p}\cdot\mathbf{x}}{\hbar}}\,\hat{\psi}^\dagger(\mathbf{x})\,|\mathrm{vac}\rangle^\pm \ . \tag{1.79}$$

So we conclude

$$\hat{a}^\dagger(\mathbf{p}) = \int_{\mathbb{R}^3} \frac{\mathrm{d}\lambda^3(\mathbf{x})}{\sqrt{2\pi\hbar}^3} \mathrm{e}^{i\frac{\mathbf{p}\cdot\mathbf{x}}{\hbar}}\,\hat{\psi}^\dagger(\mathbf{x}) \tag{1.80}$$

and vice versa

$$\hat{\psi}^\dagger(\mathbf{x}) = \int_{\mathbb{R}^3} \frac{\mathrm{d}\lambda^3(\mathbf{p})}{\sqrt{2\pi\hbar}^3} \mathrm{e}^{-i\frac{\mathbf{x}\cdot\mathbf{p}}{\hbar}}\,\hat{a}^\dagger(\mathbf{p}) \ . \tag{1.81}$$

1.5. Quantum master equations

In this subsection we turn to the time evolution of quantum systems. We restrict ourselves to Markovian (memoryless) models. This means that the present state of the system suffices to predict its future. To this end we start from an abstract level by introducing the so-called quantum dynamical semigroup and presenting its generator. The semigroup property reflects the restriction to Markovian models. After that we show some symmetries of the generator. The major part is then dedicated to time evolution comparable to the Heisenberg picture and the Ehrenfest equations of motion. The difference between the standard and the general case are stressed. Finally we present the famous Caldeira-Legget master equation.

Quantum dynamical semigroup Since our goal is understanding and inventing general models of friction, we start from an axiomatic point of view as it can be found in [18]. It is a well known fact that the most general map from a quantum state to another quantum state is a completely-positive trace-preserving (CPTP) map, also known as a quantum channel. Consider a time evolution for quantum states that is described by continuous single parameter family of quantum channels $(\Lambda_t)_{t\geq 0}$. In case the family is continuous (at least in the ultra weak sense) and the property

$$\Lambda_{t_2+t_1} = \Lambda_{t_2}\Lambda_{t_1} \tag{1.82}$$

holds true for all $t_1, t_2 \geq 0$, we call the family a quantum dynamical semigroup. The time evolution of a state $\hat{\rho}(0)$ at time $t_0 = 0$ is then given by

$$\hat{\rho}(t) = \Lambda_t \left[\hat{\rho}(0)\right] \ . \tag{1.83}$$

Note that equation (1.82) implies the Markovianity of the time evolution because the present state of the system $\hat{\rho}(t)$ always suffices to calculate its future as

$$\hat{\rho}(t+\Delta t) = \Lambda_{t+\Delta t}\left[\hat{\rho}(0)\right] \overset{\text{semigroup}}{=} \Lambda_{\Delta t}\left[\Lambda_t\left[\hat{\rho}(0)\right]\right] = \Lambda_{\Delta t}\left[\hat{\rho}(t)\right] \ . \tag{1.84}$$

One can show with help of the Kraus decomposition of the channels Λ_t that,in the finite dimensional case, we can arrive at an Lindblad master equation called differential equation for $\hat{\rho}(t)$

$$\frac{\mathrm{d}}{\mathrm{d}t}\hat{\rho}(t) = \mathcal{L}\hat{\rho}(t) =: -\frac{i}{\hbar}\left[\hat{H}, \hat{\rho}\right] + \underbrace{\sum_k \gamma_k \left(\hat{L}_k \hat{\rho} \hat{L}_k^\dagger - \frac{1}{2}\left\{\hat{\rho}, \hat{L}_k^\dagger \hat{L}_k\right\}\right)}_{=:\mathcal{D}\hat{\rho}} \tag{1.85}$$

where $\mathcal{L}$ is the generator of the semigroup and is also called Linbladian/Liouvillian. The $\hat{L}_k$ are called Lindblad operators and the γ_k are positive rates. The Hermitian operator $\hat{H}$ can be seen as a Hamiltonian that generates the reversible coherent part of the time evolution. It is complemented by the dissipator $\mathcal{D}$ that consists of additional terms which are able to introduce irreversible dynamics. These terms are typically used to

describe open quantum systems.

We will call linear maps that map operators on operators super operators.

Symmetries of the generator Every Lindbladian is invariant under a permutation of the Lindblad operators weighted with the entries of a unitary. we can transform the Lindblad operators and the Hamiltonian in certain ways without changing the generator $\mathcal{L}$. Given the entries u_{ij} of an unitary matrix we can write

$$\sqrt{\gamma_i}\hat{L}_i \longmapsto \sqrt{\gamma_i'}\hat{L}_i' := \sum_j u_{ij}\sqrt{\gamma_j}\hat{L}_j \ . \tag{1.86}$$

In addition, the Lindbladian is also invariant under the combined gauge transformation of Lindblad operators and Hamiltonian. Considering the complex numbers a_i and the real number b we have

$$\hat{L}_i \longmapsto \hat{L}_i' := \hat{L}_i + a_i \tag{1.87}$$

$$\hat{H} \longmapsto \hat{H}' = \frac{1}{2i}\sum_j \gamma_j \left(a_j^* \hat{L}_j - a_j \hat{L}_j^\dagger\right) + b \ . \tag{1.88}$$

Especially the first kind of transformation will become important when we motivate single-particle master equations and then try to generalize them to the multi particle case.

Heisenberg- and Ehrenfest equation analogues As a straightforward generalization of the master equation (1.85) we can consider a time-dependent Lindbladian $\mathcal{L}(t)$ with operators $\hat{H}(t)$ and $\hat{L}_j(t)$. This modifies the semigroup property to

$$\Lambda_{t_2,t_0} = \Lambda_{t_2,t_1}\Lambda_{t_1,t_0} \tag{1.89}$$

since the dynamic lost the translation invariance with respect to time.

Many master equations used in practice, including that of collapse models, are often too complicated to be solved analytically without approximations. Nevertheless, we may still gain insight about the described dynamics and possible approximations by looking at the time evolution of relevant observables and their expectation values.

We start with the master equation

$$\frac{\mathrm{d}}{\mathrm{d}t}\hat{\rho}(t) = \mathcal{L}(t)\hat{\rho}(t) \tag{1.90}$$

with the solution $\hat{\rho}(t) = \Lambda_{t,t_0}[\hat{\rho}(t_0)]$. Plugging the solution back in the master equation yields the time evolution of Λ_{t,t_0} as

$$\frac{\mathrm{d}}{\mathrm{d}t}\Lambda_{t,t_0} = \mathcal{L}(t)\Lambda_{t,t_0} \ . \tag{1.91}$$

Now we can define adjoint channels $\Lambda^\dagger_{t,t_0}$ and adjoint super operators $\mathcal{L}^\dagger(t)$ through the identities

$$\mathrm{Tr}\left(\hat{A}\Lambda_{t,t_0}\left[\hat{\rho}(t_0)\right]\right) =: \mathrm{Tr}\left(\Lambda^\dagger_{t,t_0}\left[\hat{A}\right]\hat{\rho}(t_0)\right) \tag{1.92}$$

$$\mathrm{Tr}\left(\hat{A}\left(\mathcal{L}(t)\hat{B}\right)\right) =: \mathrm{Tr}\left(\left(\mathcal{L}^\dagger(t)\hat{A}\right)\hat{B}\right) \ . \tag{1.93}$$

From a mathematical standpoint these are the adjoint operators with respect to the Hilbert Schmidt scalar product. From a physical standpoint we swap the time evolution from the system state $\hat{\rho}$ to the observable $\hat{A}$ such that the time-dependent expectation values remain the same. With this we can formulate an Ehrenfest equation of motion for the observable

$$\frac{\mathrm{d}}{\mathrm{d}t}\left\langle\hat{A}\right\rangle_t = \mathrm{Tr}\left(\hat{A}\dot{\hat{\rho}}(t)\right) = \mathrm{Tr}\left(\hat{A}\left(\mathcal{L}(t)\hat{\rho}(t)\right)\right) \tag{1.94}$$

$$= \mathrm{Tr}\left(\left(\mathcal{L}^\dagger(t)\hat{A}\right)\hat{\rho}(t)\right) \tag{1.95}$$

$$= \mathrm{Tr}\left(\left(\mathcal{L}^\dagger(t)\hat{A}\right)\Lambda_{t,t_0}\left[\hat{\rho}(t_0)\right]\right) \tag{1.96}$$

$$= \mathrm{Tr}\left(\Lambda^\dagger_{t,t_0}\left[\mathcal{L}^\dagger(t)\hat{A}\right]\hat{\rho}(t_0)\right) \ , \tag{1.97}$$

where we used the definition of adjoint super operators twice. The Ehrenfest equation of motion can now be taken from equation (1.95). That expression can be rephrased like

$$\frac{\mathrm{d}}{\mathrm{d}t}\left\langle\hat{A}\right\rangle_t = \left\langle\mathcal{L}^\dagger(t)\hat{A}\right\rangle_t \ . \tag{1.98}$$

Occasionally the right hand side can be expressed as a function of $\langle\hat{A}\rangle_t$, which would result in an ordinary differential equation that is fairly easy to integrate. We will make use of this in the calculation of the equilibrium energy.

The inclined reader may have noticed that this resembles the description of unitary closed-system evolution in the Heisenberg picture. Indeed, we can formally define the time-evolved operator

$$\hat{A}_\#(t) := \Lambda^\dagger_{t,t_0}\left[\hat{A}\right] \tag{1.99}$$

starting from the initial value $\hat{A}_\#(t_0) = \hat{A}$. Together with equation (1.97) we can obtain

$$\mathrm{Tr}\left(\left(\frac{\mathrm{d}}{\mathrm{d}t}\hat{A}_\#(t)\right)\hat{\rho}(t_0)\right) = \mathrm{Tr}\left(\Lambda^\dagger_{t,t_0}\left[\mathcal{L}^\dagger(t)\hat{A}\right]\hat{\rho}(t_0)\right) \quad ,\forall\hat{\rho}(t_0) \tag{1.100}$$

from which we conclude the time evolution of the adjoint channel

$$\frac{\mathrm{d}}{\mathrm{d}t}\Lambda^\dagger_{t,t_0} = \Lambda^\dagger_{t,t_0}\left[\mathcal{L}^\dagger(t)\ \cdot\right] \ . \tag{1.101}$$

Only when the two super operators commute we get the adjoint master equation

$$\frac{\mathrm{d}}{\mathrm{d}t}\hat{A}_{\#}(t) = \mathcal{L}^{\dagger}(t)\hat{A}_{\#}(t) \ . \tag{1.102}$$

However there is a crucial difference to the Heisenberg picture operator that should be stressed here: In the special case of a unitary time evolution given by the operator $\hat{U}(t)$, the Heisenberg picture operator $\hat{A}_H(t)$ is defined as

$$\hat{A}_H(t) = \hat{U}^{\dagger}(t)\hat{A}\hat{U}(t) \ . \tag{1.103}$$

Because of the unitarity we can write

$$\hat{A}_H^2(t) = \hat{U}^{\dagger}(t)\hat{A}\hat{U}(t)\hat{U}^{\dagger}(t)\hat{A}\hat{U}(t) = \hat{U}^{\dagger}(t)\hat{A}^2\hat{U}(t) \ . \tag{1.104}$$

and

$$\left[\hat{A}_H(t), \hat{B}_H(t)\right] = \hat{U}^{\dagger}(t)\left[\hat{A}, \hat{B}\right]\hat{U}(t) \ . \tag{1.105}$$

So products and commutation relations between operators are preserved in the Heisenberg picture under unitary evolution. This is no longer the case for $\hat{A}_{\#}(t)$ evolving according to equation (1.99). In fact, we will often have

$$\left(\hat{A}_{\#}(t)\right)^2 \neq \left(\hat{A}^2\right)_{\#}(t) \ . \tag{1.106}$$

Especially canonical commutation relations will in general get lost in this picture. In practice, this means we have to solve the time evolution for every function of an operator separately. This typically results in an infinite set of coupled differential equations.

Caldeira-Legett master equation An important quantum master equation that often occurs as limiting case of more complicated equations is the Caldeira-Legget master equation of quantum brownian motion. It describes the motion of a particle that interacts with the potential $V(\hat{x})$ and is linearly coupled to a bath of harmonic oscillators. Under certain approximations, we find the equation of motion

$$\frac{\mathrm{d}}{\mathrm{d}t}\hat{\rho} = -\frac{i}{\hbar}\left[\frac{\hat{p}^2}{2m} + V(\hat{x}), \hat{\rho}\right] - \frac{i\gamma}{2\hbar}\left[\{\hat{x}, \hat{p}\}, \hat{\rho}\right] + \gamma\left(\hat{L}\hat{\rho}\hat{L}^{\dagger} - \frac{1}{2}\{\hat{\rho}, \hat{L}^{\dagger}\hat{L}\}\right) \tag{1.107}$$

with the Lindblad operator

$$\hat{L} = \sqrt{\frac{4mk_BT}{\hbar^2}}\hat{x} + i\sqrt{\frac{1}{4mk_BT}}\hat{p} \ . \tag{1.108}$$

Here we can see that the Hamiltonian gets an additional term proportional to $\{\hat{x}, \hat{p}\}$ that describes the systematic effect from the environment on the system. Note that this is exactly the generator of scale transformations that we have discussed starting in equation (1.10).

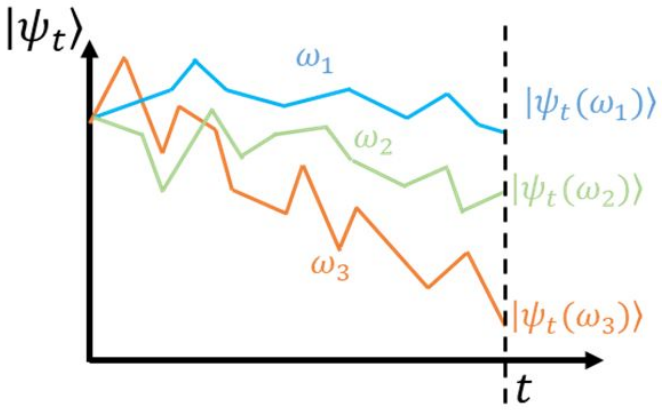

Figure 1: An schematic visualization of three random quantum trajectories. Based on random events occuring on the path we obtain an ensemble of states at time t.

1.6. Stochastic unravellings

Similar to the master equation of classical probability distributions , the quantum master equation can be understood as an ensemble-averaged description of a stochastic process in a Hilbert space.

Motivation and approach The idea is to consider a probability space $(\Omega, \mathcal{A}, \mathbb{P})$ where every realization of the process $\omega \in \Omega$ corresponds to a random path of our quantum system $|\psi_t(\omega)\rangle$ in time, also called quantum trajectory. The randomness can be due to random measurements or random interactions, for example. At a fixed time t the different paths lead to an ensemble of different states $(|\psi_t(\omega)\rangle)_{\omega\in\Omega}$, as sketched in figure 1. This classical randomness can be omitted by averaging over the ensemble with respect to the probability measure $\mathbb{P}$. We obtain the density matrix as the expectation value

$$\hat{\rho}_t := \mathbb{E}\left(|\psi\rangle_t \langle\psi|_t\right) = \int_\Omega |\psi_t(\omega)\rangle \langle\psi_t(\omega)| \, \mathrm{d}\mathbb{P}(\omega) \ . \tag{1.109}$$

We can think of the paths being generated by random events occuring at random times. Such random changes are modeled by stochastic differential equations. The most famous process used to introduce randomness is the Wiener process $(W_t)_{t\geq 0}$. For every time t W_t is a Gaussian random variable with zero mean and variance t. Alternatively, it is characterized by the following properties of its statistically independent increments $\mathrm{d}W_t = W_{t+\mathrm{d}t} - W_t$ [18],

$$\mathbb{E}\left(\mathrm{d}W_t\right) = 0, \tag{1.110}$$

$$\left(\mathrm{d}W_t\right)^2 = \mathrm{d}t \ . \tag{1.111}$$

Note that the chain rule and the product rule from standard calculus are based on neglecting terms of higher order like $\mathcal{O}(\mathrm{d}t^2)$. Equation (1.111) makes evident that those rules need to be modified for the Wiener process: In fact, the lowest order term being neglected is $\mathcal{O}(\mathrm{d}t\ \mathrm{d}W_t)$.

Stochastic Schrödinger equation In [22] the general form of a stochastic Schrödinger equation based on the Wiener process was given as

$$\mathrm{d}\left|\psi_t\right\rangle = \left(-i\hat{H} - \frac{1}{2}\gamma\left(\hat{\mathbf{A}}^\dagger - \mathbf{R}\right)\cdot\hat{\mathbf{A}} + \frac{1}{2}\gamma\left(\hat{\mathbf{A}} - \mathbf{R}\right)\cdot\mathbf{R}\right)\left|\psi_t\right\rangle\mathrm{d}t \tag{1.112}$$

$$+\left(\hat{\mathbf{A}} - \mathbf{R}\right)\cdot\mathrm{d}\mathbf{W}_t\left|\psi_t\right\rangle\ . \tag{1.113}$$

Here γ is a rate, $\hat{H}$ is a self adjoint operator, $\hat{\mathbf{A}}$ is a vector of operators $\hat{A}_i$, $\mathbf{R} = \frac{1}{2}\left\langle\psi_t\right|\left(\hat{\mathbf{A}} + \hat{\mathbf{A}}^\dagger\right)\left|\psi_t\right\rangle$, and the stochasticity comes from the vector $\mathrm{d}\mathbf{W}_t$ of independent Wiener increments $\mathrm{d}W_t^{(i)}$ obeying

$$\mathbb{E}\left(\mathrm{d}W_t^{(i)}\right) = 0 \tag{1.114}$$

$$\mathrm{d}W_t^{(i)}\mathrm{d}W_t^{(j)} = \gamma\delta_{ij}\mathrm{d}t\ . \tag{1.115}$$

The complicated non-linear deterministic term in front of the $\mathrm{d}t$ keeps the norm of the state constant, see appendix A.2. The time evolution of the density matrix $\hat{\rho}_t$ is given by the Lindblad master equation

$$\frac{\mathrm{d}}{\mathrm{d}t}\hat{\rho}_t = -i\left[\hat{H}, \hat{\rho}_t\right] + \gamma\sum_j\left(\hat{A}_j\hat{\rho}_t\hat{A}_j^\dagger - \frac{1}{2}\left\{\hat{A}_j{}^\dagger\hat{A}_j, \hat{\rho}_t\right\}\right) \tag{1.116}$$

as it is derived in appendix A.3. So we have identified the $\hat{A}_j$ as the Lindblad operators $\hat{L}_j$ and $\hat{H}$ as an Hamiltonian rescaled by $\hbar$. We call the stochastic Schrödinger equation (1.112) the stochastic unravelling of the master equation (1.116). Due to invariance of the master equation under the transformation (1.86) and (1.87) there is an infinite amount of unravellings for one master equation.

We will be concerned with master equations in which the discrete sum of Lindblad terms is replaced by a continuous integral. On the level of the Wiener unravelling, this amounts to defining a continuous family of Wiener processes $(W_t(\mathbf{x}))_{\mathbf{x}\in\mathbb{R}^3}$ with the properties

$$\mathbb{E}\left(\mathrm{d}W_t(\mathbf{x})\right) = 0 \tag{1.117}$$

$$\mathrm{d}W_t(\mathbf{x})\mathrm{d}W_t(\mathbf{y}) = \gamma\ \delta^3(\mathbf{x}-\mathbf{y})\mathrm{d}t\ . \tag{1.118}$$

Fortunately, all calculations can be carried out in the same fashion as before; all we have to do is exchanging the sums for integrals.

2. Collapse models

In this section we introduce collapse models. To this end we start with a general motivation and overview in subsection 2.1. Then we focus our view to the presently most relevant and widely studied Continuous Continuous Spontaneous Localization model (CSL) in subsection 2.2. In the final section 2.3 we discuss a more recently postulated modified version of the CSL model, which introduces dissipation as a means to curb the CSL-induced heating effect. This model will be the starting point for our own investigation in the following sections.

2.1. The case for collapse models

The measurement problem Quantum theory is a very successful theory that describes our universe on scales as small as an atom. A main feature of quantum theory lies in the superposition principle: Given two states $|\psi_1\rangle$ and $|\psi_2\rangle$ that are valid solutions to the Schrödinger equation, a superposition between them is a valid solution as well, e.g.

$$\frac{1}{\sqrt{2}}\left(|\psi_1\rangle + |\psi_2\rangle\right) \ . \tag{2.1}$$

On the contrary, our everyday experience tells us that macroscopic objects in space occupy distinct states. From this arises the question, whether our classical world could emerge from quantum mechanics in the microscopic regime. In [5] it is argued that the possibility of performing (quantum) measurements stays in direct contradiction to the linear nature of quantum evolution. In other words, the linear Schrödinger equation can not mediate between the classical and quantum world. This fundamental problem is known as the measurement problem. There are various approaches tackling this problem on different levels.

Copenhagen interpretation A possible solution is the 'right' choice of interpretation. Proponents of the Copenhagen interpretation accept the fact that there are two incompatible ways a quantum system can undergo state change. One is the continuous unitary evolution described the Schrödinger equation.

$$|\psi(t)\rangle = \exp(-\frac{i}{\hbar}\hat{H}t)\,|\psi(0)\rangle \tag{2.2}$$

The other is a discontinuous non-linear change of state whenever a measurement occurs

$$|\psi\rangle \mapsto \frac{\hat{\Pi}\,|\psi\rangle}{\sqrt{\langle\psi|\,\hat{\Pi}\,|\psi\rangle}} \tag{2.3}$$

([23]). However, by accepting the "Heisenberg cut" between microscopic quantum systems and macroscopic measurement devices, and the special role the latter play for wavefunction collapse, one implicitly assumes a division between the quantum and the

classical world.

Dynamic collapse A different approach is to modify the time evolution of quantum mechanics in such a way that state reductions of the form (2.3) occur spontaneously and sufficiently frequently on macroscopic scales. Such a time evolution needs to fulfill a list of properties as it is given in [9]:

- **Nonlinearity**: The time evolution needs to be nonlinear. Otherwise the superposition principle would be respected on all scales.
- **Stochasticity**: The measurement results in standard quantum mechanics occur randomly. Hence a time evolution reproducing such a process needs to be random as well. On the other hand, nonlinear quantum mechanics can easily lead to the possibility of superluminal signaling, as argued in [24]. Complementing the nonlinearity with a suitable stochastic term in the Schrödinger equation allows us to break the superposition principle on the level of the wave function, while keeping intact the linear evolution of state ensembles represented by a density operator. The probabilistic framework underlying quantum theory is then preserved, and unphysical effects such as superluminal communications remain impossible.
- **Amplification**: Quantum mechanics is one of the most successful physical theories in the microscopic domain. A modification of the theory must therefore have a negligible effect on microscopic systems, but should be amplified with increasing system size so as to ensure that the macroscopic objects can only be found in definite, classical states.

Given this list of properties there is still the question, relative to which basis the collapse should occur. The typical choice is the position basis. This is motivated by position probably being the least abstract physical quantity. In contrast the collapse in more abstract basis e.g. the energy basis (as it is done in [25]) can lead to problems: In case of degenerate energy levels the corresponding eigenstates could still be in strong spatial superposition. This does not agree with our observation in the macroscopic world.

In the following, we will restrict our view to markovian models as considered in subsection 1.5, where the stochasticity originates from a Poisson jump process or a (continuous) Wiener process. One of the first models of the Poissonian kind is the GRW model named after its founders Ghiradi, Rimini and Weber [7]. And one of the first continuous models is the Continuous Spontaneous Collapse model (CSL) [2]. Both models have the flaw, like basically all models for spontaneous localisation, of a steady increase in energy. Therefore both models got an dissipative extension to the dissipative GRW model [10] and the dissipative CSL model [3]. The latter can be seen as the most sophisticated Markovian collapse model. A more detailed elaboration on the motivation of collapse models and their different types can be found in [9].

Ensemble description and observable consequences The main focus throughout this thesis lies on the one particle dynamics of dissipative CSL and comparable models. To this end we use the corresponding master equation instead of the stochastic dynamics. It is noteworthy that conceptually different collapse models like dissipative GRW and dissipative CSL can lead to the same effective dynamics described by a master equation. For our considerations they are just two different stochastic unravellings (see 1.6) and we will use the term dissipative CSL interchangeably for the stochastic differential equation and the master equation.

2.2. The CSL model

In this subsection, we will introduce the continous spontanous localization (CSL) model, which is a stochastic modification of the many-particle Schrödinger equation for wave function collapse. We shall discuss the prediction of the model, as well as its flaw.

The model The CSL model is given by a universal stochastic differential equation for the wave function of arbitrary many-body systems [3]. For better distinction, we will from now on denote second quantization Lindblad operators by blackboard bold variables like $\mathbb{M}$ and $\mathbb{L}$. The stochastic differential equation reads

$$\mathrm{d}\left|\psi_t\right\rangle = \Bigg[-\frac{i}{\hbar}\hat{H}\mathrm{d}t + \frac{\sqrt{\gamma}}{m_0}\int_{\mathbb{R}^3}\mathrm{d}\lambda^3(\mathbf{y})\left[\hat{\mathbb{M}}(\mathbf{y}) - \langle\hat{\mathbb{M}}(\mathbf{y})\rangle_t\right]\mathrm{d}W_t(\mathbf{y}) \tag{2.4}$$

$$-\frac{\gamma}{2m_0^2}\int_{\mathbb{R}^3}\mathrm{d}\lambda^3(\mathbf{y})\left[\hat{\mathbb{M}}(\mathbf{y}) - \langle\hat{\mathbb{M}}(\mathbf{y})\rangle_t\right]^2\mathrm{d}t\Bigg]\left|\psi_t\right\rangle \ . \tag{2.5}$$

Here, $\hat{H}$ is a Hamiltonian, γ is a parameter determining the rate of the collapse process, and r_c is a second free model parameter that sets the length scale above which spatial superpositions are suppressed. The index j labels different particle species with corresponding mass m_j, while m_0 is a reference mass, typically chosen as the proton mass. The stochasticity is introduced by a continuous family of Wiener increments $(\mathrm{d}W_t(\mathbf{y}))_{\mathbf{y}}$ with the properties

$$\mathbb{E}\left(\mathrm{d}W_t(\mathbf{x})\right) = 0, \tag{2.6}$$

$$\mathrm{d}W_t(\mathbf{x})\mathrm{d}W_t(\mathbf{y}) \ = \delta^3(\mathbf{x}-\mathbf{y})\mathrm{d}t. \tag{2.7}$$

They couple to the motional state of the particles through the operator

$$\hat{\mathbb{M}}(\mathbf{y}) = \sum_j m_j \int_{\mathbb{R}^3} \frac{\mathrm{d}\lambda^3(\mathbf{x})}{\left(\sqrt{2\pi}r_c\right)^3} e^{-\frac{|\mathbf{x}-\mathbf{y}|^2}{2r_c^2}} \hat{\psi}_j^\dagger(\mathbf{x})\hat{\psi}_j(\mathbf{x}) \ . \tag{2.8}$$

Note that $m_j\hat{\psi}_j^\dagger(\mathbf{x})\hat{\psi}_j(\mathbf{x})$ is exactly the mass density of the j-th species with the annihilation operator $\hat{\psi}_j(\mathbf{x})$ of particles of the type j in position $\mathbf{x}$. Therefore $\hat{\mathbb{M}}(\mathbf{y})$ can be seen as a Gaussian-smeared total mass density operator at position $\mathbf{y}$. We recognize that this stochastic Schrödinger equation is the continuous version of equation (1.112) with the self adjoint operator $\hat{\mathbb{M}}(\mathbf{y})$. We will use this fact to translate the time evolution into a master equation with Lindblad operator $\hat{M}(\mathbf{y})$

$$\frac{\mathrm{d}}{\mathrm{d}t}\hat{\rho}_t = -\frac{i}{\hbar}\left[\hat{H},\hat{\rho}_t\right] + \frac{\gamma}{m_0^2}\int_{\mathbb{R}^3}\mathrm{d}\lambda^3(\mathbf{y})\left(\hat{\mathbb{M}}(\mathbf{y})\hat{\rho}_t\hat{\mathbb{M}}(\mathbf{y})^\dagger - \frac{1}{2}\left\{\hat{\mathbb{M}}^\dagger(\mathbf{y})\hat{\mathbb{M}}(\mathbf{y}),\hat{\rho}_t\right\}\right) \ . \tag{2.9}$$

The usage of the second quantization formalism ensures the exchange symmetry properties of fermions and bosons, but to investigate some basic properties we return to first quantization and consider one particle: Making use of the correspondence in equa-

tion (1.76) between single particle operators in first and second quantization, we obtain the single particle version of $\hat{\mathbb{M}}(\mathbf{y})$ simply by replacing the field operators with matrix elements in position representation

$$\hat{M}(\mathbf{y}) = m \int_{\mathbb{R}^3} \frac{\mathrm{d}\lambda^3(\mathbf{x})}{\left(\sqrt{2\pi} r_c\right)^3} e^{-\frac{|\mathbf{x}-\mathbf{y}|^2}{2r_c^2}} |\mathbf{x}\rangle \langle \mathbf{x}| = \frac{m}{\left(\sqrt{2\pi} r_c\right)^3} e^{-\frac{|\hat{\mathbf{x}}-\mathbf{y}|^2}{2r_c^2}} \ . \tag{2.10}$$

Here we used the spectral decomposition of $\hat{x}$ in the second step. Notice the similarity between this operator and the Gaussian POVM in equation 1.25: They merely differ by their normalization,

$$\int_{\mathbb{R}^3} \mathrm{d}\lambda^3(\mathbf{y}) \hat{M}^\dagger(\mathbf{y}) \hat{M}(\mathbf{y}) = \frac{m^2}{(2\pi)^3 r_c^6} \left(\sqrt{\pi} r_c\right)^3 \mathbb{1} = \frac{m^2}{8\left(\sqrt{\pi} r_c\right)^3} \mathbb{1} \ . \tag{2.11}$$

This norm can be combined with the CSL parameter γ to define an effective measurement rate but this can just be seen as a contribution to the rate γ, which leaves us with the dissipative part of the master equation like

$$\frac{\mathrm{d}}{\mathrm{d}t} \hat{\rho}_t = \Gamma \left(\int_{\mathbb{R}^3} \mathrm{d}\lambda^3(\mathbf{y}) \hat{N}(\mathbf{y}) \hat{\rho}_t \hat{N}^\dagger(\mathbf{y}) - \hat{\rho}_t \right) \tag{2.12}$$

with the rescaled operator

$$\hat{N}(\mathbf{y}) := \left(\sqrt{\pi} r_c\right)^{-\frac{3}{2}} \mathrm{e}^{-\frac{|\hat{\mathbf{x}}-\mathbf{y}|^2}{2r_c^2}} \ . \tag{2.13}$$

and redefined rate

$$\Gamma := \frac{m^2 \gamma}{8 m_0^2 \left(\sqrt{\pi} r_c\right)^3} \ . \tag{2.14}$$

Consequences The main feature of the time evolution described by (2.12) is the suppression of position space superpositions. In order to see this explicitly, we shall ignore the system Hamiltonian $\hat{H}$ for the moment and focus our attention on the Lindblad term. In position representation, this leads to

$$\left(\frac{\mathrm{d}}{\mathrm{d}\left(\Gamma t\right)} + 1 \right) \langle \mathbf{z}_1 | \hat{\rho}_t | \mathbf{z}_2 \rangle = \int_{\mathbb{R}^3} \mathrm{d}\lambda^3(\mathbf{y}) \langle \mathbf{z}_1 | \hat{N}(\mathbf{y}) \hat{\rho}_t \hat{N}^\dagger(\mathbf{y}) | \mathbf{z_2} \rangle \tag{2.15}$$

$$= \frac{1}{\left(\sqrt{\pi} r_c\right)^3} \int_{\mathbb{R}^3} \mathrm{d}\lambda^3(\mathbf{y}) \mathrm{e}^{-\frac{|\mathbf{z}_1-\mathbf{y}|^2}{2r_c^2}} e^{-\frac{|\mathbf{z}_2-\mathbf{y}|^2}{2r_c^2}} \langle \mathbf{z}_1 | \hat{\rho}_t | \mathbf{z}_2 \rangle \tag{2.16}$$

$$= \frac{1}{\left(\sqrt{\pi} r_c\right)^3} \mathrm{e}^{-\frac{(\mathbf{z}_1-\mathbf{z}_2)^2}{4r_c^2}} \langle \mathbf{z}_1 | \hat{\rho}_t | \mathbf{z}_2 \rangle \int_{\mathbb{R}^3} \mathrm{d}\lambda^3(\mathbf{a}) \mathrm{e}^{-\frac{\mathbf{a}^2}{r_c^2}} \tag{2.17}$$

$$= \mathrm{e}^{-\frac{(\mathbf{z}_1-\mathbf{z}_2)^2}{4r_c^2}} \langle \mathbf{z}_1 | \hat{\rho}_t | \mathbf{z}_2 \rangle \ . \tag{2.18}$$

In the third step we completed the square like

$$(\mathbf{z_1}-\mathbf{y})^2+(\mathbf{z_1}-\mathbf{y})^2=2\left[\mathbf{y}-\frac{1}{2}(\mathbf{z_1}+\mathbf{z_2})\right]^2+\frac{1}{2}(\mathbf{z}_1-\mathbf{z}_2)^2 \tag{2.19}$$

followed by the change of variable $\mathbf{a}(\mathbf{y})=\mathbf{y}-\frac{1}{2}(\mathbf{z_1}+\mathbf{z_2})$. Finally, after carrying out the integral, we can see the solution

$$\langle\mathbf{z}_1|\,\hat{\rho}_t\,|\mathbf{z}_2\rangle=\exp\left[\Gamma\left(\mathrm{e}^{-\frac{(\mathbf{z}_1-\mathbf{z}_2)^2}{4r_c^2}}-1\right)t\right]\langle\mathbf{z}_1|\,\hat{\rho}_0\,|\mathbf{z}_2\rangle \tag{2.20}$$

that decays the faster the bigger the distance $|\mathbf{z}_1-\mathbf{z}_2|$ is, compared to the scale r_c. Thus the single particle CSL master equation (2.12) fulfills its purpose: It gradually destroys spatial superpositions of the wave function with a rate $\propto\Gamma\propto m^2$ growing with the particle mass.

However, the model has an unavoidable downside, we will investigate now. To this end we consider a free particle with Hamiltonian $\hat{H}=\frac{\hat{\mathbf{p}}^2}{2m}$ and investigate on the expectation value of the kinetic energy $\langle\hat{H}\rangle_t$. We will now use the master equation to obtain a Ehrenfest equation of motion for $\langle\hat{H}\rangle_t$. The general idea was already discussed in subsection 1.5. We get

$$\frac{\mathrm{d}}{\mathrm{d}t}\langle\hat{H}\rangle_t=\mathrm{Tr}\left(\hat{H}\frac{\mathrm{d}}{\mathrm{d}t}\hat{\rho}_t\right) \tag{2.21}$$

$$=\mathrm{Tr}\left(\frac{i}{\hbar}\left[\hat{H},\hat{H}\right]\hat{\rho}_t+\hat{H}\Gamma\left(\int_{\mathbb{R}^3}\mathrm{d}\lambda^3(\mathbf{y})\hat{N}(\mathbf{y})\hat{\rho}_t\hat{N}^\dagger(\mathbf{y})-\hat{\rho}_t\right)\right)\ . \tag{2.22}$$

Using the fact that $\hat{H}$ commutes with itself we can simplify further by writing one expectation value on the left hand side yields

$$\left(\frac{\mathrm{d}}{\mathrm{d}(\Gamma t)}+1\right)\langle\hat{H}\rangle_t=\mathrm{Tr}\left(\hat{H}\int_{\mathbb{R}^3}\mathrm{d}\lambda^3(\mathbf{y})\hat{N}(\mathbf{y})\hat{\rho}_t\hat{N}^\dagger(\mathbf{y})\right) \tag{2.23}$$

$$=\frac{1}{2m}\sqrt{\frac{r_c^2}{\pi\hbar^2}}^3\mathrm{Tr}\left(\hat{\mathbf{p}}^2\int_{\mathbb{R}^3}\mathrm{d}\lambda^3(\mathbf{q})\mathrm{e}^{-\frac{r_c^2}{\hbar^2}\mathbf{q}^2}\mathrm{e}^{i\frac{\mathbf{q}\cdot\hat{\mathbf{x}}}{\hbar}}\ \hat{\rho}_t\ \mathrm{e}^{-i\frac{\mathbf{q}\cdot\hat{\mathbf{x}}}{\hbar}}\right) \tag{2.24}$$

$$=\frac{1}{2m}\sqrt{\frac{r_c^2}{\pi\hbar^2}}^3\int_{\mathbb{R}^3}\mathrm{d}\lambda^3(\mathbf{q})\mathrm{e}^{-\frac{r_c^2}{\hbar^2}\mathbf{q}^2}\mathrm{Tr}\left(\mathrm{e}^{-i\frac{\mathbf{q}\cdot\hat{\mathbf{x}}}{\hbar}}\ \hat{\mathbf{p}}^2\ \mathrm{e}^{i\frac{\mathbf{q}\cdot\hat{\mathbf{x}}}{\hbar}}\hat{\rho}_t\right) \tag{2.25}$$

$$=\frac{1}{2m}\sqrt{\frac{r_c^2}{\pi\hbar^2}}^3\int_{\mathbb{R}^3}\mathrm{d}\lambda^3(\mathbf{q})\mathrm{e}^{-\frac{r_c^2}{\hbar^2}\mathbf{q}^2}\left\langle(\hat{\mathbf{p}}+\mathbf{q})^2\right\rangle_t \tag{2.26}$$

$$=\langle\hat{H}\rangle_t+\frac{1}{2m}\sqrt{\frac{r_c^2}{\pi\hbar^2}}^3\int_{\mathbb{R}^3}\mathrm{d}\lambda^3(\mathbf{q})\ \mathbf{q}^2\ \mathrm{e}^{-\frac{r_c^2}{\hbar^2}\mathbf{q}^2} \tag{2.27}$$

$$=\langle\hat{H}\rangle_t+\frac{1}{2m}\frac{3\hbar^2}{2r_c^2}\ . \tag{2.28}$$

In the second line we used the Fourier transform of the measurement operators as it was introduced in 1.2, in the third step we pulled the integral out of the trace and used the cyclic invariance of the trace, in the third step we used the definition of the kick operator (compare equation (1.3)), in the fourth step we used the linearity of the expectation value and that the Gaussian has zero mean, and finally we evaluated the integral with help of (A.27) from appendix A.4. By rephrasing the last expression we obtain the ordinary differential equation

$$\frac{\mathrm{d}}{\mathrm{d}t}\langle \hat{H} \rangle_t = \gamma \frac{3m\hbar^2}{32\sqrt{\pi}^3 r_c^5 m_0^2} \tag{2.29}$$

which shows that the kinetic energy of the particle increases constantly. This shows that the CSL effect is always accompanied by a constant heating power that slowly but steadily increases the kinetic energy of particles to infinity. As a remedy, we will now consider a modified CSL model in which dissipation limits the heating effect.

2.3. The dissipative CSL-model

In this subsection we will introduce the dissipative CSL (dCSL) model, as first formulated in [3] . It incorporates friction into the Lindblad operators $\hat{\mathbb{M}}(\mathbf{y})$ of the original CSL dissipator, such that the CSL-induced heating does not exceed a finite (parameter dependent) amount of energy. However, adding frictions comes at the cost of breaking the Galilei invariance of the model.

The model The dCSL model is characterized by the two free parameters γ,r_c of the original CSL model and a new third one, the velocity scale v_η at which dissipation sets in. The stochastic differential equation for the wave function of many body system reads

$$\mathrm{d}\left|\psi_t\right\rangle = \Bigg[-\frac{i}{\hbar}\left[\hat{H},\hat{\rho}\right]\mathrm{d}t + \frac{\sqrt{\gamma}}{m_0}\int_{\mathbb{R}^3}\mathrm{d}\lambda^3(\mathbf{y})\left[\hat{\mathbb{L}}(\mathbf{y}) - r_t(\mathbf{y})\right]\mathrm{d}W_t(\mathbf{y}) \tag{2.30}$$

$$- \frac{\gamma}{2m_0^2}\int_{\mathbb{R}^3}\mathrm{d}\lambda^3(\mathbf{y})\left[\hat{\mathbb{L}}^\dagger(\mathbf{y})\hat{\mathbb{L}}(\mathbf{y}) - 2r_t(\mathbf{y})\hat{\mathbb{L}}(\mathbf{y}) + r_t^2(\mathbf{y})\right]\mathrm{d}t\Bigg]\left|\psi_t\right\rangle \ , \tag{2.31}$$

where

$$\hat{\mathbb{L}}(\mathbf{y}) := \sum_j \frac{m_j}{(1+k_j)^3}\int_{\mathbb{R}^3}\frac{\mathrm{d}\lambda^3(\mathbf{x})}{(2\pi r_c)^3}\mathrm{e}^{-\frac{(\mathbf{x}-\mathbf{y})^2}{2r_c^2(1+k_j)^2}}\hat{\psi}_j^\dagger(\mathbf{x})\hat{\psi}_j\left(\frac{1-k_j}{1+k_j}\mathbf{x} + \frac{2k_j}{1+k_j}\mathbf{y}\right) \ , \tag{2.32}$$

with

$$r_t(\mathbf{y}) := \frac{1}{2}\left\langle\psi_t\right|\left(\hat{\mathbb{L}}(\mathbf{y}) + \hat{\mathbb{L}}^\dagger(\mathbf{y})\right)\left|\psi_t\right\rangle \ , \quad k_j := \frac{\hbar}{2m_j v_\eta r_c} \ . \tag{2.33}$$

The new velocity scale enters through the mass-dependent constants k_j. They vanish for $v_\eta \to \infty$, in which case the dCSL model converges to the original CSL model (2.4). It is noteworthy that for $k_j = 0\ \forall j$ the non dissipative model (equation (2.4)) is retrieved. Recalling section 1.6 the dCSL state equation can be seen as a stochastic unravelling of the master equation

$$\frac{\mathrm{d}}{\mathrm{d}t}\hat{\rho}_t = -\frac{i}{\hbar}\left[\hat{H},\hat{\rho}_t\right] + \frac{\gamma}{m_0^2}\int_{\mathbb{R}^3}\mathrm{d}\lambda^3(\mathbf{y})\left(\hat{\mathbb{L}}(\mathbf{y})\hat{\rho}_t\hat{\mathbb{L}}(\mathbf{y})^\dagger - \frac{1}{2}\left\{\hat{\mathbb{L}}^\dagger(\mathbf{y})\hat{\mathbb{L}}(\mathbf{y}),\hat{\rho}_t\right\}\right) \ . \tag{2.34}$$

This master equation is all we need to describe the observable consequences of the dCSL model.

Consequences For a better understanding of the action of the Lindblad operators $\hat{\mathbb{L}}(\mathbf{y})$ it is instructive to express them in terms of field operators in momentum space. The transformation rules are given in equation (1.80) and completely carried out in

appendix A.5. We obtain

$$\hat{\mathbb{L}}(\mathbf{y}) = \sum_j m_j \int_{\mathbb{R}^6} \frac{\mathrm{d}\lambda^6(\mathbf{Q},\mathbf{P})}{(2\pi\hbar)^3} \mathrm{e}^{-i\frac{\mathbf{y}\cdot\mathbf{Q}}{\hbar}} \mathrm{e}^{-\frac{r_c^2}{2\hbar^2}((1+k_j)\mathbf{Q}+2k_j\mathbf{P})^2} \hat{a}_j^\dagger(\mathbf{P}+\mathbf{Q})\hat{a}_j(\mathbf{P}) \ . \tag{2.35}$$

The intuition, why this leads to dissipation, can be seen from reading equation (2.35) from right to left: For every given particle species j, the operator describes a redistribution of momentum: The field operators annihilate a particle at some momentum $\mathbf{P}$ and create a new one at a shifted momentum $\mathbf{P}+\mathbf{Q}$. The Gaussian function under the integral maximizes when its argument is zero, which makes it most likely that the momentum kick be $\mathbf{Q}_{max} = -\frac{2k_j}{1+k_j}\mathbf{P}$. The kick points exactly opposite to the initial momentum $\mathbf{P}$ of the particle, which mimics a velocity-dependent friction force on average. This makes it plausible that the dCSL model can effectively slow particles down.

To show that this indeed bounds the CSL-induced heating to a finite energy-scale, we again consider the single-particle Lindblad operator,

$$\hat{L}(\mathbf{y}) = m \int_{\mathbb{R}^6} \frac{\mathrm{d}\lambda^6(\mathbf{Q},\mathbf{P})}{(2\pi\hbar)^3} \mathrm{e}^{-i\frac{\mathbf{y}\cdot\mathbf{Q}}{\hbar}} \mathrm{e}^{-\frac{r_c^2}{2\hbar^2}((1+k)\mathbf{Q}+2k\mathbf{P})^2} |\mathbf{P}+\mathbf{Q}\rangle \langle\mathbf{P}| \tag{2.36}$$

$$= m \int_{\mathbb{R}^6} \frac{\mathrm{d}\lambda^6(\mathbf{Q},\mathbf{P})}{(2\pi\hbar)^3} \mathrm{e}^{i\frac{\mathbf{Q}\cdot(\hat{\mathbf{x}}-\mathbf{y})}{\hbar}} \mathrm{e}^{-\frac{r_c^2}{2\hbar^2}((1+k)\mathbf{Q}+2k\mathbf{P})^2} |\mathbf{P}\rangle \langle\mathbf{P}| \tag{2.37}$$

$$= m \int_{\mathbb{R}^3} \frac{\mathrm{d}\lambda^3(\mathbf{Q})}{(2\pi\hbar)^3} \mathrm{e}^{i\frac{\mathbf{Q}\cdot(\hat{\mathbf{x}}-\mathbf{y})}{\hbar}} \mathrm{e}^{-\frac{r_c^2}{2\hbar^2}((1+k)\mathbf{Q}+2k\hat{\mathbf{p}})^2} \tag{2.38}$$

with

$$k := \frac{\hbar}{2mv_\eta r_c} \ . \tag{2.39}$$

Here, we expressed $|\mathbf{P}+\mathbf{Q}\rangle$ by means of the kick operator $\exp(i\mathbf{Q}\hat{\mathbf{x}}/\hbar)$ and used the spectral decomposition of $\hat{\mathbf{p}}$ in the last step. We can now calculate the equation of motion for the mean kinetic energy $\langle\hat{H}\rangle_t = \langle\frac{\hat{\mathbf{p}}^2}{2m}\rangle_t$ of a free particle in full analogy to subsection 2.2. We first notice that the single-particle Lindblad operators are again a resolution of the identity up to constant,

$$\int_{\mathbb{R}^3} \mathrm{d}^3\lambda(\mathbf{y}) \hat{L}^\dagger(\mathbf{y})\hat{L}(\mathbf{y}) \tag{2.40}$$

$$= m^2 \int_{\mathbb{R}^6} \frac{\mathrm{d}\lambda^6(\mathbf{Q},\mathbf{P})}{(2\pi\hbar)^6} \mathrm{e}^{-\frac{r_c^2}{2\hbar^2}((1+k)\mathbf{Q}+2k\hat{\mathbf{p}})^2} \mathrm{e}^{-i\frac{\mathbf{Q}\cdot\hat{\mathbf{x}}}{\hbar}} \mathrm{e}^{+i\frac{\mathbf{P}\cdot\hat{\mathbf{x}}}{\hbar}} \mathrm{e}^{-\frac{r_c^2}{2\hbar^2}((1+k)\mathbf{P}+2k\hat{\mathbf{p}})^2} \tag{2.41}$$

$$\times \int_{\mathbb{R}^3} \mathrm{d}\lambda^3(\mathbf{y}) \mathrm{e}^{\frac{i}{\hbar}\mathbf{y}\cdot(\mathbf{Q}-\mathbf{P})} \tag{2.42}$$

$$= m^2 \int_{\mathbb{R}^3} \frac{\mathrm{d}\lambda^3(\mathbf{Q})}{(2\pi\hbar)^3} \mathrm{e}^{-\frac{r_c^2}{\hbar^2}((1+k)\mathbf{Q}+2k\hat{\mathbf{p}})^2} \tag{2.43}$$

$$= \frac{m^2}{(2\pi\hbar)^3} \left(\frac{\sqrt{\pi}\hbar}{(1+k)r_c}\right)^3 \mathbb{1} \ . \tag{2.44}$$

Here we made use of the integral representation of the δ-function in the $\mathbf{y}$ integral. Similarly, we can simplify the expression

$$\int_{\mathbb{R}^3} \mathrm{d}\lambda^3(\mathbf{y}) \hat{L}(\mathbf{y}) \hat{\rho}_t \hat{L}^\dagger(\mathbf{y}) \tag{2.45}$$

$$= m^2 \int_{\mathbb{R}^6} \frac{\mathrm{d}^6\lambda(\mathbf{Q},\mathbf{P})}{(2\pi\hbar)^6} \mathrm{e}^{+i\frac{\mathbf{Q}\cdot\hat{\mathbf{x}}}{\hbar}} \mathrm{e}^{-\frac{r_c^2}{2\hbar^2}((1+k)\mathbf{Q}+2k\hat{\mathbf{p}})^2} \hat{\rho}_t \mathrm{e}^{-\frac{r_c^2}{2\hbar^2}((1+k)\mathbf{P}+2k\hat{\mathbf{p}})^2} \mathrm{e}^{-i\frac{\mathbf{P}\cdot\hat{\mathbf{x}}}{\hbar}} \tag{2.46}$$

$$\int_{\mathbb{R}^3} \mathrm{d}\lambda^3(\mathbf{y}) \mathrm{e}^{\frac{i}{\hbar}\mathbf{y}\cdot(\mathbf{Q}-\mathbf{P})} \tag{2.47}$$

$$= m^2 \int_{\mathbb{R}^3} \frac{\mathrm{d}^3\lambda(\mathbf{Q})}{(2\pi\hbar)^3} \mathrm{e}^{+i\frac{\mathbf{Q}\cdot\hat{\mathbf{x}}}{\hbar}} \mathrm{e}^{-\frac{r_c^2}{2\hbar^2}((1+k)\mathbf{Q}+2k\hat{\mathbf{p}})^2} \hat{\rho}_t \mathrm{e}^{-\frac{r_c^2}{2\hbar^2}((1+k)\mathbf{Q}+2k\hat{\mathbf{p}})^2} \mathrm{e}^{-i\frac{\mathbf{Q}\cdot\hat{\mathbf{x}}}{\hbar}} \ . \tag{2.48}$$

Using these two results (2.44) and (2.48), we can calculate

$$\frac{\mathrm{d}}{\mathrm{d}t}\langle \hat{H} \rangle_t = \mathrm{Tr}\left[\frac{\hat{\mathbf{p}}^2}{2m}\frac{\gamma}{m_0^2}\left(\int_{\mathbb{R}^3} \mathrm{d}\lambda^3(\mathbf{y}) \left(\hat{L}(\mathbf{y})\hat{\rho}_t\hat{L}(\mathbf{y})^\dagger - \frac{1}{2}\left\{\hat{L}^\dagger(\mathbf{y})\hat{L}(\mathbf{y}), \hat{\rho}_t\right\}\right)\right)\right] \tag{2.49}$$

$$= \frac{\gamma}{2mm_0^2}\mathrm{Tr}\left(\hat{\mathbf{p}}^2 \int_{\mathbb{R}^3} \mathrm{d}\lambda^3(\mathbf{y}) \hat{L}(\mathbf{y})\hat{\rho}_t\hat{L}(\mathbf{y})^\dagger\right) - \frac{\gamma}{m_0^2}\frac{m^2}{(2\pi\hbar)^3}\left(\frac{\sqrt{\pi}\hbar}{(1+k)r_c}\right)^3 \langle \hat{H} \rangle \ . \tag{2.50}$$

The main work is now to evaluate

$$\mathrm{Tr}\left(\hat{\mathbf{p}}^2 \int_{\mathbb{R}^3} \mathrm{d}\lambda^3(\mathbf{y}) \hat{L}(\mathbf{y}) \hat{\rho}_t \hat{L}^\dagger(\mathbf{y})\right) \tag{2.51}$$

$$= m^2 \ \mathrm{Tr}\left(\hat{\mathbf{p}}^2 \int_{\mathbb{R}^3} \frac{\mathrm{d}^3\lambda(\mathbf{Q})}{(2\pi\hbar)^3} \mathrm{e}^{+i\frac{\mathbf{Q}\cdot\hat{\mathbf{x}}}{\hbar}} \mathrm{e}^{-\frac{r_c^2}{2\hbar^2}((1+k)\mathbf{Q}+2k\hat{\mathbf{p}})^2} \hat{\rho}_t \mathrm{e}^{-\frac{r_c^2}{2\hbar^2}((1+k)\mathbf{Q}+2k\hat{\mathbf{p}})^2} \mathrm{e}^{-i\frac{\mathbf{Q}\cdot\hat{\mathbf{x}}}{\hbar}}\right) \tag{2.52}$$

$$= m^2 \ \int_{\mathbb{R}^3} \frac{\mathrm{d}^3\lambda(\mathbf{Q})}{(2\pi\hbar)^3} \mathrm{Tr}\left(\mathrm{e}^{-\frac{r_c^2}{2\hbar^2}((1+k)\mathbf{Q}+2k\hat{\mathbf{p}})^2} \left(\mathrm{e}^{-i\frac{\mathbf{Q}\cdot\hat{\mathbf{x}}}{\hbar}} \hat{\mathbf{p}}^2 \mathrm{e}^{+i\frac{\mathbf{Q}\cdot\hat{\mathbf{x}}}{\hbar}}\right) \mathrm{e}^{-\frac{r_c^2}{2\hbar^2}((1+k)\mathbf{Q}+2k\hat{\mathbf{p}})^2} \hat{\rho}_t\right) \tag{2.53}$$

$$= m^2 \ \int_{\mathbb{R}^3} \frac{\mathrm{d}^3\lambda(\mathbf{Q})}{(2\pi\hbar)^3} \mathrm{Tr}\left(\mathrm{e}^{-\frac{r_c^2}{2\hbar^2}((1+k)\mathbf{Q}+2k\hat{\mathbf{p}})^2} (\hat{\mathbf{p}}+\mathbf{Q})^2 \mathrm{e}^{-\frac{r_c^2}{2\hbar^2}((1+k)\mathbf{Q}+2k\hat{\mathbf{p}})^2} \hat{\rho}_t\right) \tag{2.54}$$

$$= m^2 \ \int_{\mathbb{R}^3} \frac{\mathrm{d}^3\lambda(\mathbf{Q})}{(2\pi\hbar)^3} \mathrm{Tr}\left((\hat{\mathbf{p}}+\mathbf{Q})^2 \mathrm{e}^{-\frac{r_c^2}{\hbar^2}((1+k)\mathbf{Q}+2k\hat{\mathbf{p}})^2} \hat{\rho}_t\right) \tag{2.55}$$

$$= m^2 \ \int_{\mathbb{R}^6} \frac{\mathrm{d}^6\lambda(\mathbf{Q},\mathbf{p})}{(2\pi\hbar)^3} (\mathbf{p}+\mathbf{Q})^2 \mathrm{e}^{-\frac{r_c^2}{\hbar^2}((1+k)\mathbf{Q}+2k\mathbf{p})^2} \langle \mathbf{p}| \hat{\rho}_t |\mathbf{p}\rangle \tag{2.56}$$

$$= m^2 \ \int_{\mathbb{R}^6} \frac{\mathrm{d}^6\lambda(\mathbf{R},\mathbf{p})}{(2\pi\hbar)^3} \left(\frac{1-k}{1+k}\mathbf{p}+\mathbf{R}\right)^2 \mathrm{e}^{-\frac{(1+k)^2r_c^2}{\hbar^2}\mathbf{R}^2} \langle \mathbf{p}| \hat{\rho}_t |\mathbf{p}\rangle \tag{2.57}$$

$$= m^2 \ \int_{\mathbb{R}^3} \frac{\mathrm{d}^3\lambda(\mathbf{R})}{(2\pi\hbar)^3} \left[\left(\frac{1-k}{1+k}\right)^2 \langle \hat{\mathbf{p}}^2 \rangle_t + \mathbf{R}^2\right] \mathrm{e}^{-\frac{(1+k)^2r_c^2}{\hbar^2}\mathbf{R}^2} \tag{2.58}$$

$$= \frac{m^2}{(2\pi\hbar)^3}\left(\frac{\sqrt{\pi}\hbar}{(1+k)r_c}\right)^3 \left[\left(\frac{1-k}{1+k}\right)^2 \langle \hat{\mathbf{p}}^2 \rangle_t + \frac{3\hbar^2}{2(1+k)^2r_c^2}\right] \ , \tag{2.59}$$

which follows by using the canonical operator algebra outlined in appendix A.1. In line 7, we performed a change of variable to

$$\mathbf{R}(\mathbf{Q}) := \mathbf{Q} + \frac{2k}{1+k}\mathbf{p} \ , \tag{2.60}$$

and carried out the remaining Gaussian integral. Now we can plug everything back into the equation of motion, which yields

$$\frac{\mathrm{d}}{\mathrm{d}t}\left\langle \hat{H}\right\rangle_t = \underbrace{\left(\frac{m}{m_0}\right)^2 \frac{\gamma}{(1+k)^5\left(2\sqrt{\pi}r_c\right)^3}}_{=:\Gamma_k/(4k)} \left[\frac{3\hbar^2}{4mr_c^2} - 4k\left\langle \hat{H}\right\rangle_t\right] \ . \tag{2.61}$$

It is noteworthy that for $k = 0$ the term proportional to $\left\langle \hat{H}\right\rangle_t$ on the right hand side vanishes and we recover the constant original heating rate in (2.29). In contrast, the above equation (2.61) describes equilibration of the kinetic energy to the fix point

$$\left\langle \hat{H}\right\rangle_{eq} := \frac{3\hbar^2}{16mkr_c^2} \ , \tag{2.62}$$

$$\left\langle \hat{H}\right\rangle_t = \left\langle \hat{H}\right\rangle_{eq} + \left(\left\langle \hat{H}\right\rangle_0 - \left\langle \hat{H}\right\rangle_{eq}\right)\mathrm{e}^{-\Gamma_k t} \ . \tag{2.63}$$

From this we can see that the kinetic energy of a free pariticle under the influence of dissipative CSL will eventually equilibrate to the finite energy $\left\langle \hat{H}\right\rangle_{eq}$.

Effective temperature Following the discussion in [3] we can assign an effective temperature to the equilibrium energy by virtue of the equipartition theorem $\left\langle \hat{H}\right\rangle_{eq} = k_B T/2$

$$T = \frac{\hbar^2}{8k_B mkr_c^2} = \frac{\hbar v_\eta}{4k_B r_c} \ . \tag{2.64}$$

This temperature seems to be a universal feature of the dCSL model as it does not depend on the particle mass. However, we will argue in subsection 6.7 that the universality is lost in the case of a harmonic oscillator.

3. Measurement feedback interpretation of dissipative CSL

In subsection 2.3 introducing the dCSL model we followed the reasoning in [3] and worked primarily with the momentum representation of the Lindblad operators $\hat{\mathbb{L}}(\mathbf{y})$. In contrast to that we will now show how to understand the dynamics in the position representation. While the dCSL model drew inspiration from microscopic descriptions of decoherence and Brownian motion based on scattering theory like [26] and [12], we choose a more operational approach. To this end, we decompose the Lindblad operators into a position measurement and a feedback unitary in subsection 3.1. Then we arrive at the effective time evolution of a system under random measurements of the type above in subsection 3.2. The properties of the feedback unitary are further investigated in subsection 3.3. Finally we interpret this protocol in subsection 3.4.

3.1. The measurement feedback protocol

We start by reformulating the Lindblad operator $\hat{\mathbb{L}}(\mathbf{y})$ as a Gaussian position measurement followed by a feedback unitary. The single-particle operator in consideration is

$$\hat{L}(\mathbf{y}) := \frac{m}{(1+k)^3} \int_{\mathbb{R}^3} \frac{\mathrm{d}\lambda^3(\mathbf{x})}{(2\pi r_c)^3} \mathrm{e}^{-\frac{(\mathbf{x}-\mathbf{y})^2}{2r_c^2(1+k)^2}} |\mathbf{x}\rangle \left\langle \frac{1-k}{1+k}\mathbf{x} + \frac{2k}{1+k}\mathbf{y} \right| \ . \tag{3.1}$$

We begin our decomposition with a measurement of the position of the particle. It is plausible that this reduces superpositions in the position basis. To not collapse the whole wave function into one point we choose the Gaussian POVM introduced in subsection 1.2. We will see that the right choice of parameters is $\sigma^2 = r_c^2(1-k)^2/2$ yielding the measurement operators associated to the measurement outcomes $\mathbf{y}$

$$\hat{M}_{\mathbf{y}} := \sqrt{\hat{E}_{\mathbf{y}}} = \frac{1}{\pi^{3/4} r_c^{3/2} |1-k|^{3/2}} \mathrm{e}^{-\frac{(\hat{\mathbf{x}}-\mathbf{y})^2}{2(1-k)^2 r_c^2}} \ . \tag{3.2}$$

Now let us consider the outcome-dependent feedback operation $\hat{U}_{\mathbf{y}}$. This is a unitary operation, as we will show in 3.3.

$$\hat{U}_{\mathbf{y}} := \sqrt{\left|\frac{1+k}{1-k}\right|}^3 \int_{\mathbb{R}^3} \mathrm{d}\lambda^3(\mathbf{z}) \left| \frac{1+k}{1-k}\mathbf{z} - \frac{2k}{1-k}\mathbf{y} \right\rangle \langle \mathbf{z}| \ . \tag{3.3}$$

Note that $\hat{U}_{\mathbf{y}}$ can be expressed as a scale transformation followed by a position displacement as we will show 3.3. It turns out that the dCSL Lindblad operator (3.1) can be obtained, up to a constant prefactor, by combining the measurement operator (3.2) with

the feedback unitary (3.3)

$$\hat{U}_{\mathbf{y}}\hat{M}_{\mathbf{y}} = \sqrt{\left|\frac{1+k}{1-k}\right|}^{3} \frac{1}{\pi^{3/4} r_c^{3/2} |1-k|^{3/2}} \int_{\mathbb{R}^3} \mathrm{d}\lambda^3(\mathbf{z}) \left|\frac{1+k}{1-k}\mathbf{z} - \frac{2k}{1-k}\mathbf{y}\right\rangle \langle \mathbf{z}| \, \mathrm{e}^{-\frac{(\mathbf{z}-\mathbf{y})^2}{2(1-k)^2 r_c^2}} \tag{3.4}$$

$$= \frac{|1+k|^{3/2}}{\pi^{3/4} r_c^{3/2} |1-k|^3} \int_{\mathbb{R}^3} \mathrm{d}\lambda^3(\mathbf{z}) \mathrm{e}^{-\frac{(\mathbf{z}-\mathbf{y})^2}{2(1-k)^2 r_c^2}} \left|\frac{1+k}{1-k}\mathbf{z} - \frac{2k}{1-k}\mathbf{y}\right\rangle \langle \mathbf{z}| \tag{3.5}$$

$$= \frac{1}{\pi^{3/4} r_c^{3/2} (1+k)^{3/2}} \int_{\mathbb{R}^3} \mathrm{d}\lambda^3(\mathbf{x}) \mathrm{e}^{-\frac{(\mathbf{x}-\mathbf{y})^2}{2(1+k)^2 r_c^2}} |\mathbf{x}\rangle \left\langle \frac{1-k}{1+k}\mathbf{x} + \frac{2k}{1+k}\mathbf{y}\right| \tag{3.6}$$

$$= \frac{[2\sqrt{\pi}(1+k) r_c]^{3/2}}{m} \hat{L}(\mathbf{y}) \ . \tag{3.7}$$

We changed the integration variable following

$$\mathbf{z}(\mathbf{x}) = \frac{1-k}{1+k}\mathbf{x} + \frac{2k}{1+k}\mathbf{y} \ . \tag{3.8}$$

The additional factor in front of $\hat{L}(\mathbf{y})$ is due to the fact that $\hat{U}_{\mathbf{y}}\hat{M}_{\mathbf{y}}$ is normalized to be a measurement operator.

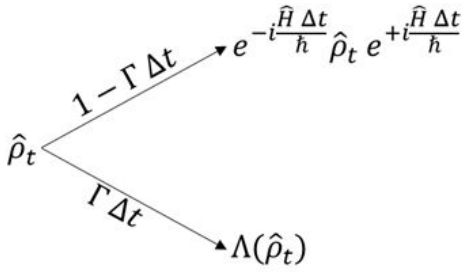

Figure 2: Poisson process, that gives rise to discontinuous jumps at random times. When no jump occurs, the system evolves unitarily according to the Schrödinger equation

3.2. Time evolution from consecutive measurements

Using the understanding of $\hat{L}(\mathbf{y})$ as a measurement with feedback, we generate the time evolution of dCSL. For the further discussion it is convenient to introduce a channel Λ that describes the average effect of the measurement when the measurement result is ignored or inaccessible.

$$\Lambda\left(\hat{\rho}\right) := \int_{\mathbb{R}^3} \mathrm{d}\lambda(\mathbf{y})\ \hat{U}_{\mathbf{y}}\hat{M}_{\mathbf{y}}\hat{\rho}\hat{M}_{\mathbf{y}}^{\dagger}\hat{U}_{\mathbf{y}}^{\dagger}\ . \tag{3.9}$$

The dCSL master equation can be understood as stochastic process in which such a measurement occurs at random times, with an average rate Γ. TO see this, consider the following Poisson process for the evolution of the particle state, as sketched in figure 2: For every small time step from t to $t+\Delta t$, the particle state $\hat{\rho}_t$ either gets measured with probability $\Gamma\Delta t$, or it evolves unitarily according to its free Hamiltonian $\hat{H}$ with probability $(1-\Gamma\Delta t)$. To arrive at a master equation for this kind of evolution we expand everything in orders of Δt. Up to first order the Schrödinger equation yields

$$\mathrm{e}^{-i\frac{\hat{H}\Delta t}{\hbar}}\hat{\rho}_t\ \mathrm{e}^{+i\frac{\hat{H}\Delta t}{\hbar}} = \hat{\rho}_t - \frac{i\Delta t}{\hbar}\left[\hat{H},\hat{\rho}_t\right] + \mathcal{O}(\Delta t^2)\ . \tag{3.10}$$

If we do not know whether a measurement occurred (i.e. which path the state took in figure 2), the correct statistical description of $\hat{\rho}_{t+\Delta t}$ is the convex combination

$$\hat{\rho}_{t+\Delta t} = (1-\Gamma\Delta t)\left(\hat{\rho}_t - \frac{i\Delta t}{\hbar}\left[\hat{H},\hat{\rho}_t\right]\right) + \Gamma\Delta t\ \Lambda\left(\hat{\rho}_t\right) + \mathcal{O}(\Delta t^2) \tag{3.11}$$

$$= \hat{\rho}_t + \Delta t\left(-\frac{i}{\hbar}\left[\hat{H},\hat{\rho}_t\right] + \Gamma\left(\Lambda\left(\hat{\rho}_t\right) - \hat{\rho}_t\right)\right) + \mathcal{O}(\Delta t^2)\ . \tag{3.12}$$

This yields the master equation as

$$\frac{\mathrm{d}}{\mathrm{d}t}\hat{\rho}_t = \lim_{\Delta t\to 0}\frac{\hat{\rho}_{t+\Delta t}-\hat{\rho}_t}{\Delta t} = -\frac{i}{\hbar}\left[\hat{H},\hat{\rho}_t\right] + \Gamma\left(\Lambda\left(\hat{\rho}_t\right) - \hat{\rho}_t\right)\ . \tag{3.13}$$

The equation has the form of a Lindblad generator (1.85), as the the Lindblad operators of the above measurement channel (3.9) are a resolution of indentity. Hence the usual anticommutator term in (1.85) simplifies as

$$\hat{\rho}_t = \left(\int_{\mathbb{R}^3} \mathrm{d}\lambda^3(\mathbf{y}) \hat{E}_{\mathbf{y}}^\dagger \hat{E}_{\mathbf{y}} \right) \hat{\rho}_t \tag{3.14}$$

$$= \left(\int_{\mathbb{R}^3} \mathrm{d}\lambda^3(\mathbf{y}) \hat{M}_{\mathbf{y}}^\dagger \hat{U}_{\mathbf{y}}^\dagger \hat{U}_{\mathbf{y}} \hat{M}_{\mathbf{y}} \right) \hat{\rho}_t \tag{3.15}$$

$$\propto \left(\int_{\mathbb{R}^3} \mathrm{d}\lambda^3(\mathbf{y}) \hat{L}^\dagger(\mathbf{y}) \hat{L}(\mathbf{y}) \right) \hat{\rho}_t \tag{3.16}$$

$$= \frac{1}{2} \int_{\mathbb{R}^3} \mathrm{d}\lambda^3(\mathbf{y}) \left\{ \hat{L}^\dagger(\mathbf{y}) \hat{L}(\mathbf{y}), \hat{\rho}_t \right\} \ . \tag{3.17}$$

Finally, in order to match the measurement master equation (3.13) the dCSL master equation (2.34), we choose the measurement rate

$$\Gamma = \left(\frac{m}{m_0} \right)^2 \frac{\gamma}{\left[2\sqrt{\pi}(1+k) r_c \right]^3} \ . \tag{3.18}$$

Summarizing, we have shown that the single-particle dynamics of the dissipative CSL model can be described by random (Gaussian) position measurements followed by an outcome dependent feedback unitary, which is performed at random times.

3.3. Properties of the unitary

The unitarity of the operator family $\hat{U}_{\mathbf{y}}$ is shown in this subsection. Then we show that they can be decomposed into a translation operator and a scale transformation. The unitarity follows from straightforward calculation

$$\hat{U}_{\mathbf{y}}^{\dagger}\hat{U}_{\mathbf{y}} = \left|\frac{1+k}{1-k}\right|^3 \int_{\mathbb{R}^6} \mathrm{d}\lambda(\mathbf{z},\mathbf{z}')\, |\mathbf{z}'\rangle \left\langle \frac{1+k}{1-k}\mathbf{z}' - \frac{2k}{1-k}\mathbf{y} \middle| \frac{1+k}{1-k}\mathbf{z} - \frac{2k}{1-k}\mathbf{y} \right\rangle \langle \mathbf{z}| \tag{3.19}$$

$$= \left|\frac{1+k}{1-k}\right|^3 \int_{\mathbb{R}^6} \mathrm{d}\lambda(\mathbf{z},\mathbf{z}')\; \delta^{(3)}\left(\left(\frac{1+k}{1-k}\right)(\mathbf{z}-\mathbf{z}')\right) |\mathbf{z}'\rangle \langle \mathbf{z}| \tag{3.20}$$

$$= \int_{\mathbb{R}^3} \mathrm{d}\lambda(\mathbf{z})\, |\mathbf{z}\rangle \langle \mathbf{z}| = \mathbb{1}\ . \tag{3.21}$$

In the same manner, we can see that $\hat{U}_{\mathbf{y}}\hat{U}_{\mathbf{y}}^{\dagger} = \mathbb{1}$, and therefore the operator $\hat{U}_{\mathbf{y}}$ is unitary.

For better understanding, we can factorize the unitary $\hat{U}_{\mathbf{y}}$ into a translation operator an a scale transformation,

$$\hat{U}_{\mathbf{y}} = \sqrt{\left|\frac{1+k}{1-k}\right|}^3 \int_{\mathbb{R}^3} \mathrm{d}\lambda^3(\mathbf{z}) \left|\frac{1+k}{1-k}\mathbf{z} - \frac{2k}{1-k}\mathbf{y}\right\rangle \langle \mathbf{z}| \tag{3.22}$$

$$= \sqrt{\left|\frac{1+k}{1-k}\right|}^3 \int_{\mathbb{R}^3} \mathrm{d}\lambda^3(\mathbf{z})\; \mathrm{e}^{\frac{i}{\hbar}\frac{2k}{1-k}\mathbf{y}\cdot\hat{\mathbf{p}}} \left|\frac{1+k}{1-k}\mathbf{z}\right\rangle \langle \mathbf{z}| \tag{3.23}$$

$$= \mathrm{e}^{\frac{i}{\hbar}\frac{2k}{1-k}\mathbf{y}\cdot\hat{\mathbf{p}}} \int_{\mathbb{R}^3} \mathrm{d}\lambda^3(\mathbf{z}) \left(\sqrt{\left|\frac{1+k}{1-k}\right|}^3 \left|\frac{1+k}{1-k}\mathbf{z}\right\rangle\right) \langle \mathbf{z}| \tag{3.24}$$

$$= \mathrm{e}^{\frac{i}{\hbar}\frac{2k}{1-k}\mathbf{y}\cdot\hat{\mathbf{p}}} \int_{\mathbb{R}^3} \mathrm{d}\lambda^3(\mathbf{z}) \left(\hat{S}_K |\mathbf{z}\rangle\right) \langle \mathbf{z}| \tag{3.25}$$

$$= \mathrm{e}^{\frac{i}{\hbar}\frac{2k}{1-k}\mathbf{y}\cdot\hat{\mathbf{p}}} \hat{S}_K\ . \tag{3.26}$$

where we made use of the definition (1.13) of the unitary scale transformation $\hat{S}_K$ by the scale factor $K = \frac{1-k}{1+k}$. With this we can express $\hat{U}_{\mathbf{y}}$ in an elegant way by the operator exponentials

$$\hat{U}_{\mathbf{y}} = \exp\left(\frac{i}{\hbar}\frac{2k}{1-k}\mathbf{y}\cdot\hat{\mathbf{p}}\right) \exp\left(\frac{i}{\hbar}\ln\left(\frac{1-k}{1+k}\right)\frac{\{\hat{\mathbf{x}},\hat{\mathbf{p}}\}}{2}\right) \tag{3.27}$$

with the anti-commutator $\{\hat{\mathbf{x}},\hat{\mathbf{p}}\} := \hat{\mathbf{x}}\cdot\hat{\mathbf{p}} + \hat{\mathbf{p}}\cdot\hat{\mathbf{x}}$. In subsection 1.1 we learned about the effect of translation operators and scaling transformations on $\hat{\mathbf{x}}$ and $\hat{\mathbf{p}}$. Now we can use

this to derive the transformation of position and momentum operators under $\hat{U}_{\mathbf{y}}$,

$$\hat{U}_{\mathbf{y}}^{\dagger}\ \hat{\mathbf{x}}\ \hat{U}_{\mathbf{y}} = \hat{S}_K^{\dagger}\left(\hat{\mathbf{x}} - \frac{2k}{1-k}\mathbf{y}\right)\hat{S}_K = \frac{1+k}{1-k}\hat{\mathbf{x}} - \frac{2k}{1-k}\mathbf{y} \tag{3.28}$$

$$\hat{U}_{\mathbf{y}}^{\dagger}\ \hat{\mathbf{p}}\ \hat{U}_{\mathbf{y}} = \hat{S}_K^{\dagger}\hat{\mathbf{p}}\hat{S}_K = \frac{1-k}{1+k}\hat{\mathbf{p}}\ . \tag{3.29}$$

These properties of $\hat{U}_{\mathbf{y}}$ and its adjoint operator $\hat{U}_{\mathbf{y}}$ are a big help for the Interpretation of the model in the following subsection 3.4.

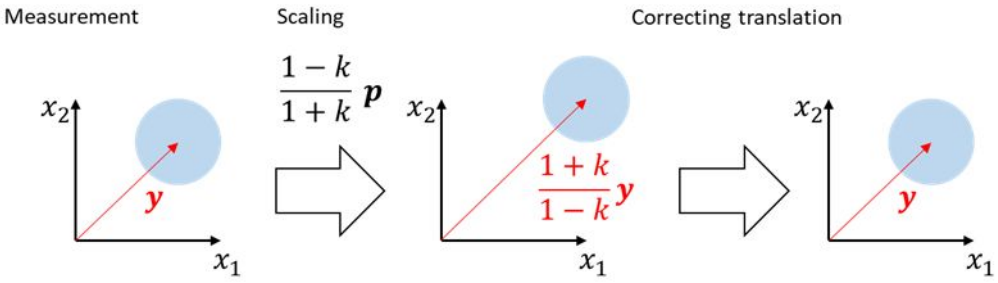

Figure 3: Physical interpretation of dissipative CSL as a measurement feedback protocol: The position is approximately determined by the Gaussian position measurement. The scaling transformation reduces the kinetic energy but lets the particles position drift away from the origin. A following translation corrects drift and keeps the kinetic energy reduced.

3.4. Physical interpretation of the protocol

In the preceeding subsections we went through the mathematical description of the measurement feedback protocol. Now we can use this to get an intuitive understanding on how the dissipative CSL model works: We learned in subsection 3.2 that the time evolution can be explained by random applications of the channel Λ. Therefore, we can focus on gaining intuition for Λ. In 3.1 the channel was interpreted as a Gaussian position measurement, as introduced in 1.2, followed by a feedback unitary. The position measurement alone describes the CSL model and therefore introduces spatial decoherence and heating.

After the measurement the scaling operation $\hat{S}_K$ is applied to the system. This reduces the kinetic energy, as can be seen from subsection 1.1 by

$$\hat{S}_K^\dagger\ \hat{\mathbf{p}}^2\ \hat{S}_K = \left(\hat{S}_K^\dagger \hat{\mathbf{p}} \hat{S}_K\right)\left(\hat{S}_K^\dagger \hat{\mathbf{p}} \hat{S}_K\right) = \left(\frac{1-k}{1+k}\right)^2 \hat{\mathbf{p}}^2\ . \tag{3.30}$$

Unfortunately, this breaks the homogeneity of space because the position operator transforms like

$$\hat{S}_K^\dagger\ \hat{\mathbf{x}}\ \hat{S}_K = \frac{1+k}{1-k}\hat{\mathbf{x}}\ . \tag{3.31}$$

This can be understood as the position $\mathbf{y}$ drifting away from the origin

$$\mathbf{y} \longmapsto \frac{1+k}{1-k}\mathbf{y}\ . \tag{3.32}$$

Therefore this assigns a special role to the origin and breaks a fundamental symmetry of space. To avoid this symmetry breaking, a measurement result dependent kick operator is applied that shifts the particle back to its original position

$$\frac{1+k}{1-k}\mathbf{y} \longmapsto \frac{1+k}{1-k}\mathbf{y} - \frac{2k}{1-k}\mathbf{y} = \mathbf{y}\ . \tag{3.33}$$

Since the translation operator is a function of momentum, the momentum stays unchanged in this last step.

Hence the position measurement plays two roles: On the one hand the measurement introduces decoherence in the position basis. On the other hand the measurement result $\mathbf{y}$ can be used in combination with a scaling transformation to reduce the kinetic energy without breaking physical symmetries.

The preceding section exemplifies how measurement feedback models can be understood intuitively. On the other hand, we can use physical intuition to build up models from measurements and feedback unitaries. We will follow the latter approach in the next section.

4. General measurement-based models

In section 3 we have seen that the one particle case of dissipative CSL can be interpreted as a measurement feedback protocol. We will now take this protocol as an inspiration to construct general models for friction in quantum dynamics. In subsection 4.1 we introduce the general model.The Ehrenfest equations of motion for functions in $\hat{\mathbf{x}}$ or $\hat{\mathbf{p}}$ are derived in subsection 4.2. After that we have a closer look on two specified models in subsections 4.3 and 4.4, the constant Coulomb-like friction and the linear Stokes-like friction.

4.1. The general model

Setup So far, we have employed the standard Gaussian POVM scheme to describe the measurement of the continuous observables position and momentum at finite precision. Here, we introduce a generalized POVM scheme based on arbitrary (non-Gaussian) probability distributions. Consider a general probability density $\mathcal{P}$ fulfilling the typical properties

$$\mathcal{P}(\mathbf{p}) \geq 0 \quad \forall \mathbf{p} \in \mathbb{R}^3 \tag{4.1}$$

$$\int_{\mathbb{R}^3} \mathrm{d}\lambda^3(\mathbf{p}) \mathcal{P}(\mathbf{p}) = 1 \ . \tag{4.2}$$

From this properties in combination with the spectral decomposition of $\hat{\mathbf{p}}$ we find in complete analogy to subsection 1.2 that

$$\hat{N}_{\mathbf{q}} := \sqrt{\mathcal{P}(\hat{\mathbf{p}} - \mathbf{q})} \tag{4.3}$$

is the measurement operator of a valid POVM with effects $\hat{N}_{\mathbf{q}}^\dagger \hat{N}_{\mathbf{q}}$. This can be seen as a weak measurement of the particle momentum. Consider now a simple control protocol on a moving quantum particle, in which the so defined momentum measurement is performed and, conditioned on the obtained outcome $\mathbf{q}$, a unitary feedback operation is applied to slow the particle down. For the feedback operation, we can assume a simple momentum kick transferring the momentum $-\alpha \mathbf{f}(\mathbf{q})$ upon measurement of $\mathbf{q}$. Here we introduce the free, tunable parameter $\alpha > 0$ for flexibility. The kick strength function $\mathbf{f} : \mathbb{R}^3 \to \mathbb{R}^3$ defines kick strength and kick direction for every $\mathbf{q}$ individually.

$$\hat{W}_{\mathbf{q}} := \mathrm{e}^{-\frac{i\alpha}{\hbar} \mathbf{f}(\mathbf{q}) \cdot \hat{\mathbf{x}}} \ . \tag{4.4}$$

The combined effect of the measurement and the feedback unitary $\hat{W}_{\mathbf{q}}$ yields the channel

$$\Lambda(\hat{\rho}) := \int_{\mathbb{R}^3} \mathrm{d}\lambda^3(\mathbf{q}) \ \hat{W}_{\mathbf{q}} \hat{N}_{\mathbf{q}} \ \hat{\rho} \ \hat{N}_{\mathbf{q}}^\dagger \hat{W}_{\mathbf{q}}^\dagger \ . \tag{4.5}$$

Analogous to subsection 3.2, random measurements with rate Γ define a master equation, we will now study

$$\frac{\mathrm{d}}{\mathrm{d}t}\hat{\rho}_t = \Gamma\left(\Lambda\left(\hat{\rho}_t\right) - \hat{\rho}_t\right) \ , \tag{4.6}$$

Omitting the contribution of the particle´s Hamiltonian for the moment, the expectation value of any observable $\hat{B}$ evolves under the measurement feedback channel according to

$$\left(\frac{\mathrm{d}}{\mathrm{d}t} + \Gamma\right)\langle\hat{B}\rangle_t = \Gamma\ \mathrm{Tr}\left(\hat{B}\Lambda(\hat{\rho}_t)\right) \tag{4.7}$$

For the Ehrenfest equations of motion it suffices to derive $\mathrm{Tr}\left(\hat{B}\hat{\rho}_t\right)$. As we will see later, $\alpha\Gamma\mathbf{f}(\mathbf{q})$ plays the role of an effective friction force.

General properties Before we go into explicit measurement feedback models we will stay at the abstract level, with α, Γ, $\mathbf{f}$ and $\mathcal{P}$ unspecified .

It is useful to introduce the Fourier transform of the measurement operators

$$\mathcal{F}\left[\sqrt{\mathcal{P}}\right](\mathbf{X}) := \frac{1}{(2\pi\hbar)^3}\int_{\mathbb{R}^3}\mathrm{d}\lambda^3(\mathbf{p})\ \mathrm{e}^{-i\frac{\mathbf{X}\cdot\mathbf{p}}{\hbar}}\sqrt{\mathcal{P}(\mathbf{p})} \tag{4.8}$$

$$\hat{N}_{\mathbf{q}} = \int_{\mathbb{R}^3}\mathrm{d}\lambda^3(\mathbf{X})\ \mathrm{e}^{i\frac{\mathbf{X}\cdot(\hat{\mathbf{p}}-\mathbf{q})}{\hbar}}\mathcal{F}\left[\sqrt{\mathcal{P}}\right](\mathbf{X}) \ . \tag{4.9}$$

With this we can rephrase

$$\int_{\mathbb{R}^3}\mathrm{d}\lambda^3(\mathbf{q})\ \hat{N}_{\mathbf{q}}\ \hat{\rho}\ \hat{N}_{\mathbf{q}}^{\dagger} = \int_{\mathbb{R}^6}\mathrm{d}\lambda^6(\mathbf{X},\mathbf{Y})\ \mathcal{F}\left[\sqrt{\mathcal{P}}\right](\mathbf{X})\mathcal{F}\left[\sqrt{\mathcal{P}}\right]^*(\mathbf{Y})\ \mathrm{e}^{i\frac{\mathbf{X}\cdot\hat{\mathbf{p}}}{\hbar}}\hat{\rho}\ \mathrm{e}^{-i\frac{\mathbf{Y}\cdot\hat{\mathbf{p}}}{\hbar}} \tag{4.10}$$

$$\times\int_{\mathbb{R}^3}\mathrm{d}\lambda^3(\mathbf{q})\mathrm{e}^{i\frac{\mathbf{q}\cdot(\mathbf{Y}-\mathbf{X})}{\hbar}} \tag{4.11}$$

$$= \int_{\mathbb{R}^3}\mathrm{d}\lambda^3(\mathbf{X})\ (2\pi\hbar)^3\left|\mathcal{F}\left[\sqrt{\mathcal{P}}\right](\mathbf{X})\right|^2\mathrm{e}^{i\frac{\mathbf{X}\cdot\hat{\mathbf{p}}}{\hbar}}\hat{\rho}\ \mathrm{e}^{-i\frac{\mathbf{X}\cdot\hat{\mathbf{p}}}{\hbar}} \tag{4.12}$$

$$= \int_{\mathbb{R}^3}\mathrm{d}\lambda^3(\mathbf{X})\ \mathcal{Q}(\mathbf{X})\ \mathrm{e}^{i\frac{\mathbf{X}\cdot\hat{\mathbf{p}}}{\hbar}}\hat{\rho}\ \mathrm{e}^{-i\frac{\mathbf{X}\cdot\hat{\mathbf{p}}}{\hbar}} \ , \tag{4.13}$$

where we identified and integrated a delta function in the first step and then introduced the function

$$\mathcal{Q}(\mathbf{X}) := (2\pi\hbar)^3\left|\mathcal{F}\left[\sqrt{\mathcal{P}}\right](\mathbf{X})\right|^2 \ . \tag{4.14}$$

The function is positive and, by virtue of Plancherel´s theorem, normalized to

$$\int_{\mathbb{R}^3}\mathrm{d}\lambda^3(\mathbf{X})\mathcal{Q}(\mathbf{X}) = \int_{\mathbb{R}^3}\mathrm{d}\lambda^3(\mathbf{X})(2\pi\hbar)^3\left|\mathcal{F}\left[\sqrt{\mathcal{P}}\right](\mathbf{X})\right|^2 \tag{4.15}$$

$$= \int_{\mathbb{R}^3}\mathrm{d}\lambda^3(\mathbf{p})\left|\sqrt{\mathcal{P}(\mathbf{p})}\right|^2 = \int_{\mathbb{R}^3}\mathrm{d}\lambda^3(\mathbf{p})\mathcal{P}(\mathbf{p}) = 1 \ . \tag{4.16}$$

Therefore, $\mathcal{Q}$ is a probability density. We will see soon that $\mathcal{P}$ occurs in the equations of motion of moments of $\hat{\mathbf{p}}$, while $\mathcal{Q}$ occurs in the equations for moments of $\hat{\mathbf{x}}$.

From the definition of $\mathcal{Q}$ we can see that it is an even function since

$$\left|\mathcal{F}\left[\sqrt{\mathcal{P}}\right](\mathbf{X})\right|^2 = \mathcal{F}\left[\sqrt{\mathcal{P}}\right]^*(\mathbf{X})\mathcal{F}\left[\sqrt{\mathcal{P}}\right](\mathbf{X}) = \mathcal{F}\left[\sqrt{\mathcal{P}}\right](-\mathbf{X})\mathcal{F}\left[\sqrt{\mathcal{P}}\right](\mathbf{X}) \tag{4.17}$$

is symmetric under the action $\mathbf{X} \mapsto -\mathbf{X}$. This also means that $\mathbf{X}\mathcal{Q}(\mathbf{X})$ is odd and therefore the expectation value of $\mathbf{X}$ with respect to $\mathcal{Q}$ is zero (provided the integral exists). This will be used to simplify the equations of motion of $\langle\hat{\mathbf{x}}^n\rangle$.

In addition, we can show that the measurement feedback channel (4.5) is covariant under translations, regardless of the chosen $\mathcal{P}$,α ,and $\mathbf{f}$,

$$\Lambda\left(\mathrm{e}^{i\frac{\mathbf{z}\cdot\hat{\mathbf{p}}}{\hbar}}\hat{\rho}\,\mathrm{e}^{-i\frac{\mathbf{z}\cdot\hat{\mathbf{p}}}{\hbar}}\right) = \int_{\mathbb{R}^3}\mathrm{d}\lambda^3(\mathbf{q})\;\hat{W}_{\mathbf{q}}\hat{N}_{\mathbf{q}}\mathrm{e}^{i\frac{\mathbf{z}\cdot\hat{\mathbf{p}}}{\hbar}}\;\hat{\rho}\;\mathrm{e}^{-i\frac{\mathbf{z}\cdot\hat{\mathbf{p}}}{\hbar}}\hat{N}_{\mathbf{q}}^\dagger\hat{W}_{\mathbf{q}}^\dagger \tag{4.18}$$

$$= \int_{\mathbb{R}^3}\mathrm{d}\lambda^3(\mathbf{q})\;\hat{W}_{\mathbf{q}}\mathrm{e}^{i\frac{\mathbf{z}\cdot\hat{\mathbf{p}}}{\hbar}}\hat{N}_{\mathbf{q}}\;\hat{\rho}\;\hat{N}_{\mathbf{q}}^\dagger\mathrm{e}^{-i\frac{\mathbf{z}\cdot\hat{\mathbf{p}}}{\hbar}}\hat{W}_{\mathbf{q}}^\dagger \tag{4.19}$$

$$= \mathrm{e}^{i\frac{\mathbf{z}\cdot\hat{\mathbf{p}}}{\hbar}}\left(\int_{\mathbb{R}^3}\mathrm{d}\lambda^3(\mathbf{q})\;\hat{W}_{\mathbf{q}}\mathrm{e}^{i\frac{\alpha\mathbf{z}\cdot\mathbf{f}(\mathbf{q})}{\hbar}}\hat{N}_{\mathbf{q}}\;\hat{\rho}\;\hat{N}_{\mathbf{q}}^\dagger\mathrm{e}^{-i\frac{\alpha\mathbf{z}\cdot\mathbf{f}(\mathbf{q})}{\hbar}}\hat{W}_{\mathbf{q}}^\dagger\right)\mathrm{e}^{-i\frac{\mathbf{z}\cdot\hat{\mathbf{p}}}{\hbar}} \tag{4.20}$$

$$= \mathrm{e}^{i\frac{\mathbf{z}\cdot\hat{\mathbf{p}}}{\hbar}}\Lambda(\hat{\rho})\mathrm{e}^{-i\frac{\mathbf{z}\cdot\hat{\mathbf{p}}}{\hbar}}\;, \tag{4.21}$$

where we used that $\hat{N}_{\mathbf{q}}$ commutes with any translation since both operators are just functions of $\hat{\mathbf{p}}$ and then used the Baker-Campbell-Hausdorf formula to see

$$\hat{W}_{\mathbf{q}}\mathrm{e}^{i\frac{\mathbf{z}\cdot\hat{\mathbf{p}}}{\hbar}} = \mathrm{e}^{i\frac{\mathbf{z}\cdot\hat{\mathbf{p}}}{\hbar}}\;\hat{W}_{\mathbf{q}}\;\mathrm{e}^{i\frac{\alpha\mathbf{z}\cdot\mathbf{f}(\mathbf{q})}{\hbar}}\;. \tag{4.22}$$

The two additional phases $\mathrm{e}^{\pm i\frac{\alpha\mathbf{z}\cdot\mathbf{f}(\mathbf{q})}{\hbar}}$ cancel out.

This framework will now be used to construct models in analogy to classical friction forces. For mathematical convenience it is necessary to keep a Gaussian probability distribution in the exemplary cases.

As kick strength function $\mathbf{f}$ we will mainly consider $\mathbf{f}(\mathbf{q}) \propto \mathbf{q}$ and $\mathbf{f}(\mathbf{q}) \propto \mathbf{q}/|\mathbf{q}|$, leading to a constant and a linear. friction.

4.2. Ehrenfest equations of motion for general measurement-based models of friction

We investigate on the general equations of motion of statistical moments under the measurement-based friction, we introduced in subsection 4.1. As stated in the last subsection it suffices to focus on the evaluation of

$$\langle \hat{B} \rangle_{\Lambda(\hat{\rho})} = \mathrm{Tr}\left(\hat{B} \Lambda(\hat{\rho}_t) \right) \ . \tag{4.23}$$

For a compact notation of the following general results, we use the notion of classical $\mathbb{E}[\cdot]$ and quantum $\langle \cdot \rangle$ expectation value. The classical expectation value with respect to the probability density $\mathcal{P}$ is denoted as

$$\mathbb{E}_{\mathcal{P}(\mathbf{q})}[f(\mathbf{q})] := \int_{\mathbb{R}^3} \mathrm{d}\lambda^3(\mathbf{q}) \ \mathcal{P}(\mathbf{q}) f(\mathbf{q}) \ . \tag{4.24}$$

Functions of momentum Suppose we have a function of the momentum operator $F(\hat{\mathbf{p}})$ and want to calculate the quantum expectation value in the transformed state $\Lambda(\hat{\rho})$. We start calculating

$$\begin{aligned}
\langle F(\hat{\mathbf{p}}) \rangle_{\Lambda(\rho)} &= \mathrm{Tr}\left(F(\hat{\mathbf{p}}) \Lambda(\rho) \right) && (4.25)\\
&= \int_{\mathbb{R}^3} \mathrm{d}\lambda^3(\mathbf{q}) \ \mathrm{Tr}\left(F(\hat{\mathbf{p}}) \ \hat{W}_{\mathbf{q}} \hat{N}_{\mathbf{q}} \ \hat{\rho} \ \hat{N}_{\mathbf{q}}^\dagger \hat{W}_{\mathbf{q}}^\dagger \right) && (4.26)\\
&= \int_{\mathbb{R}^3} \mathrm{d}\lambda^3(\mathbf{q}) \ \mathrm{Tr}\left(\hat{W}_{\mathbf{q}}^\dagger \ F(\hat{\mathbf{p}}) \ \hat{W}_{\mathbf{q}} \hat{N}_{\mathbf{q}} \ \hat{\rho} \ \hat{N}_{\mathbf{q}}^\dagger \right) && (4.27)\\
&= \int_{\mathbb{R}^3} \mathrm{d}\lambda^3(\mathbf{q}) \ \mathrm{Tr}\left(F(\hat{\mathbf{p}} - \alpha \mathbf{f}(\mathbf{q})) \hat{N}_{\mathbf{q}} \ \hat{\rho} \ \hat{N}_{\mathbf{q}}^\dagger \right) && (4.28)\\
&= \int_{\mathbb{R}^3} \mathrm{d}\lambda^3(\mathbf{q}) \ \mathrm{Tr}\left(F(\hat{\mathbf{p}} - \alpha \mathbf{f}(\mathbf{q})) \sqrt{\mathcal{P}(\hat{\mathbf{p}} - \mathbf{q})} \ \hat{\rho} \ \sqrt{\mathcal{P}(\hat{\mathbf{p}} - \mathbf{q})} \right) && (4.29)\\
&= \int_{\mathbb{R}^3} \mathrm{d}\lambda^3(\mathbf{q}) \ \mathrm{Tr}\left(F(\hat{\mathbf{p}} - \alpha \mathbf{f}(\mathbf{q})) \mathcal{P}(\hat{\mathbf{p}} - \mathbf{q}) \ \hat{\rho} \ \right) && (4.30)\\
&= \int_{\mathbb{R}^3} \mathrm{d}\lambda^3(\mathbf{q}) \ \mathrm{Tr}\left(F(\hat{\mathbf{p}} - \alpha \mathbf{f}(\mathbf{q})) \mathcal{P}(\hat{\mathbf{p}} - \mathbf{q}) \ \hat{\rho} \ \right) && (4.31)\\
&= \int_{\mathbb{R}^6} \mathrm{d}\lambda^6(\mathbf{q}, \mathbf{p}) \ F(\mathbf{p} - \alpha \mathbf{f}(\mathbf{q})) \mathcal{P}(\mathbf{p} - \mathbf{q}) \langle \mathbf{p} | \hat{\rho} | \mathbf{p} \rangle && (4.32)\\
&= \int_{\mathbb{R}^6} \mathrm{d}\lambda^6(\mathbf{Q}, \mathbf{p}) \ F(\mathbf{p} - \alpha \mathbf{f}(\mathbf{p} - \mathbf{Q})) \mathcal{P}(\mathbf{Q}) \langle \mathbf{p} | \hat{\rho} | \mathbf{p} \rangle && (4.33)\\
&= \int_{\mathbb{R}^3} \mathrm{d}\lambda^3(\mathbf{p}) \ \langle \mathbf{p} | \, \mathbb{E}_{\mathcal{P}(\mathbf{Q})}[F(\mathbf{p} - \alpha \mathbf{f}(\mathbf{p} - \mathbf{Q}))] \, \hat{\rho} \, | \mathbf{p} \rangle && (4.34)\\
&= \left\langle \mathbb{E}_{\mathcal{P}(\mathbf{Q})}[F(\hat{\mathbf{p}} - \alpha \mathbf{f}(\hat{\mathbf{p}} - \mathbf{Q}))] \right\rangle_{\hat{\rho}} \ . && (4.35)
\end{aligned}$$

We applied the kick operators to the function $F(\hat{p})$ and then used the cyclic property of the trace and the fact that functions of the momentum operator commute. Finally we

used the spectral theorem to substitute $\mathbf{Q}(\mathbf{q}) = \mathbf{p} - \mathbf{q}$ and then expressed the $\mathbf{Q}$-integral as a classical expectation value.

The last line describes a double expectation value over the classical momentum kick distribution $\mathcal{P}$ and the particle´s quantum state $\hat{\rho}$.

Functions of position A similar expression can be found for functions of the position operator $G(\hat{\mathbf{x}})$. The probability distribution $\mathcal{Q}$, introduced in 4.1, enables us to use a compact notation

$$\begin{aligned}
\left\langle G(\hat{\mathbf{x}})\right\rangle_{\Lambda(\hat{\rho})} &= \mathrm{Tr}\left(G(\hat{\mathbf{x}})\Lambda(\hat{\rho})\right) && (4.36)\\
&= \int_{\mathbb{R}^3} \mathrm{d}\lambda^3(\mathbf{q})\ \mathrm{Tr}\left(G(\hat{\mathbf{x}})\ \hat{W}_{\mathbf{q}}\hat{N}_{\mathbf{q}}\ \hat{\rho}\ \hat{N}_{\mathbf{q}}^\dagger\hat{W}_{\mathbf{q}}^\dagger\right) && (4.37)\\
&= \int_{\mathbb{R}^3} \mathrm{d}\lambda^3(\mathbf{q})\ \mathrm{Tr}\left(\hat{W}_{\mathbf{q}}^\dagger G(\hat{\mathbf{x}})\hat{W}_{\mathbf{q}}\ \hat{N}_{\mathbf{q}}\ \hat{\rho}\ \hat{N}_{\mathbf{q}}^\dagger\right) && (4.38)\\
&= \int_{\mathbb{R}^3} \mathrm{d}\lambda^3(\mathbf{q})\ \mathrm{Tr}\left(G(\hat{\mathbf{x}})\ \hat{N}_{\mathbf{q}}\ \hat{\rho}\ \hat{N}_{\mathbf{q}}^\dagger\right) && (4.39)\\
&= \int_{\mathbb{R}^3} \mathrm{d}\lambda^3(\mathbf{X})\mathcal{Q}(\mathbf{X})\mathrm{Tr}\left(\mathrm{e}^{-i\frac{\mathbf{X}\cdot\hat{\mathbf{p}}}{\hbar}}G(\hat{\mathbf{x}})\mathrm{e}^{+i\frac{\mathbf{X}\cdot\hat{\mathbf{p}}}{\hbar}}\hat{\rho}\right) && (4.40)\\
&= \int_{\mathbb{R}^3} \mathrm{d}\lambda^3(\mathbf{X})\mathcal{Q}(\mathbf{X})\mathrm{Tr}\left(G(\hat{\mathbf{x}}-\mathbf{X})\hat{\rho}\right) && (4.41)\\
&= \int_{\mathbb{R}^3} \mathrm{d}\lambda^3(\mathbf{X})\mathcal{Q}(\mathbf{X})\left\langle G(\hat{\mathbf{x}}-\mathbf{X})\right\rangle_{\hat{\rho}} && (4.42)\\
&= \mathbb{E}_{\mathcal{Q}(\mathbf{X})}\left[\left\langle G(\hat{\mathbf{x}}-\mathbf{X})\right\rangle_{\hat{\rho}}\right]\ , && (4.43)
\end{aligned}$$

where we used $\hat{W}_{\mathbf{q}}^\dagger G(\hat{\mathbf{x}})\hat{W}_{\mathbf{q}} = G(\hat{\mathbf{x}})$. Then we expressed $\hat{N}_{\mathbf{q}}$ by its Fourier transform, introduced in equation (4.13). Finally we applied the translation operators on $G(\hat{\mathbf{x}})$ and then expressed the integral as a classical expectation value. Therefore, the time evolution of any function of $\hat{\mathbf{x}}$ is independent of the choice of α and $\mathbf{f}$.

First and second moments The impact of the measurement feedback channel (4.5) on the particle motion can be well described by the expectation values of second order polynomials in position and momentum. We can now use our general expression for this special cases

$$\left\langle\hat{\mathbf{x}}\right\rangle_{\Lambda(\hat{\rho})} = \mathbb{E}_{\mathcal{Q}(\mathbf{X})}\left[\left\langle\hat{\mathbf{x}}-\mathbf{X}\right\rangle_{\hat{\rho}}\right] = \mathbb{E}_{\mathcal{Q}(\mathbf{X})}[1]\left\langle\hat{\mathbf{x}}\right\rangle_{\hat{\rho}} - \mathbb{E}_{\mathcal{Q}(\mathbf{X})}\left[\mathbf{X}\right] = \left\langle\hat{\mathbf{x}}\right\rangle_{\hat{\rho}}\ , \tag{4.44}$$

where we used the linearity of both expectation values and the normalization of $\mathcal{Q}$ as $\mathbb{E}_{\mathcal{Q}}[1] = 1$ and that the expectation value $\mathbb{E}_{\mathcal{Q}(\mathbf{X})}\left[\mathbf{X}\right] = 0$. In the same fashion we can

calculate

$$\langle \hat{\mathbf{x}}^2 \rangle_{\Lambda(\hat{\rho})} = \langle \hat{\mathbf{x}}^2 \rangle_{\hat{\rho}} - 2\mathbb{E}_{\mathcal{Q}(\mathbf{X})}[\mathbf{X}] \cdot \langle \hat{\mathbf{x}} \rangle_{\hat{\rho}} + \mathbb{E}_{\mathcal{Q}(\mathbf{X})}\left[\mathbf{X}^2\right] \tag{4.45}$$

$$= \langle \hat{\mathbf{x}}^2 \rangle_{\hat{\rho}} + \mathbb{E}_{\mathcal{Q}(\mathbf{X})}\left[\mathbf{X}^2\right] \ . \tag{4.46}$$

With equation (4.7) we get the equations of motion

$$\frac{\mathrm{d}}{\mathrm{d}t} \langle \hat{\mathbf{x}} \rangle_t = 0 \tag{4.47}$$

and

$$\frac{\mathrm{d}}{\mathrm{d}t} \langle \hat{\mathbf{x}}^2 \rangle_t = \Gamma \ \mathbb{E}_{\mathcal{Q}(\mathbf{X})}\left[\mathbf{X}^2\right] \tag{4.48}$$

This yields a direct connection between the variance of the quantum statistics $\Delta^2(\hat{\mathbf{x}})_t := \langle \hat{\mathbf{x}}^2 \rangle_t - \langle \hat{\mathbf{x}} \rangle_t^2$ and the variance $\mathbb{V}_{\mathcal{Q}(\mathbf{X})}[\mathbf{X}] := \mathbb{E}_{\mathcal{Q}(\mathbf{X})}[\mathbf{X}^2] - \mathbb{E}_{\mathcal{Q}(\mathbf{X})}[\mathbf{X}]$ of the classical distribution $\mathcal{Q}$

$$\frac{\mathrm{d}}{\mathrm{d}t} \Delta^2(\hat{\mathbf{x}})_t = \Gamma \ \mathbb{V}_{\mathcal{Q}(\mathbf{X})}[\mathbf{X}] \ . \tag{4.49}$$

Note that the coherent time evolution is omitted in above equation. In practice the coherent term has to be added. In the case of $\hat{\mathbf{p}}$, the general equations of motions do not admit an explicit solution. But they still give a hint on the general dynamics, so

$$\langle \hat{\mathbf{p}} \rangle_{\Lambda(\hat{\rho})} = \left\langle \mathbb{E}_{\mathcal{P}(\mathbf{Q})}[\hat{\mathbf{p}} - \alpha \mathbf{f}(\hat{\mathbf{p}} - \cdot)] \right\rangle_{\hat{\rho}} = \left\langle \mathbb{E}_{\mathcal{P}(\mathbf{Q})}[1]\hat{\mathbf{p}} - \alpha \mathbb{E}_{\mathcal{P}(\mathbf{Q})}(\mathbf{f}(\hat{\mathbf{p}} - \mathbf{Q})) \right\rangle_{\hat{\rho}} \tag{4.50}$$

$$= \langle \hat{\mathbf{p}} \rangle_{\hat{\rho}} - \alpha \left\langle \mathbb{E}_{\mathcal{P}(\mathbf{Q})}[\mathbf{f}(\hat{\mathbf{p}} - \mathbf{Q})] \right\rangle_{\hat{\rho}} \tag{4.51}$$

and

$$\langle \hat{\mathbf{p}}^2 \rangle_{\Lambda(\hat{\rho})} = \langle \hat{\mathbf{p}}^2 \rangle_{\hat{\rho}} - 2\alpha \left\langle \hat{\mathbf{p}} \cdot \mathbb{E}_{\mathcal{P}(\mathbf{Q})}[\mathbf{f}(\hat{\mathbf{p}} - \mathbf{Q})] \right\rangle_{\hat{\rho}} + \alpha^2 \left\langle \mathbb{E}_{\mathcal{P}(\mathbf{Q})}\left[\mathbf{f}^2(\hat{\mathbf{p}} - \mathbf{Q})\right] \right\rangle_{\hat{\rho}} \ . \tag{4.52}$$

These yield the equation of motion

$$\frac{\mathrm{d}}{\mathrm{d}t} \langle \hat{\mathbf{p}} \rangle_t = -\alpha\Gamma \left\langle \mathbb{E}_{\mathcal{P}(\mathbf{Q})}[\mathbf{f}(\hat{\mathbf{p}} - \mathbf{Q})] \right\rangle_t \ . \tag{4.53}$$

This change of the average momentum can be seen as an effective momentum dependent force that is applied to the particle. We see that the force $F(\hat{\mathbf{p}})$ has the form of the smeared out kick strength function $\mathbf{f}$. The second moment in $\hat{\mathbf{p}}$ evolves according to

$$\frac{\mathrm{d}}{\mathrm{d}t} \langle \hat{\mathbf{p}}^2 \rangle_t = -2\alpha\Gamma \left\langle \hat{\mathbf{p}} \cdot \mathbb{E}_{\mathcal{P}(\mathbf{Q})}[\mathbf{f}(\hat{\mathbf{p}} - \mathbf{Q})] \right\rangle_{\hat{\rho}} + \alpha^2\Gamma \left\langle \mathbb{E}_{\mathcal{P}(\mathbf{Q})}\left[\mathbf{f}^2(\hat{\mathbf{p}} - \mathbf{Q})\right] \right\rangle_{\hat{\rho}} \ . \tag{4.54}$$

From these equations we can learn that the general equation of motions for moments of $\hat{\mathbf{p}}$ just depend on momentum itself. So thinking classically we can just create momentum dependent forces.

With this general features of measurement-feedback models for friction at hand, we shall now discuss exemplary cases realizing Stokes and Coulomb friction.

4.3. Stokes friction

Linear friction forces are frequently used in physics. They typically are used in the damped harmonic oscillator in mechanics or, being more abstract, in electronic LC-circuits. This type of force is also exerted on objects moving through viscid fluids, as it is known from classical fluid dynamics. In this subsection we will introduce choices for $\mathcal{P}$, α ,and $\mathbf{f}$ that lead to similar dynamics of the statistical moments.

Setup As mentioned in subsection 4.1 we will from now on focus on a Gaussian probability density

$$\mathcal{P}(\mathbf{q}) = \left(2\pi p_c^2\right)^{-3/2} \mathrm{e}^{-\frac{\mathbf{q}^2}{2p_c^2}} \tag{4.55}$$

with zero mean and the standard deviation p_c. This keeps the calculations manageable and assures that all moments of $\mathcal{P}$ and $\mathcal{Q}$ exist. To formalize the following derivations we go back to equation (4.53)

$$\mathbb{E}_{\mathcal{P}(\mathbf{q})}\left[\mathbf{f}(\mathbf{p}-\mathbf{q})\right] := \int_{\mathbb{R}^3} \mathrm{d}\lambda(\mathbf{q})\ \mathbf{f}(\mathbf{p}-\mathbf{q})\mathcal{P}(\mathbf{q}) \tag{4.56}$$

such that

$$\frac{\mathrm{d}}{\mathrm{d}t}\left\langle\hat{\mathbf{p}}\right\rangle_t = -\alpha\Gamma\left\langle\mathbb{E}_{\mathcal{P}(\mathbf{q})}\left[\mathbf{f}(\hat{\mathbf{p}}-\mathbf{q})\right]\right\rangle\ . \tag{4.57}$$

Conclusively, our goal is to achieve $\mathbb{E}_{\mathcal{P}(\mathbf{Q})}\left[\mathbf{f}(\hat{\mathbf{p}}-\mathbf{Q})\right] \propto \mathbf{p}$. It can be seen that a possible choice is $\mathbf{f}(\mathbf{q}) = \mathbf{q}$ as

$$\mathbb{E}_{\mathcal{P}(\mathbf{Q})}\left[\mathbf{f}(\mathbf{p}-\mathbf{Q})\right] = \int_{\mathbb{R}^3} \mathrm{d}\lambda(\mathbf{q})\ (\mathbf{p}-\mathbf{q})\mathcal{P}(\mathbf{q}) = \mathbf{p}\underbrace{\int_{\mathbb{R}^3} \mathrm{d}\lambda(\mathbf{q})\mathcal{P}(\mathbf{q})}_{=1} - \underbrace{\int_{\mathbb{R}^3} \mathrm{d}\lambda(\mathbf{q})\ \mathbf{q}\mathcal{P}(\mathbf{q})}_{=0} = \mathbf{p}\ . \tag{4.58}$$

This choice is plausible since the force is the expectation value of the smeared out $\mathbf{f}$. Therefore the best Ansatz to get a particular momentum dependent force $\mathbf{F}(\mathbf{q})$ is to choose the same dependence for the kick strength function $\mathbf{f}(\mathbf{q}) \propto \mathbf{F}(\mathbf{q})$. Plugging everything together the Lindblad operator for the Stokes friction becomes

$$\hat{L}_{\mathrm{st}}(\mathbf{q}) := \left(2\pi p_c^2\right)^{-3/4} \mathrm{e}^{-i\frac{\alpha}{\hbar}\mathbf{q}\cdot\hat{\mathbf{x}}} \mathrm{e}^{-\frac{(\hat{\mathbf{p}}-\mathbf{q})^2}{4p_c^2}}\ . \tag{4.59}$$

Connection to dissipative CSL It turns out that the master equation (4.6) based on the here defined Lindblad operators (4.59) corresponds to the single-particle dissipative CSL model. This is not obvious since we have to do a gauge transformation of the form (1.86) beforehand, which mixes the Lindblad operators with the entries of unitary. Instead of the entries u_{ij} in the discrete case, we now have to use a function $u(\mathbf{y},\mathbf{q})$ and integrate over $\mathbf{q}$. Instead of the unitarity the analogous property

$$\int_{\mathbb{R}^3} \mathrm{d}\lambda(\mathbf{q})\ u^*(\mathbf{z},\mathbf{q})u(\mathbf{y},\mathbf{q}) = \delta^{(3)}(\mathbf{z}-\mathbf{y}) \tag{4.60}$$

ensures the invariance of the dynamics. The Lindblad operators (2.38) for the dCSL model depend on the free parameters r_c and k. We arrive at the same Lindblad operator if we express the free parameters α and p_c of our measurement feedback description as

$$\alpha = \frac{2k}{1+k}, \tag{4.61}$$

$$p_c = \frac{\hbar}{2\sqrt{2}r_c k}. \tag{4.62}$$

In order to show the equivalence to the dCSL Lindblad operator explicitly, consider the transformation function

$$u(\mathbf{y},\mathbf{q}) = \left(\frac{2k}{1+k}\right)^{3/2} \frac{1}{\sqrt{2\pi\hbar}^3} \mathrm{e}^{i\frac{2k}{1+k}\frac{\mathbf{y}\cdot\mathbf{q}}{\hbar}} \ . \tag{4.63}$$

Note that we obtain the same rate

$$\Gamma = \left(\frac{m}{m_0}\right)^2 \frac{\gamma}{\left[2\sqrt{\pi}(1+k)r_c\right]^3} \tag{4.64}$$

as for the measurement feedback interpretation of CSL in 3 since our Lindblad operators are normalized in the same way both times. We obtain

$$\hat{L}_{\mathrm{st}}(\mathbf{q}) \longmapsto \int_{\mathbb{R}^3} \mathrm{d}\lambda(\mathbf{q})\ u(\mathbf{y},\mathbf{q})\hat{L}_{st}(\mathbf{q}) \tag{4.65}$$

$$= \frac{1}{\sqrt{2\pi\hbar}^3}\left(\frac{2k}{1+k}\right)^{3/2}\sqrt{\frac{2r_c k}{\sqrt{\pi}\hbar}}^3 \int_{\mathbb{R}^3} \mathrm{d}\lambda(\mathbf{q})\ \mathrm{e}^{i\frac{2k}{1+k}\frac{(\mathbf{y}-\hat{\mathbf{x}})\cdot\mathbf{q}}{\hbar}} \mathrm{e}^{-\frac{r_c^2}{2\hbar^2}(2k\hat{\mathbf{p}}-2k\mathbf{q})^2} \tag{4.66}$$

$$= \frac{1}{\sqrt{2\pi\hbar}^3}\sqrt{\frac{(1+k)r_c}{\sqrt{\pi}\hbar}}^3 \int_{\mathbb{R}^3} \mathrm{d}\lambda(\mathbf{Q})\ \mathrm{e}^{\frac{i}{\hbar}\mathbf{Q}\cdot(\hat{\mathbf{x}}-\mathbf{y})} \mathrm{e}^{-\frac{r_c^2}{2\hbar^2}((1+k)\mathbf{Q}+2k\hat{\mathbf{p}})^2} \tag{4.67}$$

$$= \frac{\sqrt{2\pi\hbar}^3}{m}\sqrt{\frac{(1+k)r_c}{\sqrt{\pi}\hbar}}^3 \hat{L}_{\mathrm{DCSL}}(\mathbf{y}) \ , \tag{4.68}$$

where we changed the integration variable $\mathbf{Q}(\mathbf{q}) = -\frac{2k}{1+k}\mathbf{q}$ and identified the Lindblad operator from 2.38. Summarizing, we introduced the single-particle dCSL model in 2.3 and interpreted it in 3 as a position measurement with scaling transformation and translation as feedback. Now we have another interpretation as a measurement based model of Stokes friction.

The consequences of this time evolution on the statisical moments in $\hat{\mathbf{x}}$ and $\hat{\mathbf{p}}$ will be discussed in detail in section 6.

4.4. Coulomb friction

Coulomb friction is one of the first types of friction that occur in the context of classical mechanics. It typically arises from an Object being pressed onto a surface. It is oriented in the opposite direction of the objects velocity but its strength depends on the normal force of the surface.

Setup For us Coulomb friction just means that we are looking for a model with a drag force that only depends on the momentums direction. Using the definition from equation (4.56) we choose

$$\mathbf{f}(\mathbf{q}) = \frac{\mathbf{q}}{|\mathbf{q}|} 1_{\{|\mathbf{q}|\geq\epsilon\}}(\mathbf{q}) \tag{4.69}$$

for our kick strength function. This is a natural choice because the effective force can be seen as a smeared out version of $\mathbf{f}$. The momentum cut-off $\epsilon > 0$ adequately describes the numerical case, where the finite resolution effectively introduces a cut-off in the integral. As we will see, the analytical integration already regularizes the function and we therefore set $\epsilon = 0$ in the analytical case.

Expected evolution of momentum We need to calculate

$$\mathbf{I}_\epsilon(\mathbf{p}) = (2\pi p_c^2)^{-3/2} \int_{\mathbb{R}^3} \mathrm{d}\lambda^3(\mathbf{q})\ \frac{\mathbf{p}-\mathbf{q}}{|\mathbf{p}-\mathbf{q}|} 1_{\{|\mathbf{q}|\geq\epsilon\}}(\mathbf{p}-\mathbf{q})\ \mathrm{e}^{-\frac{\mathbf{q}^2}{2p_c^2}} \tag{4.70}$$

$$= -(2\pi p_c^2)^{-3/2} \int_{\mathbb{R}^3} \mathrm{d}\lambda^3(\mathbf{u})\ \frac{\mathbf{u}}{|\mathbf{u}|} 1_{\{|\mathbf{u}|\geq\epsilon\}}(\mathbf{u})\ \mathrm{e}^{-\frac{(\mathbf{u}+\mathbf{p})^2}{2p_c^2}}\ , \tag{4.71}$$

where we used the substitution $\mathbf{u}(\mathbf{q}) = \mathbf{q} - \mathbf{p}$. To make use of symmetry we introduce spherical coordinates $\mathbf{u}(u, \vartheta, \varphi)$ with the convention that u_z is aligned with $\mathbf{p}$. This leads to vanishing x and y componets when carrying out the φ-integration. We can also reshape the exponential of the gaussian by using

$$\mathbf{p}\cdot\mathbf{u} = pu\cos(\vartheta) \tag{4.72}$$

(Note $|\mathbf{p}| =: p$). Putting this together yields

$$\mathbf{I}_\epsilon(\mathbf{p}) = -2\pi(2\pi p_c^2)^{-3/2}\mathrm{e}^{-\frac{\mathbf{p}^2}{2p_c^2}} \frac{\mathbf{p}}{|\mathbf{p}|} \int_{+\epsilon}^{+\infty} \mathrm{d}u\ u^2 \mathrm{e}^{\frac{u^2}{2p_c^2}} \int_{-1}^{+1} \mathrm{d}\cos(\vartheta)\cos(\vartheta)\mathrm{e}^{\frac{-up\cos(\vartheta)}{p_c^2}}\ . \tag{4.73}$$

Using integration by parts on the ϑ-integral and then going over to the dimensionless variables $s(u) := u/(\sqrt{2}p_c)$ and $\xi := p/(\sqrt{2}p_c)$ yields the intermediate result

$$\mathbf{I}_\epsilon(\mathbf{p}) = \frac{2}{\sqrt{2\pi}} \frac{\mathbf{p}}{|\mathbf{p}|} \mathrm{e}^{\frac{-\mathbf{p}^2}{2p_c^2}} \left[2\left(\frac{p_c}{p}\right) \int_{\epsilon/(\sqrt{2}p_c)}^{+\infty} \mathrm{d}s\ s\cosh(2\xi s)\mathrm{e}^{-s^2} \right. \tag{4.74}$$

$$\left. +\sqrt{2}\left(\frac{p_c}{p}\right)^2 \int_{\epsilon/(\sqrt{2}p_c)}^{+\infty} \mathrm{d}s \sinh(2\xi s)\mathrm{e}^{-s^2} \right]. \tag{4.75}$$

The evaluation of the remaining integrals can be found in appendix B.1. Using those results gives us the full solution

$$\mathbf{I}_\epsilon(\mathbf{p}) = \frac{\mathbf{p}}{|\mathbf{p}|}\left[\frac{1}{2}\left(1-\left(\frac{p_c}{p}\right)^2\right)\Delta\mathrm{erf}(\xi,\epsilon) + \sqrt{\frac{2}{\pi}}\left(\frac{p_c}{p}\right)\mathrm{e}^{-\frac{\epsilon^2+p^2}{2p_c^2}}\cosh\left(\frac{\epsilon p}{p_c^2}\right)\right] , \tag{4.76}$$

with the short hand notation

$$\Delta\mathrm{erf}(\xi,\epsilon) := \mathrm{erf}\left(\frac{\epsilon}{\sqrt{2}p_c}+\xi\right) - \mathrm{erf}\left(\frac{\epsilon}{\sqrt{2}p_c}-\xi\right) \tag{4.77}$$

$$= \mathrm{erf}\left(\frac{\epsilon+p}{\sqrt{2}p_c}\right) - \mathrm{erf}\left(\frac{\epsilon-p}{\sqrt{2}p_c}\right) . \tag{4.78}$$

We see that the limit $\epsilon \to 0$ is well defined and set

$$\mathbf{I}(\mathbf{p}) = I_{\epsilon=0}(\mathbf{p}) = \frac{\mathbf{p}}{|\mathbf{p}|}\underbrace{\left[\left(1-\left(\frac{p_c}{p}\right)^2\right)\mathrm{erf}\left(\frac{p}{\sqrt{2}p_c}\right) + \sqrt{\frac{2}{\pi}}\left(\frac{p_c}{p}\right)\mathrm{e}^{-\frac{p^2}{2p_c^2}}\right]}_{=:F(p)} . \tag{4.79}$$

So we did get a $\mathbf{I}(\mathbf{p})$ that is approximately of the Coulomb form, but modified with an additional momentum dependent factor $F(|\mathbf{p}|)$. For big $|\mathbf{p}|/p_c$ the factor F approaches $\mathrm{erf}\left(p/(\sqrt{2}p_c)\right)$ asymptotically. On the other hand erf is the cumulative distribution function of the normalized gaussian probability distribution. It therefore approaches 1 for big p/p_c. So we can conclude that particles occupying states with high absolute momenta compared to the resolution p_c experience a force that is approximately

$$\frac{\mathrm{d}}{\mathrm{d}t}\langle\hat{\mathbf{p}}\rangle_t \approx -\alpha\Gamma\left\langle\frac{\hat{\mathbf{p}}}{|\hat{\mathbf{p}}|}\right\rangle_t , \tag{4.80}$$

which resembles the Coulomb friction force we wanted to model.

Kinetic energy We can now even use equation (4.54) for the Ehrenfest equation of motion of the kinetic energy. Therefore we need

$$\mathbf{p}\cdot\mathbb{E}_{\mathcal{P}(\mathbf{q})}(\mathbf{f}(\mathbf{p}-\mathbf{q})) = \mathbf{p}\cdot I(\mathbf{p}) = \mathbf{p}\cdot\frac{\mathbf{p}}{|\mathbf{p}|}F(\mathbf{p}) = |\mathbf{p}|F(\mathbf{p}) \tag{4.81}$$

and the new term

$$\mathbb{E}_{\mathcal{P}(\mathbf{q})}\left(\mathbf{f}^2(\mathbf{p}-\mathbf{q})\right) =: \Pi(\mathbf{p}) . \tag{4.82}$$

For the same reason as above, we go through the calculation with cut-off ϵ in appendix B.2. Here we just note that $\mathbf{f}^2 = 1$ almost everywhere and therefore

$$\Pi(\mathbf{p}) = \mathbb{E}_{\mathcal{P}}(1) = 1 . \tag{4.83}$$

All in all this yields the equation of motion

$$\frac{\mathrm{d}}{\mathrm{d}t}\langle\hat{\mathbf{p}}^2\rangle_t = -2\alpha\Gamma\,\langle\,|\hat{\mathbf{p}}|\;F(\hat{\mathbf{p}})\,\rangle_t + \alpha^2\Gamma\ . \tag{4.84}$$

From this we can find a lower bound for the expected absolute momentum in equilibrium

$$\langle\,|\hat{\mathbf{p}}|\,\rangle_{eq} \geq \langle\,|\hat{\mathbf{p}}|\;F(\hat{\mathbf{p}})\,\rangle_{eq} = \frac{\alpha}{2}\ , \tag{4.85}$$

which gives another physical meaning to α.

5. Characteristic function and equilibrium

In this section we investigate how and to what state a single-particle equilibrates under dissipative CSL. To this end, we start in 5.1 by deriving the time evolution of a state´s characteristic function under dissipative CSL, as introduced in 1.3. Then we argue that the equilibrium state of a particle cannot in general be a Gibbs state, with one known exception: A free (spatially unconfined) particle will asymptotically converge to its improper Gibbs state, as we will show in the final subsection 5.3.

5.1. Characteristic function under dissipative CSL

Let us start by formulating our single-particle measurement-feedback master equation from 4 in the characteristic function representation of the particle state. We restrict our view to the case of linear Stokes friction, which corresponds to the single-particle dissipation CSL model and yields mathematically tractable expressions. The time evolution of the characteristic function

$$G_t(\mathbf{k}_1, \mathbf{k}_2) := \mathrm{Tr}\left(\mathrm{e}^{i(\mathbf{k}_1\cdot\hat{\mathbf{x}}+\mathbf{k}_2\cdot\hat{\mathbf{p}})}\hat{\rho}_t\right) \tag{5.1}$$

is obtained by differentiating both sides with respect to t and inserting the master equation (4.6). If we once again omit the particle Hamiltonian $\hat{H}$ to single out the dCSL contribution, we arrive at

$$\frac{\mathrm{d}}{\mathrm{d}t}G_t(\mathbf{k}_1, \mathbf{k}_2) = \mathrm{Tr}\left(\mathrm{e}^{i(\mathbf{k}_1\cdot\hat{\mathbf{x}}+\mathbf{k}_2\cdot\hat{\mathbf{p}})}\frac{\mathrm{d}}{\mathrm{d}t}\hat{\rho}_t\right) = \mathrm{Tr}\left(\mathrm{e}^{i(\mathbf{k}_1\cdot\hat{\mathbf{x}}+\mathbf{k}_2\cdot\hat{\mathbf{p}})}\Gamma\left(\Lambda(\hat{\rho})-\hat{\rho}\right)\right). \tag{5.2}$$

Shifting the characteristic function of $\hat{\rho}$ that appears on the right hand side to the left, yields

$$\left(\frac{\mathrm{d}}{\mathrm{d}t}+\Gamma\right)G_t(\mathbf{k}_1, \mathbf{k}_2) = \Gamma\ \mathrm{Tr}\left(\mathrm{e}^{i(\mathbf{k}_1\cdot\hat{\mathbf{x}}+\mathbf{k}_2\cdot\hat{\mathbf{p}})}\Lambda(\hat{\rho})\right)\ . \tag{5.3}$$

The remaining term can be expanded with the help of the Baker-Campbell-Hausdorf formula,

$$\mathrm{e}^{i(\mathbf{k}_1\cdot\hat{\mathbf{x}}+\mathbf{k}_2\cdot\hat{\mathbf{p}})} = \mathrm{e}^{i\mathbf{k}_1\cdot\hat{\mathbf{x}}}\mathrm{e}^{i\mathbf{k}_2\cdot\hat{\mathbf{p}}}\mathrm{e}^{i\hbar\frac{\mathbf{k}_1\cdot\mathbf{k}_2}{2}}. \tag{5.4}$$

Carrying out the trace in momentum representation, the right hand side of (5.3) becomes

$$\mathrm{RHS}/\Gamma = \mathrm{e}^{i\hbar\frac{\mathbf{k}_1\cdot\mathbf{k}_2}{2}}\int_{\mathbb{R}^3}\mathrm{d}\lambda(\mathbf{p})\,\langle\mathbf{p}|\,\mathrm{e}^{i\mathbf{k}_1\cdot\hat{\mathbf{x}}}\mathrm{e}^{i\mathbf{k}_2\cdot\hat{\mathbf{p}}}\Lambda(\hat{\rho})\,|\mathbf{p}\rangle \tag{5.5}$$

$$= \mathrm{e}^{-i\hbar\frac{\mathbf{k}_1\cdot\mathbf{k}_2}{2}}\int_{\mathbb{R}^3}\mathrm{d}\lambda(\mathbf{p})\ \mathrm{e}^{i\mathbf{k}_2\cdot\mathbf{p}}\,\langle\mathbf{p}-\hbar\mathbf{k}_1|\,\Lambda(\hat{\rho})\,|\mathbf{p}\rangle \tag{5.6}$$

$$= \mathrm{e}^{-i\hbar\frac{\mathbf{k}_1\cdot\mathbf{k}_2}{2}}\int_{\mathbb{R}^3}\mathrm{d}\lambda(\mathbf{p})\ \mathrm{e}^{i\mathbf{k}_2\cdot\mathbf{p}}\int_{\mathbb{R}^3}\mathrm{d}\lambda(\mathbf{q}) \tag{5.7}$$

$$\langle\mathbf{p}+\alpha\mathbf{q}-\hbar\mathbf{k}_1|\,\sqrt{\mathcal{P}(\hat{\mathbf{p}}-\mathbf{q})}\hat{\rho}\sqrt{\mathcal{P}(\hat{\mathbf{p}}-\mathbf{q})}\,|\mathbf{p}+\alpha\mathbf{q}\rangle\ . \tag{5.8}$$

Here we plugged in the channel of Stokes friction given in equation (4.59). Now we can act the $\sqrt{\mathcal{P}}$-operators on the corresponding eigenstates. To keep overview we substitute $\mathbf{P}(\mathbf{p}) := \mathbf{p} + \alpha\mathbf{q}$ and get

$$\mathrm{RHS}/\Gamma = \mathrm{e}^{-i\hbar\frac{\mathbf{k}_1\cdot\mathbf{k}_2}{2}} \int_{\mathbb{R}^6} \mathrm{d}\lambda^6(\mathbf{q},\mathbf{P})\ \mathrm{e}^{i\mathbf{k}_2\cdot(\mathbf{P}-\alpha\mathbf{q})} \sqrt{\mathcal{P}\left(\mathbf{P}-\mathbf{q}-\hbar\mathbf{k}_1\right)} \tag{5.9}$$

$$\sqrt{\mathcal{P}\left(\mathbf{P}-\mathbf{q}\right)}\left\langle\mathbf{P}-\hbar\mathbf{k}_1\right|\hat{\rho}\left|\mathbf{P}\right\rangle\ . \tag{5.10}$$

After reordering the integrals we now substitute $\mathbf{Q}(\mathbf{q}) = \mathbf{P} - \mathbf{q}$ which yields

$$\mathrm{RHS}/\Gamma = \mathrm{e}^{-i\hbar\frac{\mathbf{k}_1\cdot\mathbf{k}_2}{2}} \int_{\mathbb{R}^3} \mathrm{d}\lambda(\mathbf{P})\mathrm{e}^{i(1-\alpha)\mathbf{k}_2\cdot\mathbf{P}} \left\langle\mathbf{P}-\hbar\mathbf{k}_1\right|\hat{\rho}\left|\mathbf{P}\right\rangle\ \mathrm{Int}(\mathbf{k}_1,\mathbf{k}_2)\ . \tag{5.11}$$

As we see, $\mathrm{Int}(\mathbf{k}_1,\mathbf{k}_2)$ does not depend on $\mathbf{P}$ and so the $\mathbf{P}$-integral yields the characteristic function,

$$\mathrm{RHS}/\Gamma = \mathrm{e}^{-i\alpha\hbar\frac{\mathbf{k}_1\cdot\mathbf{k}_2}{2}}\ G_t(\mathbf{k}_1,(1-\alpha)\mathbf{k}_2)\ \mathrm{Int}(\mathbf{k}_1,\mathbf{k}_2). \tag{5.12}$$

This expression can be integrated using the tools from appendix A.4,

$$\mathrm{Int}(\mathbf{k}_1,\mathbf{k}_2) = \left(2\pi p_c^2\right)^{-3/2}\mathrm{e}^{-\frac{\hbar^2\mathbf{k}_1^2}{4p_c^2}} \int_{\mathbb{R}^3}\mathrm{d}\lambda(\mathbf{Q})\mathrm{e}^{i\alpha\mathbf{k}_2\cdot\mathbf{Q}}\mathrm{e}^{\frac{\hbar\mathbf{k}_1\cdot\mathbf{Q}}{2p_c^2}}\mathrm{e}^{-\frac{\mathbf{Q}^2}{2p_c^2}} \tag{5.13}$$

$$= \exp\left(-\frac{\hbar^2\mathbf{k}_1^2}{8p_c^2} + i\alpha\hbar\frac{\mathbf{k}_1\cdot\mathbf{k}_2}{2} - \frac{\alpha^2p_c^2}{2}\mathbf{k}_2^2\right). \tag{5.14}$$

Putting everything together we get the non-coherent of the time evolution of the characteristic function

$$\left(\frac{\mathrm{d}}{\mathrm{d}t}+\Gamma\right)G_t(\mathbf{k}_1,\mathbf{k}_2) = \Gamma\ \exp\left(-\frac{\hbar^2\mathbf{k}_1^2}{8p_c^2} - \frac{\alpha^2p_c^2}{2}\mathbf{k}_2^2\right)G_t(\mathbf{k}_1,(1-\alpha)\mathbf{k}_2) \tag{5.15}$$

$$= \Gamma\ \exp\left(-k^2r_c^2\mathbf{k}_1^2 - \frac{\hbar^2}{4(1+k)^2r_c^2}\mathbf{k}_2^2\right)G_t\left(\mathbf{k}_1,\frac{1-k}{1+k}\mathbf{k}_2\right)\ , \tag{5.16}$$

where the second line is expressed in the parameters of dissipative CSL. It is remarkable that the non-coherent time evolution due to dCSL is completely given by an algebraic expressions. This will be helpful in the next subsection when we investigate on the characteristic function in equilibrium.

5.2. Characteristic function in equilibrium

In subsection 5.1 we found a differential equation (5.15) describing the non-coherent time evolution of the characteristic function $G_t(\mathbf{k}_1, \mathbf{k}_2)$ under dissipative CSL. We will now derive an equilibrium condition for the characteristic function of states ρ that are invariant under the unitary time evolution of the system. These obey $\left[\hat{H}, \hat{\rho}\right] = 0$. For these states to be in equilibrium it is sufficient to set the time derivative in (5.15) to zero. This yields

$$G_{\mathrm{eq}}(\mathbf{k}_1, \mathbf{k}_2) = \exp\left(-k^2 r_c^2 \mathbf{k}_1^2 - \frac{\hbar^2}{4(1+k)^2 r_c^2}\mathbf{k}_2^2\right) G_{eq}\left(\mathbf{k}_1, \frac{1-k}{1+k}\mathbf{k}_2\right) \ . \tag{5.17}$$

For better overview, we introduce rescaled parameters

$$\mathbf{s}_1 := k r_c \mathbf{k}_1 \ , \tag{5.18}$$

$$\mathbf{s}_2 := \frac{\hbar}{2(1+k) r_c}\mathbf{k}_2 \ , \tag{5.19}$$

$$\zeta := \frac{1-k}{1+k} \ , \tag{5.20}$$

and define

$$F(\mathbf{s}_1, \mathbf{s}_2) := G_{\mathrm{eq}}\left(\frac{\mathbf{s}_1}{k r_c}, \frac{2(1+k) r_c}{\hbar}\mathbf{s}_2\right) \ . \tag{5.21}$$

With this rescalings the condition (5.17) becomes

$$F(\mathbf{s}_1, \mathbf{s}_2) = \mathrm{e}^{-\left(\mathbf{s}_1^2 + \mathbf{s}_2^2\right)} \ F(\mathbf{s}_1, \zeta \mathbf{s}_2) \ . \tag{5.22}$$

Note that for the typical choice of $k \in (0, 1)$ we also have $\zeta \in (0, 1)$. We can now use this expression to argue, why the equilibrium state can not exactly be a Gibbs state with respect to the particle Hamiltonian of the form

$$\hat{\rho}_{\mathrm{eq}} = \frac{1}{Z} e^{-\beta \hat{H}} \quad : \tag{5.23}$$

Since $\left[\hat{\rho}_{\mathrm{eq}}, \hat{H}\right] = 0$, the free time evolution vanishes on its own and we can focus on the dissipative CSL part and G_{eq} fulfills equation (5.17) (and F the analogous one). By applying the above identity (5.22) n times recursively, we find that F must fulfill

$$|F(\mathbf{s}_1, \zeta^n \mathbf{s}_2)| = \exp\left(n\mathbf{s}_1^2 + \sum_{k=0}^{n-1} \zeta^{2k} \mathbf{s}_2^2\right) |F(\mathbf{s}_1, \mathbf{s}_2)| \tag{5.24}$$

$$\geq \big(\underbrace{\mathrm{e}^{\mathbf{s}_1^2}}_{>1}\big)^n \ |F(\mathbf{s}_1, \mathbf{s}_2)| \ . \tag{5.25}$$

This implies that, even though the sequence of ζ powers converges to zero, the absolute function value grows exponentially with n, unless $\mathbf{s}_1 = 0$. As a consequence we conclude that if $F \neq 0$ at any point which is not of the form $(\mathbf{s}_1, 0)$ or $(0, \mathbf{s}_2)$) then F is already unbounded since the right hand side in equation (5.25) increases infinitely. However, a bounded function fulfilling $F(\mathbf{s}_1, \mathbf{s}_2) = 0$ unless $\mathbf{s}_1 = 0$ or $\mathbf{s}_2 = 0$ is zero almost everywhere with respect to the six dimensional Lebesgue measure. Hence, this leads to a contradiction since the corresponding Wigner function was zero as well. We therefore conclude that F and with that G_{eq} are highly singular at the coordinate axes. This singularity leads to infinite statistical moments when applying i.e. equation (1.49) Therefore typical Gibbs states can not be in equilibrium under dissipative CSL. That this does not hold true if one allows for idealized states with a distributional characteristic function is illustrated in the next subsection.

5.3. The special case of a free particle

In the last subsection we concluded that proper Gibbs states can not be the equilibrium state under dissipative CSL. We will now show that the improper (i.e. non-normalizable) Gibbs state of a free particle leads to G becoming a distribution. This generalized G will fulfill the condition (5.17).

Characteristic function of a free particle The free particle Hamiltonian is

$$\hat{H} = \frac{\hat{\mathbf{p}}^2}{2m} \ , \tag{5.26}$$

which immediately implies that the partition function Z of the corresponding Gibbs state diverges,

$$Z = \mathrm{Tr}\left(e^{-\beta\hat{H}}\right) = \int_{\mathbb{R}^3} \mathrm{d}\lambda^3(\mathbf{p}) \, \langle \mathbf{p}| \, e^{-\beta\hat{H}} \, |\mathbf{p}\rangle = \int_{\mathbb{R}^3} \mathrm{d}\lambda^3(\mathbf{p}) \mathrm{e}^{-\beta\mathbf{p}^2/(2m)} \delta^{(3)}(0) = \infty \ . \tag{5.27}$$

We can circumvent this normalization problem by confining the particle to a box of volume V. As explained in detail in appendix C.1 we obtain for asymptotically big V

$$Z = \frac{V}{\lambda_{\mathrm{th}}^3} \ , \tag{5.28}$$

where λ_{th} is the thermal wavelength

$$\lambda_{\mathrm{th}} := \hbar\sqrt{\frac{mk_BT}{2\pi}} \ . \tag{5.29}$$

This yields the Gibbs-state

$$\hat{\rho}_{\mathrm{th}} = \frac{\lambda_{th}^3}{V} \mathrm{e}^{-\beta\hat{\mathbf{p}}^2/(2m)} \tag{5.30}$$

for which we can now derive the characteristic function

$$\begin{aligned}
G_{\mathrm{th}}(\mathbf{k}_1, \mathbf{k}_2) &= \mathrm{Tr}\left(\mathrm{e}^{i(\mathbf{k}_1\cdot\hat{\mathbf{x}} + \mathbf{k}_2\cdot\hat{\mathbf{p}})} \ \hat{\rho}_{th}\right) && (5.31)\\
&= \mathrm{e}^{i\hbar\frac{\mathbf{k}_1\cdot\mathbf{k}_2}{2}} \frac{\lambda_{th}^3}{V} \int_{\mathbb{R}^3} \mathrm{d}\lambda^3(\mathbf{p}) \, \langle \mathbf{p}| \, \mathrm{e}^{i\mathbf{k}_1\cdot\hat{\mathbf{x}}} \mathrm{e}^{i\mathbf{k}_2\cdot\hat{\mathbf{p}}} \mathrm{e}^{-\beta\hat{\mathbf{p}}^2/(2m)} \, |\mathbf{p}\rangle && (5.32)\\
&= \mathrm{e}^{-i\hbar\frac{\mathbf{k}_1\cdot\mathbf{k}_2}{2}} \frac{\lambda_{th}^3}{V} \int_{\mathbb{R}^3} \mathrm{d}\lambda^3(\mathbf{p}) \ \mathrm{e}^{i\mathbf{k}_2\cdot\mathbf{p}} \ \mathrm{e}^{-\beta\mathbf{p}^2/(2m)} \, \langle \mathbf{p} - \hbar\mathbf{k}_1 | \mathbf{p}\rangle && (5.33)\\
&= \delta^{(3)}(\hbar\mathbf{k}_1) \frac{\lambda_{th}^3}{V} \int_{\mathbb{R}^3} \mathrm{d}\lambda^3(\mathbf{p}) \ \mathrm{e}^{i\mathbf{k}_2\cdot\mathbf{p}} \ \mathrm{e}^{-\beta\mathbf{p}^2/(2m)} && (5.34)\\
&= \delta^{(3)}(\hbar\mathbf{k}_1) \frac{\lambda_{th}^3}{V} (2\pi\hbar)^3 \lambda_{th}^3 \mathrm{e}^{-m\mathbf{k}_2^2/(2\beta)} && (5.35)\\
&= \frac{(2\pi)^3}{V} \delta^{(3)}(\mathbf{k}_1) \exp\left(-\frac{m}{2\beta}\mathbf{k}_2^2\right) \ , && (5.36)
\end{aligned}$$

where we used the Baker-Campbell-Hausdorf formula, applied the kick operator and identified the delta function $\langle \mathbf{p} - \hbar\mathbf{k}_1 | \mathbf{p} \rangle$. Finally we evaluated the integral as shown in appendix A.4.

Equilibrium condition We can now insert the Gibbs characteristic function(5.31) into the equilibrium condition (5.17) of the dissipative CSL model and find

$$G_{\text{th}}\left(\mathbf{k}_1, \frac{1-k}{1+k}\mathbf{k}_2\right) = \frac{(2\pi)^3}{V}\delta^{(3)}(\mathbf{k}_1)\exp\left(-\frac{m}{2\beta}\left(\frac{1-k}{1+k}\mathbf{k}_2\right)^2\right) \tag{5.37}$$

$$= \frac{(2\pi)^3}{V}\delta^{(3)}(\mathbf{k}_1)\exp\left(-\frac{m}{2\beta}\left(1 - \frac{4k}{(1+k)^2}\right)\mathbf{k}_2^2\right) \tag{5.38}$$

$$= \exp\left(\frac{m}{\beta}\frac{2k}{(1+k)^2}\mathbf{k}_2^2\right) G_{\text{th}}\left(\mathbf{k}_1, \mathbf{k}_2\right) \tag{5.39}$$

$$= \exp\left(k^2 r_c^2 \mathbf{k}_1^2 + \frac{m}{\beta}\frac{2k}{(1+k)^2}\mathbf{k}_2^2\right) G_{\text{th}}\left(\mathbf{k}_1, \mathbf{k}_2\right) \ . \tag{5.40}$$

This equality is fulfilled when the the inverse temperature β obeys

$$\frac{m}{\beta}\frac{2k}{(1+k)^2} \stackrel{!}{=} \frac{\hbar^2}{4(1+k)^2 r_c^2} \tag{5.41}$$

which proves that the equilibrium state of a free particle under dCSL is a Gibbs state of temperature

$$T = \frac{\hbar^2}{8k_B m k r_c^2} \ . \tag{5.42}$$

This is exactly the temperature given in [3] and calculated in subsection 2.3.

Note that, for the Gibbs state to fulfill the equilibrium condition, it is crucial that the characteristic function is zero for any $\mathbf{k}_1 \neq 0$. This rather pathological feature of the improper free particle Gibbs state ensures the agreement here, which no longer holds if the particle is subject to a potential that confines it spatially. We shall discuss the simplest exemplary case, a harmonic potential, in the next section.

6. Equilibration of a harmonic oscillator

We found in section 5 that, in general, the dCSL model does not thermalize the motional quantum state of a single particle to a Gibbs state. The only known exception is a free unconfined particle, which has a Gibbs state with a distribution-valued characteristic function. This shows that the dCSL model does not generally describe a thermalization process. Nevertheless, it can limit the amount of collapse-induced heating and lead to non-thermal equilibrium states of finite energy. Here we study the exemplary case of a harmonically bound particle in one dimension subject to dCSL. We numerically compute the equilibrium state under dCSL and identify the parameter regime in which is approximates a Gibbs state. We integrate the closed of equations of motion for the first and second moments of position and momentum, which allows us to identify the conditions under which equilibration to a finite energy occurs.

6.1. Dissipative CSL in the one-dimensional case

The correct one dimensional version of the dissipative CSL model will be derived in this subsection. To obtain a one dimensional equation of motion we trace out two dimensions of the equation

$$\frac{\mathrm{d}}{\mathrm{d}t}\hat{\rho} = -\frac{i}{\hbar}\left[\hat{H},\hat{\rho}\right] + \Gamma\left(\Lambda(\hat{\rho}) - \hat{\rho}\right) \tag{6.1}$$

On the left hand side we obtain

$$\mathrm{Tr}_{2,3}\left(\frac{\mathrm{d}}{\mathrm{d}t}\hat{\rho}\right) = \frac{\mathrm{d}}{\mathrm{d}t}\mathrm{Tr}_{2,3}\left(\hat{\rho}\right) = \frac{\mathrm{d}}{\mathrm{d}t}\hat{\rho}^{(1)} \ , \tag{6.2}$$

where we introduced $\hat{\rho}^{(1)} := \mathrm{Tr}_{2,3}\left(\hat{\rho}\right)$.

Coherent time evolution For completeness we start with the coherent time evolution on the right hand side: We assume the Hamiltonian is of the form

$$\hat{H} = \underbrace{\frac{\hat{p}_1^2}{2m} + \frac{1}{2}m\omega\hat{x}_1^2}_{\hat{H}_1} + \hat{H}_2 + \hat{H}_3 \ , \tag{6.3}$$

where our assumption is that each $\hat{H}_j$ only acts on the Hilbert space of the corresponding spatial direction. For every direction we choose a basis of energy eigenstates $\left(|n_j\rangle\right)_n$ fulfilling

$$\hat{H}_j\,|n_j\rangle = E_{j,n_j}\,|n_j\rangle \ . \tag{6.4}$$

Now we trace out in exactly this basis

$$\mathrm{Tr}_{2,3}\left(\left[\hat{H},\hat{\rho}\right]\right) \tag{6.5}$$

$$=\sum_{j=1}^{3}\mathrm{Tr}_{2,3}\left(\left[\hat{H}_j,\hat{\rho}\right]\right)=\sum_{j=1}^{3}\sum_{n_2,n_3\in\mathbb{N}}\langle n_2,n_3|\left[\hat{H}_j,\hat{\rho}\right]|n_2,n_3\rangle \tag{6.6}$$

$$=\left[\hat{H}_1,\sum_{n_2,n_3\in\mathbb{N}}\langle n_2,n_3|\,\hat{\rho}\,|n_2,n_3\rangle\right]+\sum_{j=2}^{3}\sum_{n_2,n_3\in\mathbb{N}}\langle n_2,n_3|\left(\hat{H}_j\hat{\rho}-\hat{\rho}\hat{H}_j\right)|n_2,n_3\rangle \tag{6.7}$$

$$=\left[\hat{H}_1,\hat{\rho}^{(1)}\right]+\sum_{j=2}^{3}\sum_{n_2,n_3\in\mathbb{N}}E_{j,n_j}\left(\underbrace{\mathrm{Tr}_{2,3}(\hat{\rho})-\mathrm{Tr}_{2,3}(\hat{\rho})}_{=0}\right) \tag{6.8}$$

$$=\left[\hat{H}_1,\hat{\rho}^{(1)}\right]\ . \tag{6.9}$$

So in this case the coherent time evolution reduces directly to the one dimensional equation.

Dissipative time evolution In the next step we investigate on the partial trace of $\Lambda(\hat{\rho})$. To keep overview we introduce some notations that will only be used in this derivation. We want to address the second and third components in particular. Therefore we set

$$\mathbf{v}_\perp := (v_2,v_3) \tag{6.10}$$

for any vector to project on the second and third component. We also define one dimensional Lindblad operators analogous to equation (4.59) as

$$\hat{L}_{\mathrm{st}}(q_j):=\left(2\pi p_c^2\right)^{-1/4}\mathrm{e}^{-i\frac{\alpha}{\hbar}q_j\hat{x}_j}\mathrm{e}^{-\frac{\left(\hat{p}_j-q_j\right)^2}{4p_c^2}} \tag{6.11}$$

such that $\hat{L}_{\mathrm{st}}(\mathbf{q})=\hat{L}_{\mathrm{st}}(q_1)\hat{L}_{\mathrm{st}}(q_2)\hat{L}_{\mathrm{st}}(q_3)=\hat{L}_{\mathrm{st}}(q_1)\hat{L}_{\mathrm{st}}(\mathbf{q}_\perp)$. With this we can write

$$\mathrm{Tr}\left(\Lambda(\hat{\rho})\right) \tag{6.12}$$

$$=\int_{\mathbb{R}^2}\mathrm{d}\lambda(\mathbf{Q}_\perp)\,\langle\mathbf{Q}_\perp|\,\Lambda(\hat{\rho})\,|\mathbf{Q}_\perp\rangle \tag{6.13}$$

$$=\int_{\mathbb{R}}\mathrm{d}q_1\hat{L}_{\mathrm{st}}(q_1)\underbrace{\left[\int_{\mathbb{R}^4}\mathrm{d}\lambda(\mathbf{q}_\perp,\mathbf{Q}_\perp)\,\langle\mathbf{Q}_\perp|\,\hat{L}_{\mathrm{st}}(\mathbf{q}_\perp)\hat{\rho}\hat{L}_{\mathrm{st}}^\dagger(\mathbf{q}_\perp)\,|\mathbf{Q}_\perp\rangle\right]}_{=:\hat{I}_{\mathrm{red}}}\hat{L}_{\mathrm{st}}^\dagger(q_1)\ . \tag{6.14}$$

Investigating $\hat{I}_{\mathrm{red}}$, we write out the Lindblad operators and apply the kicks to the momentum eigenstates

$$\hat{I}_{\mathrm{red}} = \int_{\mathbb{R}^4} \frac{\mathrm{d}\lambda(\mathbf{q}_\perp, \mathbf{Q}_\perp)}{(2\pi p_c^2)} \langle \mathbf{Q}_\perp + \alpha\mathbf{q}_\perp | \, \mathrm{e}^{-\frac{(\hat{\mathbf{p}}_\perp - \mathbf{q}_\perp)^2}{4p_c^2}} \hat{\rho} \mathrm{e}^{-\frac{(\hat{\mathbf{p}}_\perp - \mathbf{q}_\perp)^2}{4p_c^2}} | \mathbf{Q}_\perp + \alpha\mathbf{q}_\perp \rangle \tag{6.15}$$

$$= \int_{\mathbb{R}^4} \frac{\mathrm{d}\lambda(\mathbf{q}_\perp, \mathbf{Q}_\perp)}{(2\pi p_c^2)} \, \mathrm{e}^{-\frac{(\mathbf{Q}_\perp + \alpha\mathbf{q}_\perp - \mathbf{q}_\perp)}{2p_c^2}} \langle \mathbf{Q}_\perp + \alpha\mathbf{q}_\perp | \, \hat{\rho} \, | \mathbf{Q}_\perp + \alpha\mathbf{q}_\perp \rangle \tag{6.16}$$

$$= \int_{\mathbb{R}^2} \mathrm{d}\lambda^2(\mathbf{P}_\perp) \langle \mathbf{P}_\perp | \, \hat{\rho} \, | \mathbf{P}_\perp \rangle \underbrace{\int_{\mathbb{R}^2} \frac{\mathrm{d}\lambda^2(\mathbf{p}_\perp)}{(2\pi p_c^2)^{2/2}} \mathrm{e}^{-\frac{(\mathbf{P}_\perp - \mathbf{p}_\perp)^2}{2p_c^2}}}_{=1} \tag{6.17}$$

$$= \mathrm{Tr}\,(\hat{\rho}) = \hat{\rho}^{(1)} \, . \tag{6.18}$$

Combining the results for the reduced coherent (6.9) and incoherent (6.14) dynamics yields the equation of motion as

$$\frac{\mathrm{d}}{\mathrm{d}t}\hat{\rho}^{(1)} = -\frac{i}{\hbar}\left[\hat{H}_1, \hat{\rho}^{(1)}\right] + \Gamma \int_{\mathbb{R}} \mathrm{d}q_1 \, \left(\hat{L}_{\mathrm{st}}(q_1)\hat{\rho}^{(1)}\hat{L}_{\mathrm{st}}^\dagger(q_1) - \hat{\rho}^{(1)}\right) \, . \tag{6.19}$$

Hence, the time evolution for the reduced states associated to the three spatial directions decouple, and it suffices to investigate the one dimensional case. This is especially helpful for practical case studies, in which the quantum state of a particle is only ever observed along a fixed direction of motion. The other directions need not to be taken into account.

In the remainder of this section, we will operate with the reduced one-dimensional dCSL model, expressed in terms of the quadrature operators $\hat{x}$, $\hat{p}$ along a fixed direction.

6.2. Formulation in natural units

We will now set reasonable scales for the physical quantities in order to make them dimensionless. This is convenient for two reasons: On the one hand it helps to simplify equations and to identify the important quantities. On the other hand computers do not know units and therefore this step has to be done anyway for later numerical calculations. Since our main goal is to investigate on a harmonic oscillator, we start our natural formulation with this Hamiltonian

$$\hat{H} = \frac{\hat{p}^2}{2m} + \frac{1}{2}m\omega^2\hat{x}^2 \ . \tag{6.20}$$

We define the relevant scales x_0 for position, p_0 for momentum and E_0 for energy by the expectation values in the ground state $|0\rangle$

$$\langle 0|\,\hat{x}^2\,|0\rangle = \frac{\hbar}{2m\omega} =: \frac{x_0^2}{2} \ , \quad \langle 0|\,\hat{p}^2\,|0\rangle = \frac{m\hbar\omega}{2} =: \frac{p_0^2}{2} \ , \quad \langle 0|\,\hat{H}\,|0\rangle = \frac{\hbar\omega}{2} =: \frac{\hbar\omega}{2} \ . \tag{6.21}$$

For this section we will denote scales by a lower case zero e.g. t_0 as a time scale. The dimensionless properties are marked with a lower case N e.g. $t_\mathrm{N} := t/t_\mathrm{N}$. Expressed with this scales, the hamiltonian (6.20) becomes

$$\hat{H} = \hbar\omega\frac{1}{2}\left(\hat{p}_\mathrm{N}^2 + \hat{x}_\mathrm{N}^2\right) = \hbar\omega\hat{H}_\mathrm{N} \ . \tag{6.22}$$

Note that $x_0 p_0 = \hbar$ and therefore $[\hat{x}_\mathrm{N}, \hat{p}_\mathrm{N}] = i\mathbb{1}$. In the next step we express the exponentials of the one-dimensional Lindblad operator (6.11) with the scales and after a substitution we find

$$\Lambda_{\mathrm{st,N}}\left(\hat{\rho}\right) = \int_{\mathbb{R}} \mathrm{d}q_\mathrm{N} \ \hat{L}_{\mathrm{st,N}}(q_\mathrm{N})\hat{\rho}\hat{L}_{\mathrm{st,N}}^\dagger(q_\mathrm{N}) \tag{6.23}$$

with

$$\hat{L}_{\mathrm{st,N}}(q_\mathrm{N}) := \left(2\pi p_{\mathrm{cN}}^2\right)^{(-1/4)} e^{-i\alpha q_\mathrm{N}\hat{x}_\mathrm{N}} \ \mathrm{e}^{-(\hat{p}_\mathrm{N}-q_\mathrm{N})^2/\left(4p_{\mathrm{cN}}^2\right)} \tag{6.24}$$

Finally, we consider the whole time evolution to find our time scale

$$\frac{\mathrm{d}}{\mathrm{d}t}\hat{\rho} = -\frac{i}{\hbar}\left[\hbar\omega\hat{H}_\mathrm{N}, \hat{\rho}\right] + \Gamma\left(\Lambda_{\mathrm{st,N}} - \hat{\rho}\right) = \omega\left(-i\left[\hat{H}_\mathrm{N}, \hat{\rho}\right] + \frac{\Gamma}{\omega}\left(\Lambda_{\mathrm{st,N}} - \hat{\rho}\right)\right) \ . \tag{6.25}$$

We set $t_0 := 1/\omega$ or respectively $t_\mathrm{N} = \omega t$ and $\Gamma_\mathrm{N} = \Gamma/\omega$. Finally, we arrive at the completely dimensionless master equation

$$\frac{\mathrm{d}}{\mathrm{d}t_\mathrm{N}}\hat{\rho} = -i\left[\hat{H}_\mathrm{N}, \hat{\rho}\right] + \Gamma_\mathrm{N}\left(\Lambda_{\mathrm{st,N}}\left(\hat{\rho}\right) - \hat{\rho}\right) \tag{6.26}$$

that can be conveniently analyzed and simulated numerically. For convenience, we will drop the the index N if ambiguity is excluded.

6.3. Dynamics under Stokes friction: A numerical study

Complementing the analytical results that will be discussed in 6.5, we go through an exemplary numerical calculation. We investigate the harmonic motion of a single particle under the influence of Stokes friction. The details of the numerical computation are described in appendix E.

Our numerical simulation, carried out in the Fock basis, can only account for a finite Hilbert space dimension. To estimate the impact of this approximation, we track the occupation number of the highest Fock state $\langle N_{\text{Points}}| \hat{\rho}_t |N_{\text{Points}}\rangle$. The numerical cut-off should not affect the results as long as that number remains negligible.

As the initial state $|\psi_{\text{init}}\rangle$ we use a coherent state with the initial quadratures 2 in position and 3 in momentum. In complex notation this reads

$$|\psi_{\text{init}}\rangle = \left|\frac{2+i3}{\sqrt{2}}\right\rangle \ . \tag{6.27}$$

The system is monitored over a time span of $T = 12$, which is roughly the time of two oscillations of the fictionless oscillator.

Ehrenfest equations of motion In figure 4, we plot the average occupation number of the highest Fock state (as explained above), the position $\langle \hat{x} \rangle$, and the momentum $\langle \hat{p} \rangle$ as a function of time. It can be seen that the highest Fock state has reasonably small occupation such that we can trust the numerical results. The expectation values of position and momentum follow a strongly damped harmonic oscillator. They approach zero fast, making the oscillation almost invisible after less than a period. Figure 5 illustrates the equilibration of the oscillator state in terms of its kinetic, potential, and total energy. We observe that they all converge to a finite equilibrium value within the plotted time window.

Wigner function Using the same parameters as for the statistical moments, we also evaluate the Wigner function. In figures 6, 7, and 8, we see the Wigner function at the initial time point, after roughly one period, and after roughly two periods. We see that after one period the function is already centered around the origin and is smeared along the diagonal. From the figure 7 to 8, the function changes just slightly, from which we conclude that it has almost reached equilibrium. Clearly, this state can not be thermal due to its asymmetric nature.

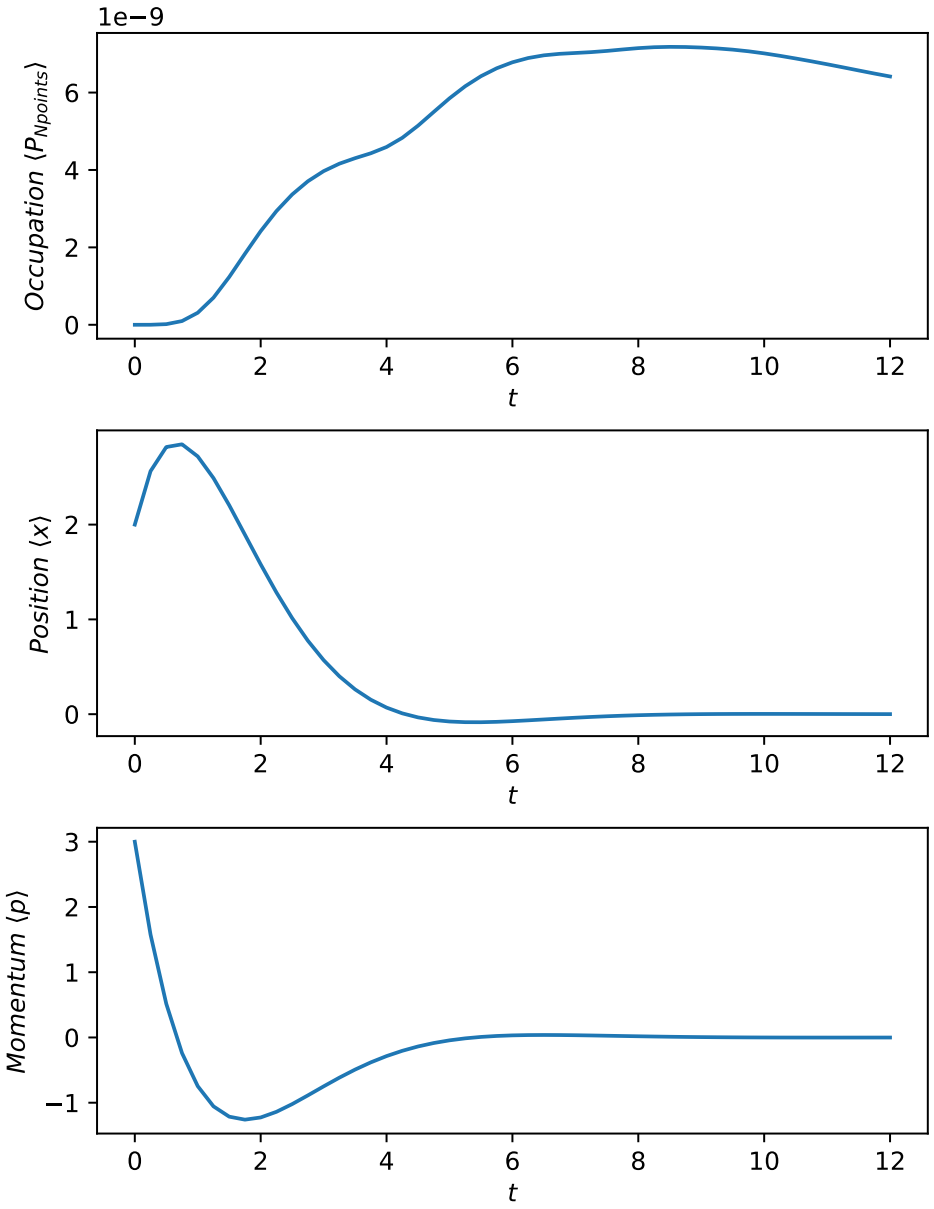

Figure 4: One-dimensional harmonic motion of a single particle under the influence of Stokes friction with parameters $\Gamma = 1.5$, $p_c = 0.5$ and $\alpha = 1$: The occupation number of the highest numerically realized Fock state (as a sanity check), the expectation value of position and the expectation value of momentum are plotted against time.

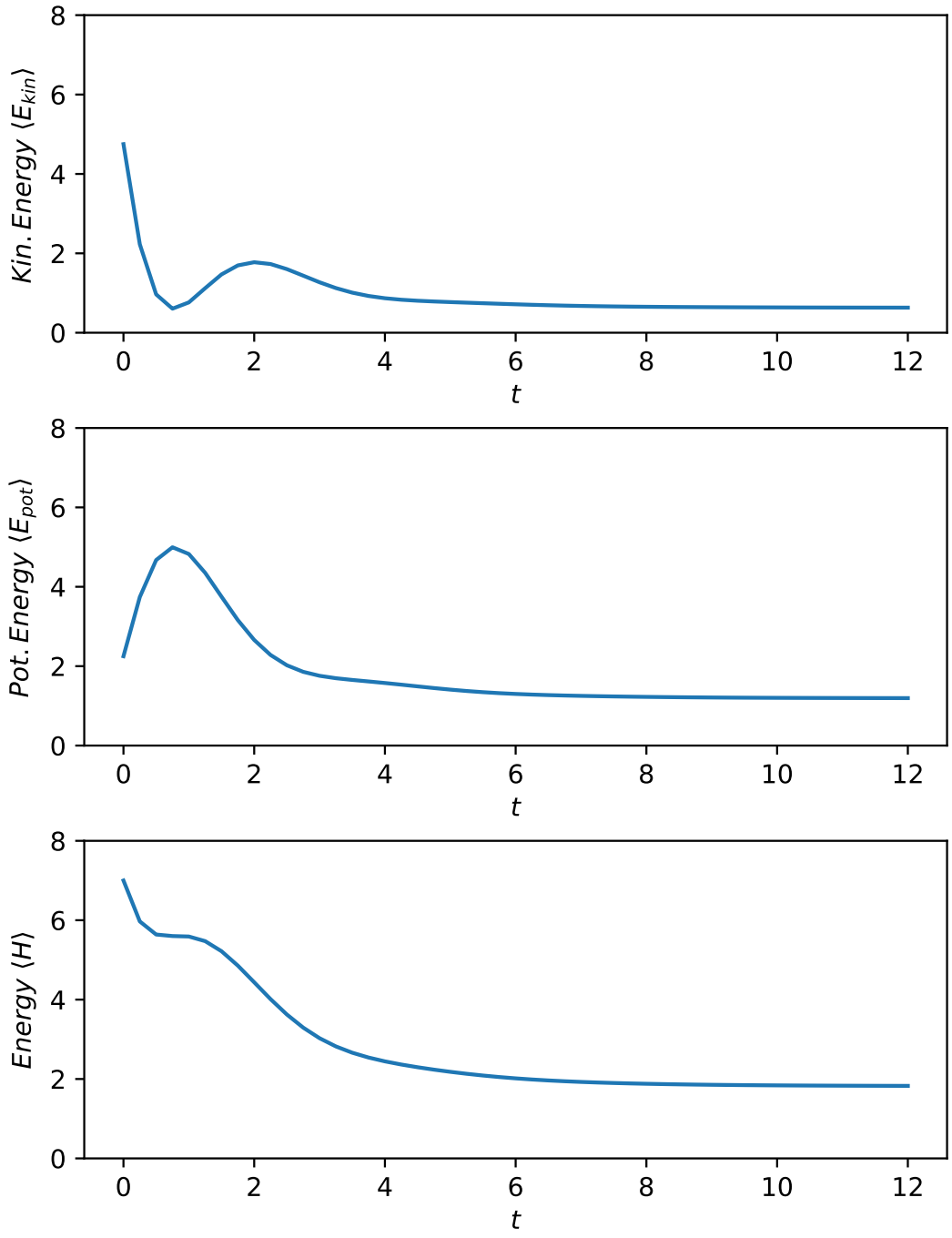

Figure 5: One-dimensional harmonic motion of a single particle under the influence of Stokes friction with the same parameters as in figure 4 : The expected kinetic energy, potential energy and the the total energy are plotted against the time.

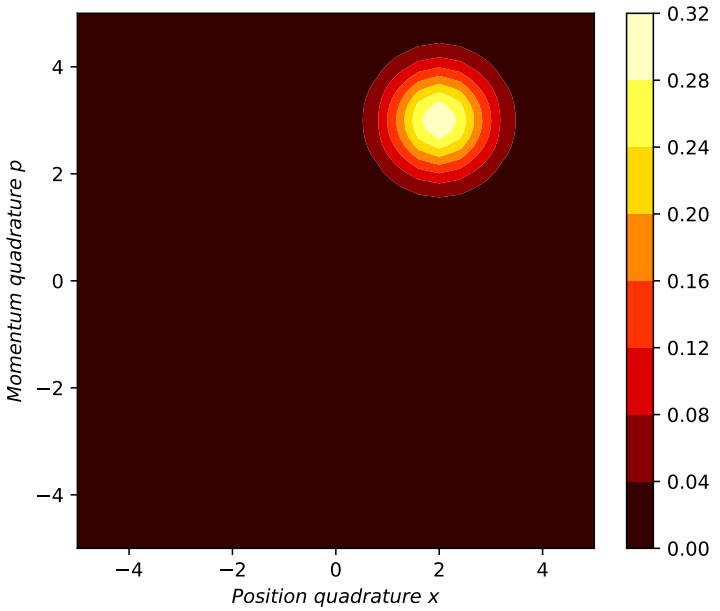

Figure 6: Wigner function of the one-dimensional motion of a single particle under Stokes friction or Coulomb friction at time $t = 0$. Parameters: $\Gamma = 1.5$, $p_c = 0.5$ and $\alpha = 1$

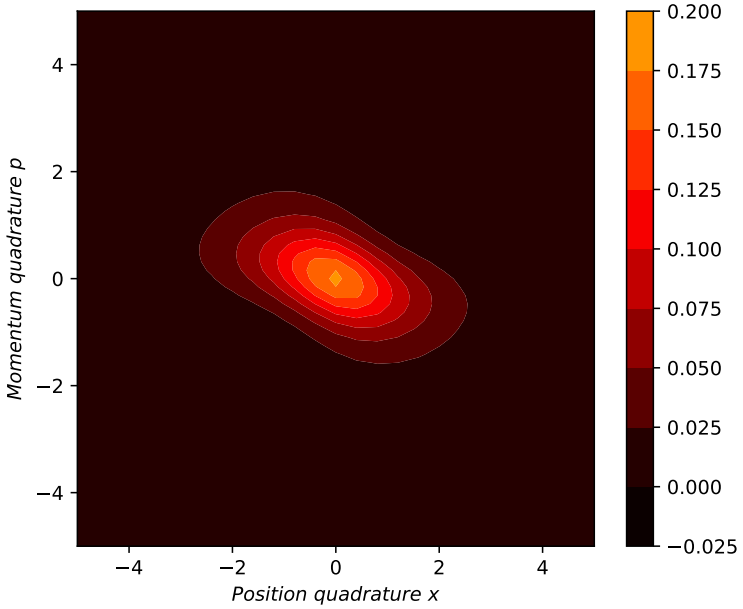

Figure 7: Wigner function of the one-dimensional motion of a single particle under Stokes friction at time $t = 6.25 \approx 2\pi$ (one period). Parameters: Same as figure 6

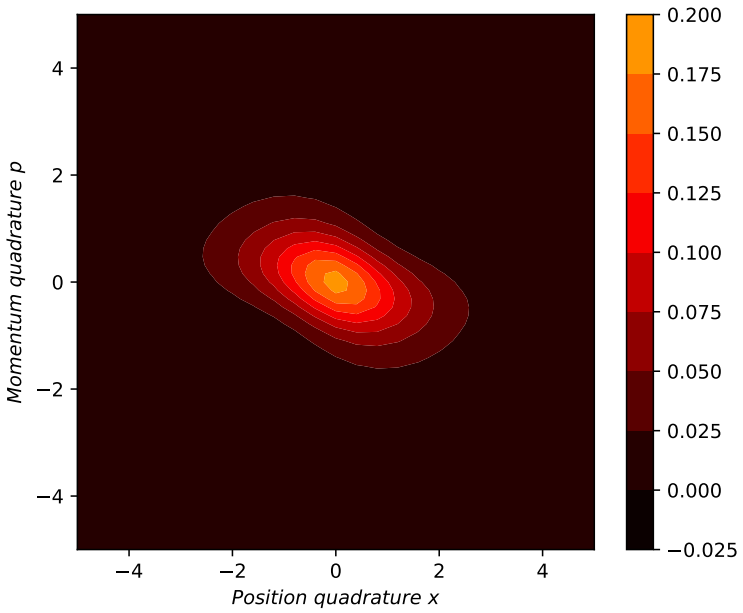

Figure 8: Wigner function of the one-dimensional motion of a single particle under Stokes friction at time $t = 12 \approx 4\pi$ (two periods). Parameters: Same as figure 6

6.4. Dynamics under Coulomb friction: A numerical study

The Coulomb friction model, we presented in subsection 4.4 is analytically not tractable. However, to get more insight into the dynamics we provide the numerical solutions to the statistical moments of the one dimensional harmonic motion of a particle under Coulomb friction. The numerical details are analogous to Stokes friction as described in E. We choose the same initial state $|\psi_{\text{init}}\rangle$ as in the stokes case (6.27).

The simulation is calculated over a time span of $T = 12$, which is roughly the time of two oscillations of the fictionless oscillator.

Ehrenfest equations of motion In figure 9 the time evolution of the occupation number of the highest Fock state (compare subsection 6.3) and the expectation values of position $\hat{x}$ and momentum $\hat{p}$ are given. We see that the occupation number stays reasonably small. Therefore, we trust the results. $\langle \hat{x} \rangle_t$ and $\langle \hat{p} \rangle_t$ look roughly like a damped harmonic oscillator and equilibrate to zero. In figure 10 we have plotted the kinetic energy, the potential energy and their sum, the total energy. All three relax fast to a finite equlibrium value.

Wigner function Finally, we investigate on the time evolution of the Wigner function. To this end, we use the same parameters as for the statistical momets. In figure 6 the initial Wigner function can be seen. In figures 11 and 12 we can see it after roughly one and two periods of the harmonic oscillator without friction. Note that the color

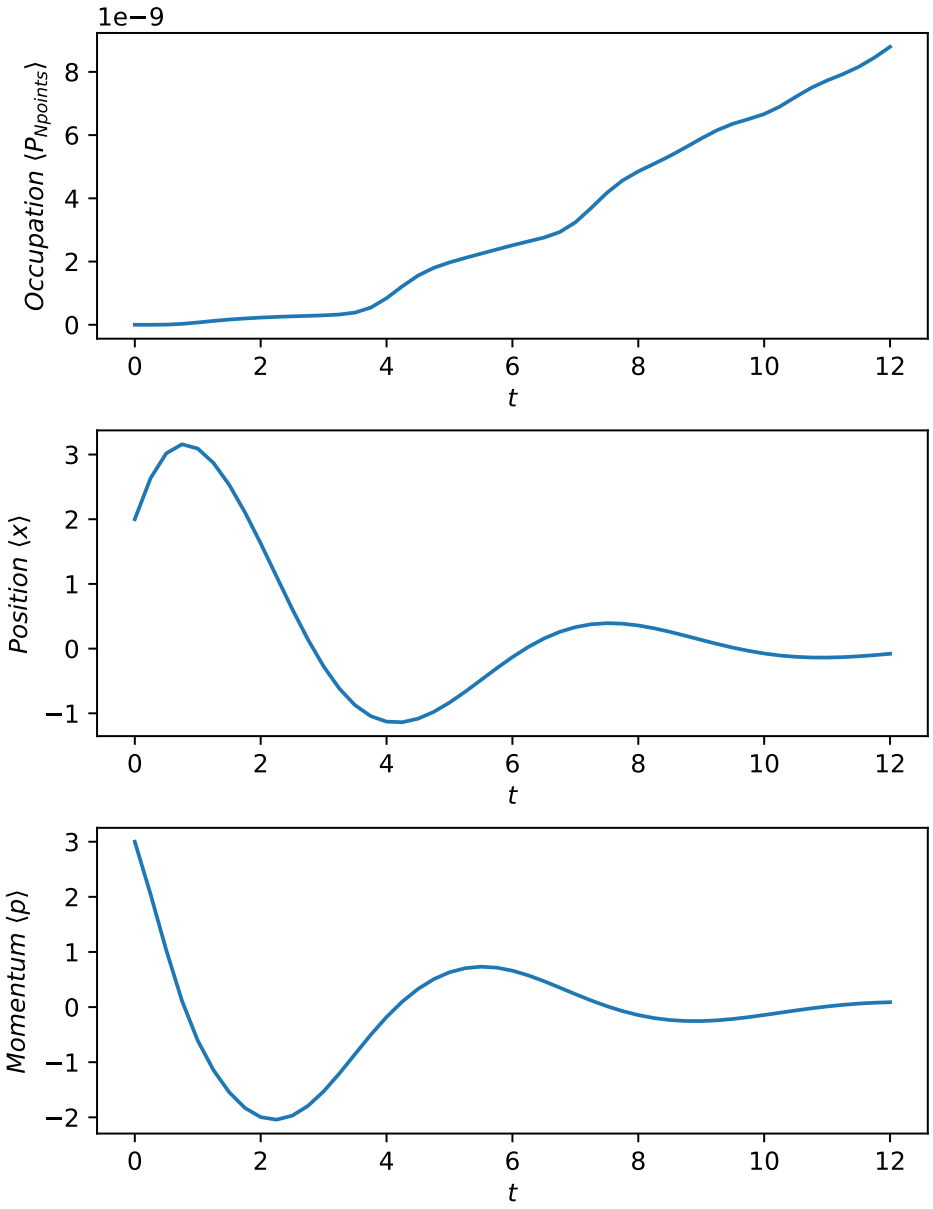

Figure 9: One-dimensional harmonic motion of a single particle under the influence of Coulomb-friction with parameters $\Gamma = 1.5$, $p_c = 0.5$ and $\alpha = 1$: The occupation number of the highest numerically realized Fock state (as a sanity check), the expectation value of position and the expectation value of momentum are plotted against time.

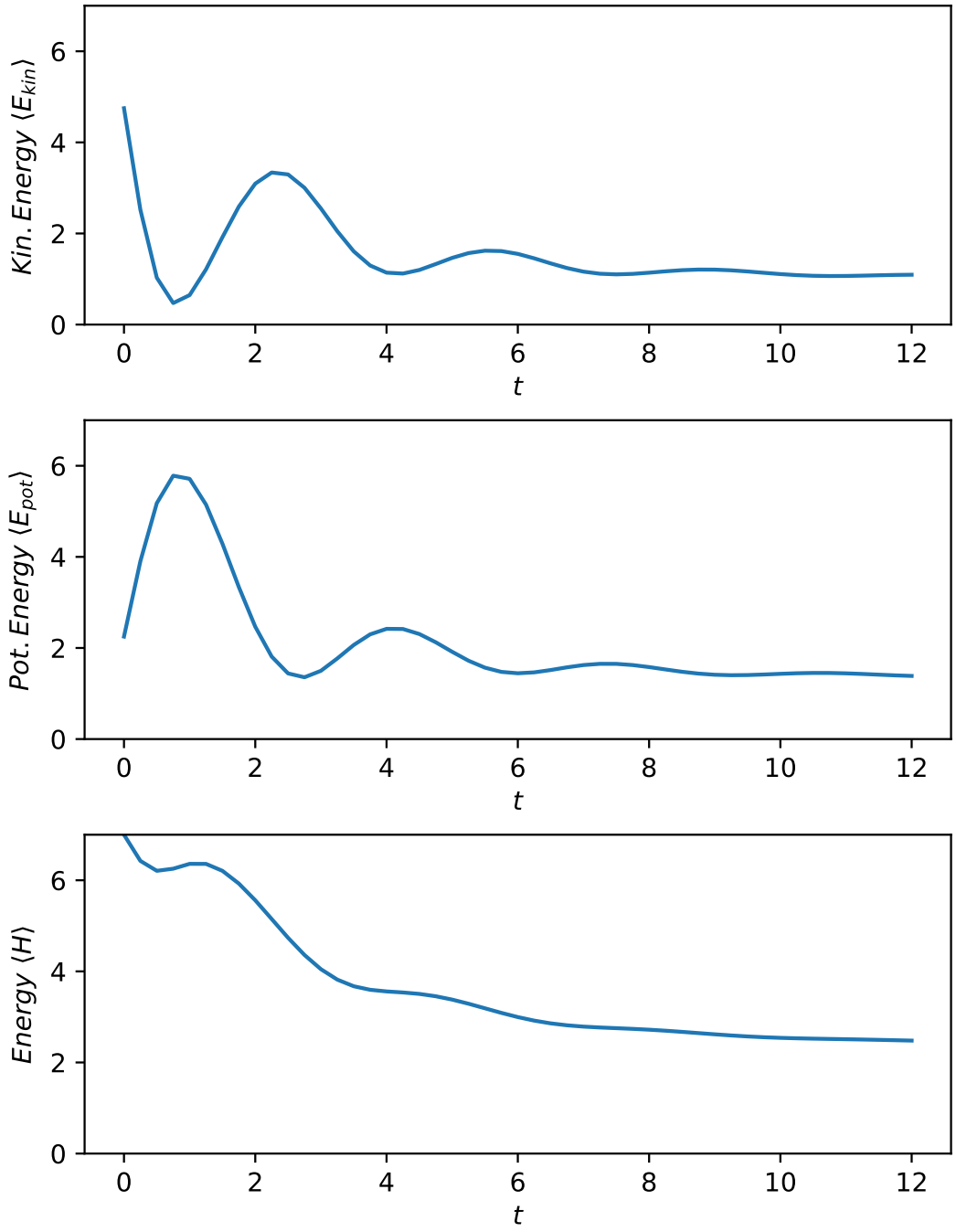

Figure 10: One-dimensional harmonic motion of a single particle under the influence of Coulomb-friction with the same parameters as in figure 9 : The expected kinetic energy, potential energy and the the total energy are plotted against the time.

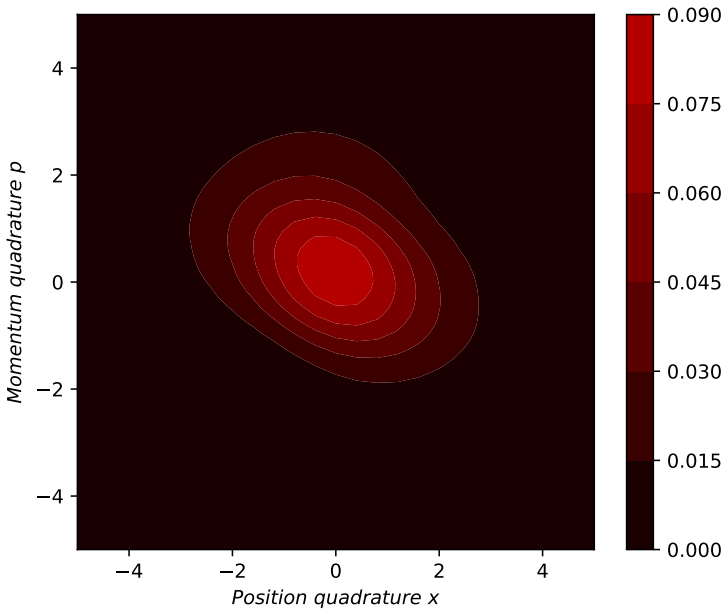

Figure 11: Wigner function of the one-dimensional motion of a single particle under Coulomb friction at time $t = 6.25 \approx 2\pi$ (one period). Parameters: $\Gamma = 1.5$, $p_c = 0.5$ and $\alpha = 1$

scheme in all three pictures is the same. After one period it is already smeared around the origin. It can be seen that the Wigner function spreads out along the diagonal, converging to a non thermal equilibrium state.

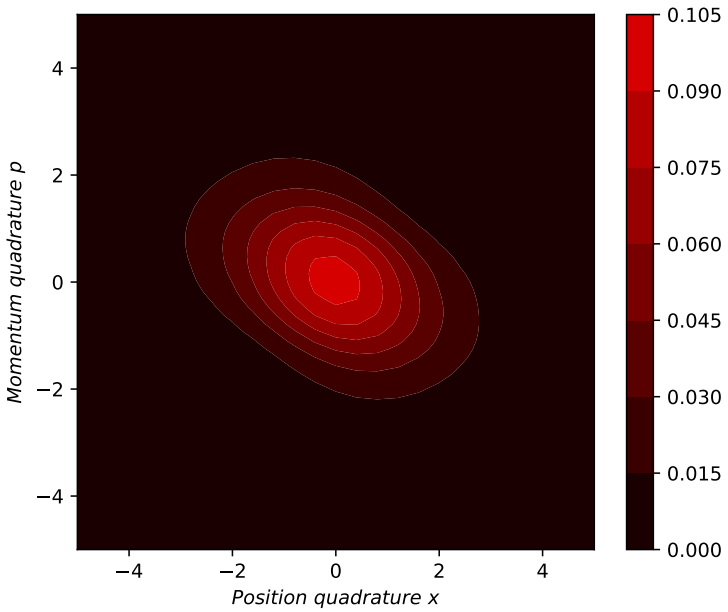

Figure 12: Wigner function of the one-dimensional motion of a single particle under Coulomb friction at time $t = 12 \approx 4\pi$ (two periods). Parameters: Same as in figure 11

6.5. Ehrenfest equations of motion for a harmonic oscillator

After we have set the stage and investigated on numerical solution, we derive the Ehrenfest equations of motion for all moments of first and second order in $\hat{x}$ and $\hat{p}$. This will help us to investigate on the energy in the thermal equilibrium. The time evolution is given by equation (6.26), where we drop all unnecessary indices and shift the bare $\hat{\rho}$ on the other side

$$\left(\frac{\mathrm{d}}{\mathrm{d}t} + \Gamma\right) \hat{\rho}_t = -i \left[\hat{H}, \hat{\rho}_t\right] + \Gamma\Lambda\left(\hat{\rho}_t\right) \ . \tag{6.28}$$

In the following, we focus on the dCSL term from for the expectation values of relevant observables as explained in 1.5,

$$\left(\frac{\mathrm{d}}{\mathrm{d}t} + \Gamma\right) \left\langle \hat{A} \right\rangle_t = -i \left\langle \left[\hat{A}, \hat{H}\right] \right\rangle_t + \Gamma \ \mathrm{Tr}\left(\hat{A} \ \Lambda(\hat{\rho}_t)\right) \ . \tag{6.29}$$

For completeness, the coherent term is calculated in C.2.

First and second moments of position or momentum We could already solve $\mathrm{Tr}\left(\hat{A} \ \Lambda(\hat{\rho}_t)\right)$ for $\hat{x}$ and $\hat{x}^2$ in the general case in subsection 4.2. We know

$$\mathrm{Tr}\left(\hat{x} \ \Lambda(\hat{\rho}_t)\right) = \langle \hat{x} \rangle_t \ . \tag{6.30}$$

For the second moment we need to calculate the Fourier transformed distribution $\mathcal{Q}$ which can be done by using a formula from appendix A.4. The dimensionless version is then

$$\mathcal{Q}(X) = \left(2\pi \ \left(\frac{1}{2p_c^2}\right)^2\right)^{(-1/2)} \mathrm{e}^{-\frac{1}{2}(2p_c)^2\mathbf{X}^2} \tag{6.31}$$

From which we can get the variance by comparison as

$$\mathbb{E}_{\mathcal{Q}(\mathbf{X})}\left((\mathbf{X})^2\right) = \mathbb{V}_{\mathcal{Q}(\mathbf{X})}\left(\mathbf{X}\right) = \frac{1}{4p_c^2} \tag{6.32}$$

and by that

$$\mathrm{Tr}\left(\hat{x}^2\Lambda(\hat{\rho}_t)\right) = \langle\hat{x}^2\rangle + \frac{1}{4p_c^2} \ . \tag{6.33}$$

The time evolution of $\langle\hat{p}\rangle_t$ was already calculated in subsection 4.3, we found

$$\mathrm{Tr}\left(\hat{p}\Lambda(\hat{\rho}_t)\right) = (1-\alpha)\left\langle\hat{p}\right\rangle_t \ . \tag{6.34}$$

The transformation for the second moment in $\hat{p}$ was already calculated in equation 2.51. We just need to translate the constants and need to consider that we are now in one instead of three dimensions

$$\mathrm{Tr}\left(\hat{p}^2 \ \Lambda(\hat{\rho})\right) = (1-\alpha)^2\left\langle\hat{p}^2\right\rangle + \alpha^2 p_c^2 \ . \tag{6.35}$$

The anti-commutator In order to obtain a closed set of equations of motion, we need to also consider the anti-commutator of $\hat{x}$ and $\hat{p}$, which has to be calculated from scratch. To this end, we shall make use of the following two identities:

$$\mathrm{e}^{i\alpha q\hat{x}}\left\{\hat{x},\hat{p}\right\}\mathrm{e}^{-i\alpha q\hat{x}} = \left\{\hat{x},\mathrm{e}^{i\alpha q\hat{x}}\hat{p}\mathrm{e}^{-i\alpha q\hat{x}}\right\} = \left\{\hat{x},\hat{p}-\alpha q\right\} = \left\{\hat{x},\hat{p}\right\} - 2\alpha q\hat{x} \ . \tag{6.36}$$

Next we need the commutator

$$\left[\hat{x},\sqrt{\mathcal{P}(\hat{p}-q)}\right] = (2\pi p_c^2)^{-1/2}\left[\hat{x},\mathrm{e}^{-\frac{(\hat{p}-q)^2}{4p_c^2}}\right] = i(2\pi p_c^2)^{-1/2}\frac{\mathrm{d}}{\mathrm{d}\hat{p}}\mathrm{e}^{-\frac{(\hat{p}-q)^2}{4p_c^2}} \tag{6.37}$$

$$= -\frac{i}{2p_c^2}(\hat{p}-q)\sqrt{\mathcal{P}(\hat{p}-q)} \ , \tag{6.38}$$

where we used equation (A.3). With this we can now tackle the equation

$$\begin{aligned}
&\mathrm{Tr}\left(\{\hat{x},\hat{p}\}\,\Lambda(\hat{\rho})\right) && (6.39)\\
&= \int_{\mathbb{R}} \mathrm{d}q\ \mathrm{Tr}\left(\{\hat{x},\hat{p}\}\,\hat{L}(q)\hat{\rho}\hat{L}^{\dagger}(q)\right) && (6.40)\\
&= \int_{\mathbb{R}} \mathrm{d}q\ \mathrm{Tr}\left(\sqrt{\mathcal{P}(\hat{p}-q)}\mathrm{e}^{i\alpha q\hat{x}}\,\{\hat{x},\hat{p}\}\,\mathrm{e}^{-i\alpha q\hat{x}}\sqrt{\mathcal{P}(\hat{p}-q)}\hat{\rho}\right) && (6.41)\\
&= \int_{\mathbb{R}} \mathrm{d}q\ \mathrm{Tr}\left(\sqrt{\mathcal{P}(\hat{p}-q)}\,\{\hat{x},\hat{p}-\alpha q\}\,\sqrt{\mathcal{P}(\hat{p}-q)}\hat{\rho}\right) && (6.42)\\
&= \underbrace{\mathrm{Tr}\left(\{\hat{x},\hat{p}\}\int_{\mathbb{R}}\mathrm{d}q\sqrt{\mathcal{P}(\hat{p}-q)}\hat{\rho}\sqrt{\mathcal{P}(\hat{p}-q)}\right)}_{=:\hat{I}} && (6.43)\\
&\quad - 2\alpha\underbrace{\int_{\mathbb{R}}\mathrm{d}q\ q\ \mathrm{Tr}\left(\sqrt{\mathcal{P}(\hat{p}-q)}\ \hat{x}\ \sqrt{\mathcal{P}(\hat{p}-q)}\hat{\rho}\right)}_{=:\hat{\Pi}}\ . && (6.44)
\end{aligned}$$

The first term in this expression can be solved by using the Fourier-transformed probability distribution $\mathcal{Q}$, as it is shown in equation (4.10). We get

$$\begin{aligned}
\hat{I} &= \int_{\mathbb{R}}\mathrm{d}X\ \mathcal{Q}(X)\mathrm{Tr}\left(\mathrm{e}^{-iX\hat{p}}\,\{\hat{x},\hat{p}\}\,\mathrm{e}^{iX\hat{p}}\hat{\rho}\right) && (6.45)\\
&= \int_{\mathbb{R}}\mathrm{d}X\ \mathcal{Q}(X)\mathrm{Tr}\left(\{\hat{x}-X,\hat{p}\}\,\hat{\rho}\right) = \langle\{\hat{x},\hat{p}\}\rangle\,, && (6.46)
\end{aligned}$$

where we used the fact that $\mathcal{Q}$ has zero mean. Using the commutator (6.38) from above, the second expression yields

$$\begin{aligned}
\hat{\Pi} &= \int_{\mathbb{R}}\mathrm{d}q\ \mathrm{Tr}\left[\mathcal{P}(\hat{p}-q)\left(\hat{x}-\frac{i}{2p_c^2}(\hat{p}-q)\right)\hat{\rho}\right] && (6.47)\\
&= \int_{\mathbb{R}}\mathrm{d}p\int_{\mathbb{R}}\mathrm{d}q\ q\mathcal{P}(p-q)\,\langle p|\left(\hat{x}-\frac{i}{2p_c^2}(p-q)\right)\hat{\rho}\,|p\rangle && (6.48)\\
&= \int_{\mathbb{R}}\mathrm{d}p\int_{\mathbb{R}}\mathrm{d}Q\ (p-Q)\mathcal{P}(Q)\,\langle p|\left(\hat{x}-\frac{i}{2p_c^2}Q\right)\hat{\rho}\,|p\rangle && (6.49)\\
&= \int_{\mathbb{R}}\mathrm{d}p\int_{\mathbb{R}}\mathrm{d}Q\ \mathcal{P}(Q)\left(p\,\langle p|\,\hat{x}\hat{\rho}\,|p\rangle + \frac{i}{2p_c^2}Q^2\,\langle p|\,\hat{\rho}\,|p\rangle\right) && (6.50)\\
&= \mathrm{Tr}\left(\hat{p}\hat{x}\hat{\rho}\right) + \frac{i}{2p_c^2}\underbrace{\int_{\mathbb{R}}\mathrm{d}Q\ Q^2\mathcal{P}(Q)}_{=p_c^2} && (6.51)\\
&= \mathrm{Tr}\left(\hat{p}\hat{x}\hat{\rho}\right) - \frac{1}{2}\left[\hat{p},\hat{x}\right] = \frac{1}{2}\left\langle\{\hat{x},\hat{p}\}\right\rangle\ , && (6.52)
\end{aligned}$$

where we substituted $Q(q) := p - q$ and left out all terms linear in Q since the probability distribution $\mathcal{P}$ has zero mean. Finally we used that $i\mathbb{1}$ is the commutator of $\hat{x}$ and $\hat{p}$. All together we have

$$\mathrm{Tr}\left(\{\hat{x},\hat{p}\}\,\Lambda(\hat{\rho}_t)\right) = (1-\alpha)\left\langle\{\hat{x},\hat{p}\}\right\rangle_t \ , \tag{6.53}$$

where we introduced the notation $\langle\hat{A}\rangle_t := \langle\hat{A}\rangle_{\hat{\rho}_t}$.

The equations of motion Collecting all the previously calculated dCSL terms as well as the coherent contributions from C.2, we can write down all equations of motions for first and second moments in $\hat{x}$ and $\hat{p}$,

$$\frac{\mathrm{d}}{\mathrm{d}t}\langle\hat{x}\rangle_t = \langle\hat{p}\rangle_t \tag{6.54}$$

$$\frac{\mathrm{d}}{\mathrm{d}t}\langle\hat{p}\rangle_t = -\langle\hat{x}\rangle_t - \alpha\Gamma\langle\hat{p}\rangle_t \tag{6.55}$$

$$\frac{\mathrm{d}}{\mathrm{d}t}\langle\hat{x}^2\rangle_t = \langle\{\hat{x},\hat{p}\}\rangle_t + \Gamma\frac{1}{4p_c^2} \tag{6.56}$$

$$\frac{\mathrm{d}}{\mathrm{d}t}\langle\{\hat{x},\hat{p}\}\rangle_t = 2\left(\langle\hat{p}^2\rangle_t - \langle\hat{x}^2\rangle_t\right) - \alpha\Gamma\langle\{\hat{x},\hat{p}\}\rangle_t \tag{6.57}$$

$$\frac{\mathrm{d}}{\mathrm{d}t}\langle\hat{p}^2\rangle_t = -\langle\{\hat{x},\hat{p}\}\rangle - \alpha\Gamma(2-\alpha)\langle\hat{p}^2\rangle_t + \alpha^2\Gamma p_c^2 \ . \tag{6.58}$$

Note that in equation (6.58) the coefficient in front of $\langle\hat{p}^2\rangle_t$ changes its sign at $\alpha = 2$, characterizing a qualitative change: The system damping becomes a heating.

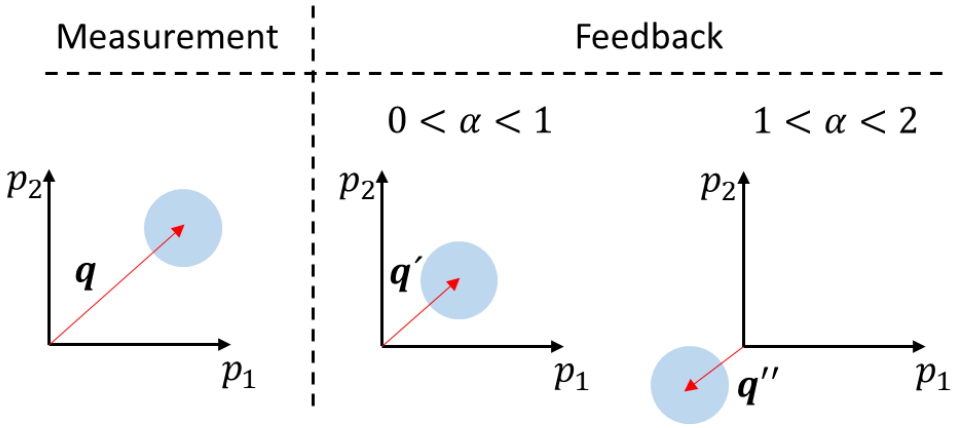

Figure 13: Measurement-feedback interpretation of the sign flip in equation (6.58). In this scenario the particle´s momentum was measured to be $\mathbf{q}$. The strength of the feedback kick depends on the parameter α: Starting from $\alpha = 0$ the momentum decreases continuously with increasing α since the particle is kicked towards the origin in momentum space. For $1 < \alpha < 2$ the momentum is kicked past the origin but the absolute momentum is still smaller than $|\mathbf{q}|$. At $\alpha = 2$ the momentum after the feedback is just $\mathbf{q}'' = -\mathbf{q}$. Finally for $\alpha > 2$, the post-feedback momentum is higher than the measured momentum, increasing the kinetic energy of the particle.

This qualitative change is sketched in figure 13: Given the momentum of our particle was measured to be $\mathbf{q}$, then for $\alpha \in (0, 1)$ the momentum is shifted towards the origin but the post-measurement momentum $\mathbf{q}'$ stays on the same side of the coordinate axes. This changes in the situation $\alpha \in (1, 2)$. Now the momentum passes the origin but still has $|\mathbf{q}''| < |\mathbf{q}|$. Increasing α even further, leads to $|\mathbf{q}''| > |\mathbf{q}|$ just on the other side of the origin. Therefore, we conclude that $\alpha \in (0, 1)$ is the natural choice of parameters.

Finally, we remark that we can find an equation of motion for the total energy by summing up the change in potential and kinetic energy. This equation is not independent from the other equations of motion

$$\frac{\mathrm{d}}{\mathrm{d}t} \langle \hat{H} \rangle_t = -\frac{\alpha\Gamma}{2}(2-\alpha) \langle \hat{p}^2 \rangle_t + \frac{\alpha^2\Gamma}{2} p_c^2 + \frac{\Gamma}{8p_c^2} \,. \tag{6.59}$$

Conclusively, the total energy of the harmonic oscillator decreases proportionally to its kinetic energy. In the next subsection we continue to investigate this system of ordinary equations of motions.

6.6. Time evolution and equilibrium

In subsection 6.5 we derived the equations of motion of the first and second statistical moments of a harmonic oscillator under the influence of dCSL. Will now use these equations to learn about the equilibration of this system.

First Moments By combining the equations for the first moments, we find

$$\left(\frac{\mathrm{d}^2}{\mathrm{d}t^2} + \alpha\Gamma\frac{\mathrm{d}}{\mathrm{d}t} + 1\right)\langle\hat{x}\rangle_t = 0 \ . \tag{6.60}$$

This is the differential equation of a damped harmonic oscillator. With the definition of the modified oscillator frequency $\omega_d := \sqrt{1-(\alpha\Gamma/2)^2}$ we find the (underdamped) solution

$$\langle\hat{x}\rangle_t = \mathrm{e}^{-\alpha\Gamma t/2}\left(\cos(\omega_d t)\,\langle\hat{x}\rangle_0 + \sin(\omega_d t)\frac{\langle\hat{p}\rangle_0 + \alpha\Gamma\,\langle\hat{x}\rangle_0/2}{\omega_d}\right) \tag{6.61}$$

$$\langle\hat{p}\rangle_t = \mathrm{e}^{-\alpha\Gamma t/2}\left(\cos(\omega_d t)\,\langle\hat{p}\rangle_0 - \sin(\omega_d t)\frac{\langle\hat{x}\rangle_0 + \alpha\Gamma\,\langle\hat{p}\rangle_0/2}{\omega_d}\right) \ . \tag{6.62}$$

From this we can learn that the expectation value of position and momentum will decay exponentially under the influence of dissipative CSL to $\langle\hat{x}\rangle_{\mathrm{eq}} = 0$ and $\langle\hat{p}\rangle_{\mathrm{eq}} = 0$.

Second moments in equilibrium For the second moments in (6.56) - (6.58), we first derive the equilibrium values by setting their time derivatives to zero. The equation of motion for $\langle\hat{x}^2\rangle$ immediately yields

$$\langle\{\hat{x},\hat{p}\}\rangle_{\mathrm{eq}} = -\frac{\Gamma}{4p_c^2} \ . \tag{6.63}$$

This can be used in the equation for the anti-commutator (6.57), which yields

$$\langle\hat{x}^2\rangle_{\mathrm{eq}} - \langle\hat{p}^2\rangle_{\mathrm{eq}} = \frac{\alpha\Gamma^2}{8p_c^2} \ . \tag{6.64}$$

We remark that this identity immediately implies that the equilibrium state does not obey the equipartition theorem $\langle\hat{x}^2\rangle = \langle\hat{p}^2\rangle$. From the last equation we then get

$$\langle\hat{p}^2\rangle_{\mathrm{eq}} = \frac{1}{4\alpha(2-\alpha)p_c^2} + \frac{\alpha p_c^2}{2-\alpha} \tag{6.65}$$

and finally

$$\langle\hat{x}^2\rangle_{\mathrm{eq}} = \frac{1}{4\alpha(2-\alpha)p_c^2} + \frac{\alpha p_c^2}{2-\alpha} + \frac{\alpha\Gamma^2}{8p_c^2} \ . \tag{6.66}$$

This also gives us the expectation value of the equilibrium energy as

$$\langle \hat{H} \rangle_{\mathrm{eq}} = \frac{1}{2} \left(\langle \hat{x}^2 \rangle_{\mathrm{eq}} + \langle \hat{p}^2 \rangle_{\mathrm{eq}} \right) = \frac{1}{4\alpha(2-\alpha)p_c^2} + \frac{\alpha p_c^2}{2-\alpha} + \frac{\alpha \Gamma^2}{16 p_c^2} \tag{6.67}$$

Note that $\langle \hat{x}^2 \rangle_{\mathrm{eq}}$ and $\langle \hat{p}^2 \rangle_{\mathrm{eq}}$ are not defined for $\alpha = 2$. This is in agreement with the explanation at the end of subsection 6.5. In figure 13 we argued why there is effectively no dissipation in the case $\alpha = 2$. Thus, a system with parameter choice $\alpha = 2$ does not equilibrate.

Dynamics of the second moments To have a better understanding of the second moments time evolution we rephrase the system of ordinary differential equations as

$$\underbrace{\frac{\mathrm{d}}{\mathrm{d}t} \begin{pmatrix} \langle \hat{x}^2 \rangle_t \\ \langle \{\hat{x}, \hat{p}\} \rangle_t \\ \langle \hat{p}^2 \rangle_t \end{pmatrix}}_{=\dot{\mathbf{v}}(t)} = \underbrace{\begin{pmatrix} 0 & 1 & 0 \\ -2 & -\alpha\Gamma & 2 \\ 0 & -1 & -\alpha\Gamma(2-\alpha) \end{pmatrix}}_{=:M} \underbrace{\begin{pmatrix} \langle \hat{x}^2 \rangle_t \\ \langle \{\hat{x}, \hat{p}\} \rangle_t \\ \langle \hat{p}^2 \rangle_t \end{pmatrix}}_{=:\mathbf{v}(t)} + \underbrace{\begin{pmatrix} \Gamma/(4p_c^2) \\ 0 \\ \alpha^2 \Gamma p_c^2 \end{pmatrix}}_{=:\mathbf{w}} . \tag{6.68}$$

In appendix C.3, we find that $\det(M) = -2\alpha\Gamma(2-\alpha)$. This expression is never zero in the nontrivial cases because $\alpha \in (0, 1]$ is a natural choice as it was argued at the end of subsection 6.5. Hence, M is invertible and we can formally express the equilibrium values of the second moments as

$$\mathbf{v}_{\mathrm{eq}} := -M^{-1}\mathbf{w} = \begin{pmatrix} \langle \hat{x}^2 \rangle_{\mathrm{eq}} \\ \langle \{\hat{x}, \hat{p}\} \rangle_{\mathrm{eq}} \\ \langle \hat{p}^2 \rangle_{\mathrm{eq}} \end{pmatrix} . \tag{6.69}$$

With this we can define a vector relative to the equilibrium as

$$\mathbf{u}(t) := \mathbf{v}(t) - \mathbf{v}_{\mathrm{eq}} \tag{6.70}$$

fulfilling the linear homogeneous equation of motion

$$\dot{\mathbf{u}}(t) = \dot{\mathbf{v}}(t) - \underbrace{\dot{\mathbf{v}}_{\mathrm{eq}}}_{=0} = M\mathbf{u}(t) + \underbrace{M\mathbf{v}_{\mathrm{eq}}}_{-\mathbf{w}} + \mathbf{w} = M\mathbf{u}(t) . \tag{6.71}$$

To understand the dynamics of $\mathbf{u}(t)$ it would be useful to find the spectral decomposition of M. Unfortunately, the closed solution to this problem is cumbersome and not very instructive. We simplify the problem by assuming that α is very small. Therefore we neglect the term in M that is of second order in α. Surprisingly this is enough to make this problem tractable. We slightly change our problem to

$$\dot{\mathbf{u}}(t) = \tilde{M}\mathbf{u}(t) \tag{6.72}$$

with

$$\tilde{M} := \begin{pmatrix} 0 & 1 & 0 \\ -2 & -\alpha\Gamma & 2 \\ 0 & -1 & -2\alpha\Gamma \end{pmatrix} . \tag{6.73}$$

As derived in appendix C.3 the eigenvalues of $\tilde{M}$ are

$$\lambda_1 = -\alpha\Gamma \tag{6.74}$$

$$\lambda_{2,3} = -\alpha\Gamma \pm i\sqrt{4 - \alpha^2\Gamma^2} \tag{6.75}$$

This shows that every solution of this system of ordinary differential equations is a linear combination of a pure decay and damped oscillations. Hence, every trajectory converges to $\mathbf{v}_{eq}$ for $t \to \infty$.

Implications on the original system matrix Up to now the decaying solutions are due to the simplified dynamics given by $\tilde{M}$. We can use the fact that the simple roots of a polynomial depend continuously on the coefficients ([27]) to learn something about the general case based on the matrix M: First we choose Γ_α in such a way that $\alpha\Gamma_\alpha =: c_0$ is constant for all α. This gives us a fixed choice of the unpertubated eigenvalues

$$\lambda_1 = -c_0 \tag{6.76}$$

$$\lambda_{2,3} = -c_0 \pm i\sqrt{4 - c_0^2} . \tag{6.77}$$

In the next step we note that for small α the matrix M approaches $\tilde{M}$ elementwise. Therefore the coefficients of their characteristic polynomials approach each other as well. Thanks to the aforementioned continuity we can find a number $\delta > 0$ for every $\epsilon > 0$ such that $|\alpha| < \delta$ implies

$$\left|\lambda_j^{(\text{true})} - \lambda_j\right| < \epsilon \quad j \in \{1, 2, 3\} \tag{6.78}$$

with the eigenvalues $\lambda_j^{(\text{true})}$ of the matrix M. This shows that with the choice $\epsilon < c_0$ the eigenvalues of the original dynamic have negative real parts as well. Consequently, we have proven that there are feasible regions in the parameter space (α, Γ) for which the second moments of a harmonic oscillator equilibrate to the values $\mathbf{v}_{\text{eq}}$.

Numerical solution We have seen by analytical reasoning that for sufficiently high Γ and sufficiently small α the second moments of a harmonic oscillator equilibrate to $\mathbf{v}_{\text{eq}}$. The numerically evaluated greatest real part of the M-eigenvalues, as plotted in figure 14 against the parameters $\alpha \in (0, 2)$ and $\Gamma \in (0, 3]$, confirms that the equilibration holds true for a wide range of parameters.

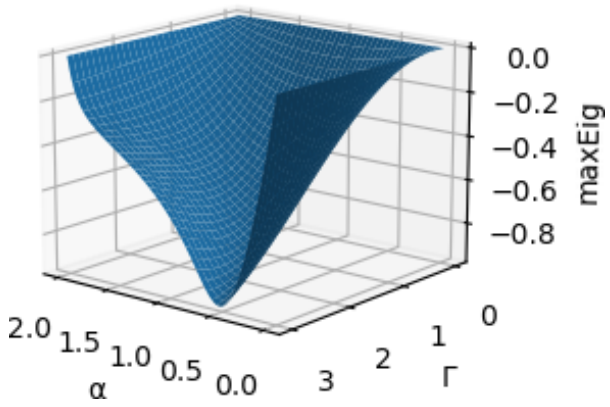

Figure 14: Largest real part of the eigenvalues of the system matrix M (6.68) plotted against the Parameters α and Γ.

6.7. Implications on the effective temperature in dissipative CSL

It is a strongly stressed feature of the dissipative CSL model in the original paper [3] that the equilibrium temperature is independent of the mass of the particle. We are now able to check this feature in case of a more complicated system like an harmonic oscillator. To this end we express our results from subsection 6.6 in the parameters from dissipative CSL (4.61),(4.62) and (4.64) that were found while showing the equivalence of Stokes friction and dCSL. In this subsection we need to reintroduce units in some results. For clarification, we denote dimensionless observables with an index N and scales by an index 0 as introduced in subsection 6.2. The relevant results are

$$\langle \hat{x}_{\mathrm{N}}^2 \rangle_{\mathrm{eq}} - \langle \hat{p}_{\mathrm{N}}^2 \rangle_{\mathrm{eq}} = \frac{\gamma_{\mathrm{N}}^2}{32\pi^3 r_{c\mathrm{N}}^4} \frac{k^3}{(1+k)^7} = \frac{\gamma^2}{32\pi^3 r_{c\mathrm{N}}^4} \left(k^3 - 7k^4 + \dots\right) = 0 + \mathcal{O}\left(k^3\right) \tag{6.79}$$

and

$$\langle \hat{H}_{\mathrm{N}} \rangle_{\mathrm{eq}} = \frac{1}{8r_{c\mathrm{N}}^2 k} + \frac{k(1+k)^2 r_{c\mathrm{N}}^2}{2} + \frac{\gamma_{\mathrm{N}}^2}{64\pi^3 r_{c\mathrm{N}}^4} \frac{k^3}{(1+k)^7} \tag{6.80}$$

$$= \frac{1}{8r_{c\mathrm{N}}^2 k} + \frac{k(1+2k) r_{c\mathrm{N}}^2}{2} + \mathcal{O}\left(k^3\right) \ . \tag{6.81}$$

Since the equilibrium state is, at best, approximately a Gibbs state, a temperature is not well defined. Therefore, T should just bee seen as a parameter characterizing the average kinetic energy per degree of freedom. For convenience we will still call it temperature. The connection is given by the Boltzmann constant k_B and does only hold when $\langle \hat{x}^2 \rangle_{\mathrm{eq}} = \langle \hat{p}^2 \rangle_{\mathrm{eq}}$. Reintroducing units in $\langle \hat{H}_{\mathrm{N}} \rangle_{\mathrm{eq}}$ we have

$$k_B T = \langle \hat{H} \rangle_{\mathrm{eq}} \ . \tag{6.82}$$

We will now consider two limiting cases in which the difference in equation (6.79) vanishes, which means the equipartition theorem is approximately true.

Small γ compared to the oscillator frequency For values $\gamma_{\mathrm{N}} \ll 1$ (in units $\gamma \ll x_0^3\omega$) we find

$$\langle \hat{H} \rangle_{\mathrm{eq}} = \frac{1}{8r_c^2 k} + \frac{k(1+k)^2 r_c^2}{2} \ . \tag{6.83}$$

Reintroducing units, this yields

$$\langle \hat{H} \rangle_{\mathrm{eq}} = \frac{1}{4k}\frac{1}{2m}\left(\frac{\hbar}{r_c}\right)^2 + k(1+k)^2\frac{m\omega^2 r_c^2}{2} \ . \tag{6.84}$$

We see that this limit is problematic for two reasons: The condition $\gamma \ll x_0\omega$ depends on the frequency of the oscillator. Therefore the parameters can not be chosen universally to fulfill this condition. On the other hand, the second term introduces a mass dependence in the temperature because of the scaling $k \propto 1/m$, which shows that dCSL can not be explained by thermalization due to the coupling to a thermal field.

$k \ll 1$ and kr_c^2 small compared to $\hbar/(2m\omega)$ If k is small enough to ignore terms of third order, we find the equilibrium energy in units as

$$\langle \hat{H} \rangle_{\mathrm{eq}} = \frac{1}{4k}\frac{1}{2m}\left(\frac{\hbar}{r_c}\right)^2 + k(1+2k)\frac{m\omega^2 r_c^2}{2} \ . \tag{6.85}$$

Analogous to the preceding case, we find that the second term introduces a mass dependence on the temperature. If we go one step further and demand

$$kr_c^2 \ll \frac{\hbar}{2m\omega} \ , \tag{6.86}$$

the first term dominates. This yields the energy

$$\langle \hat{H} \rangle_{\mathrm{eq}} = \frac{1}{4k}\frac{1}{2m}\left(\frac{\hbar}{r_c}\right)^2 \tag{6.87}$$

and the corresponding temperature

$$T = \frac{\hbar^2}{8k_B m k r_c^2} \ . \tag{6.88}$$

This is exactly the temperature that was obtained for the free particle in the original dCSL paper [3]. But the condition that has to be fulfilled depends on the frequency of the oscillator. Therefore it is not possible to find a universal choice of parameters that equilibrates every harmonic oscillator to a state corresponding to the same parameter T.

conclusion We scrutinized the effective temperature parameter T proposed in [3] to characterize the average kinetic energy per motional degree of freedom at equilibrium

under dCSL. In the case of a harmonically bound system, we identified a parameter regime in which the equilibrium is represented by the same T-parameter. However, given that this validity regime depends on the oscillator frequency (and mass), we conclude that T cannot be regarded as a universal feature of dCSL at all scales. Consequently, this indicates that the dCSL master equation cannot be interpreted as a thermalization process.

7. Consistency in many-particle models

Up to now we considered the single-particle properties of dissipative CSl and comparable models with special focus on the equilibration of the energy. In this section we will present additional conditions on the many-particle models and investigate if they are fulfilled.

7.1. Requirements for physical theories

The fundamental theories in physics fulfill certain symmetries. We will now review and investigate on the most important ones.

Symmetries of spacetime This work is formulated within the framework of non-relativistic quantum mechanics. Therefore, a natural choice of symmetry is given by Galilei covariance. However, as a consequence of the friction forces, the equations are not expected to be covariant to the full Galilei group. This is due to a fixed momentum reference frame with respect to which the friction slows down any movement. Therefore, we content ourselves with isotropy and homogeneity of space being preserved by the master equation.

Mass scaling All objects in our macroscopic world consist of a huge amount of particles. Therefore, the objects we want to describe, consist of many particles. We seek a scale-invariant theory that describes moving particles consistently on all size scales. For example, in Newtonian mechanics, the earth could be regarded a moving particle through our solar system given that it is sufficiently small and that gravitational forces are insensitive to its inner structure. Here, we similarly demand that the centre-of-mass motion of rigid compound particles be treated the same as equally heavy point masses, provided the compounds are small compared to the localization length of the CSL model.

Innocent bystander criterion For practical purposes, it is always necessary to define a system by ignoring(in some sense) its surroundings, otherwise the whole universe had to be taken into consideration in any calculation. Therefore, our model should not introduce correlations between different particles. Otherwise there would a difference in ignoring an additional particle in the first place or taking it into consideration but then tracing it out. So the tracing out of a party should not change the overall dynamics of the remaining parties.

The Goal of this section In the following subsections we will investigate on the mass-dependence of the model parameters $(\alpha_j, p_{cj}, \Gamma_j)_j$ for every particle species $j \in J$. We try to keep the aforementioned principles intact.

7.2. Mass scaling

Many-particle Lindblad operator A universal collapse model that applies to arbitrary composite systems requires a consistent many-body generalization of the single-particle master equation. This could be done in arbitrary (and arbitrarily complicated) ways, but only one possibility is known that yields tractable results, conserves particle exchange symmetry, and achieves a consistent amplification of the collapse effect with the mass scale [28]. One promotes the single-particle Lindblad operators to weighted sums of single-particle operators,

$$\sum_k \sqrt{\Gamma_k}\ \hat{L}_k\ . \tag{7.1}$$

Using the correspondence rules from section1.4, and assuming that the parameters are equal for particles of the same species, we can translate such an expression to second quantization in a straightforward manner.

The rigid body approximation In order to investigate the impact of the dCSL model on the cenre-of-mass motion of a compound object, we start from the many-body master equation for all constituent particles and assume that they are rigidly bound at fixed positions relative to the centre of mass. We can then switch to relative coordinates and trace over them to arrive at a reduced description of the centre of mass. As it is shown in appendix D.1, there is a canonical transformation that maps N single-particle operators $(\hat{\mathbf{x}}_j, \hat{\mathbf{p}}_j)_j$ onto centre of mass coordinates $(\hat{\mathbf{x}}_{\mathrm{c.m.}}, \hat{\mathbf{p}}_{\mathrm{c.m.}})$ and $N-1$ relative coordinates $(\hat{\mathbf{r}}_k, \hat{\mathbf{q}}_k)_k$. The transformation can be written as

$$\hat{\mathbf{x}}_j = \hat{\mathbf{x}}_{c.m} + \sum_{k=2}^{N} \Xi_{jk}\hat{\mathbf{r}}_k\ ;\quad \hat{\mathbf{p}}_j = \frac{m_j}{M}\hat{\mathbf{p}}_{c.m.} + \hat{\mathbf{q}}_j, \tag{7.2}$$

with a matrix Ξ_{jk} that depends on the masses of the particles.

We now idealize the compound object consisting of these particles to be rigid. Therefore the relative coordinates $\hat{\mathbf{r}}_j$ become constant numbers,

$$\hat{\mathbf{r}}_j \longmapsto \mathbf{r}_j, \tag{7.3}$$

and accordingly the corresponding relative momenta become zero,

$$\hat{\mathbf{q}}_j \longmapsto 0\ . \tag{7.4}$$

All things considered, the positions of the single particles depend on the dynamical variable $\hat{\mathbf{x}}_{c.m.}$ and on the geometry of the object given by Ξ_{jk} and the $(\mathbf{r}_k)_k$,

$$\hat{\mathbf{x}}_j = \hat{\mathbf{x}}_{c.m} + \sum_{k=2}^{N} \Xi_{jk}\mathbf{r}_k. \tag{7.5}$$

and the momenta are just fractions of the total centre of mass momentum

$$\hat{\mathbf{p}}_j = \frac{m_j}{M}\hat{\mathbf{p}}_{c.m.} \ . \tag{7.6}$$

Note that by setting the $\hat{\mathbf{r}}_j$ constant we neglected rotations of the particle.

Effects of species dependent single-particle gauge transformations We will find a many-particle generalization of a version of our stokes friction (respectively dCSL) that yields the correct mass scaling. In subsection 1.5 we learned that we can apply a gauge transformation to the Lindblad operators defined by a function $u(\mathbf{y}, \mathbf{q})$ without changing the single-particle dynamics. That this does not hold true for possible many-particle generalizations, can be exemplified with the following example: Consider two particles of different species with Lindblad operators $\hat{L}_1(\mathbf{q})$, $\hat{L}_2(\mathbf{q})$. In general, the gauge transformations can depend on the species such that we have $u_1(\mathbf{y}, \mathbf{q})$ and $u_2(\mathbf{y}, \mathbf{q})$. We get the transformed single-particle Lindblad operators $\hat{A}_1(\mathbf{y})$ and $\hat{A}_2(\mathbf{y})$ as

$$\hat{A}_j(\mathbf{y}) := \int_{\mathbb{R}^3} \mathrm{d}\lambda^3(\mathbf{q}) \ u_j(\mathbf{y}, \mathbf{q})\hat{L}_j(\mathbf{q}) \ . \tag{7.7}$$

The first term of the Lindblad master equation becomes in terms of the new operators

$$\int_{\mathbb{R}^3} \mathrm{d}\lambda^3(\mathbf{y}) \left(\hat{A}_1(\mathbf{y}) + \hat{A}_2(\mathbf{y})\right) \hat{\rho} \left(\hat{A}_1(\mathbf{y}) + \hat{A}_2(\mathbf{y})\right)^\dagger \tag{7.8}$$

$$= \int_{\mathbb{R}^3} \mathrm{d}\lambda^3(\mathbf{y}) \left(\hat{A}_1(\mathbf{y})\hat{\rho}\hat{A}_1^\dagger(\mathbf{y}) + \hat{A}_2(\mathbf{y})\hat{\rho}\hat{A}_2^\dagger(\mathbf{y})\right) \tag{7.9}$$

$$+ \int_{\mathbb{R}^3} \mathrm{d}\lambda^3(\mathbf{y}) \left(\hat{A}_1(\mathbf{y})\hat{\rho}\hat{A}_2^\dagger(\mathbf{y}) + \hat{A}_2(\mathbf{y})\hat{\rho}\hat{A}_1^\dagger(\mathbf{y})\right) \tag{7.10}$$

$$= \int_{\mathbb{R}^3} \mathrm{d}\lambda^3(\mathbf{q}) \left(\hat{L}_1(\mathbf{y})\hat{\rho}\hat{L}_1^\dagger(\mathbf{y}) + \hat{L}_2(\mathbf{y})\hat{\rho}\hat{L}_2^\dagger(\mathbf{y})\right) \tag{7.11}$$

$$+ \int_{\mathbb{R}^6} \mathrm{d}\lambda^6(\mathbf{q}_1, \mathbf{q}_2) \left[\underbrace{\left(\int_{\mathbb{R}^3} \mathrm{d}\lambda^3(\mathbf{y}) u_1(\mathbf{y}, \mathbf{q}_1) u_2^*(\mathbf{y}, \mathbf{q}_2) \right)}_{\neq \delta^{(3)}(\mathbf{q}_1 - \mathbf{q}_2)} \hat{L}_1(\mathbf{q}_1)\hat{\rho}\hat{L}_2^\dagger(\mathbf{q}_2) + \mathrm{h.c.} \right] \ , \tag{7.12}$$

where we separated the terms with Lindblad operators of one species and the terms with Lindblad operators of both species. By definition, the terms corresponding to one species can be rephrased in terms of the untransformed operators. On the other hand, the mixed terms can not be rephrased accordingly. This is due to the mixed functions u_1 and u_2 that do not yield the needed δ-function.

Finding a consistent mass scaling We have seen that the many-particle generalizations can change under species-dependent gauge transformations on the single-particle level. Therefore, we have to choose a single-particle version: The only fruitful variant,

that we found, was obtained from the original stokes friction by the transformation matrix

$$u(\mathbf{y},\mathbf{q}) = \frac{\alpha^{2/3}}{\sqrt{2\pi\hbar}^3}\exp\left(\frac{i}{\hbar}\alpha\mathbf{y}\cdot\mathbf{q}\right) . \tag{7.13}$$

This yields the (for the single-particle case) equivalent Lindblad operator with corresponding rate Γ

$$\sqrt{\Gamma}\hat{L}^{(1)}(\mathbf{y}) = \frac{\sqrt{\Gamma}\alpha^{2/3}}{\sqrt{2\pi\hbar}^3}(2\pi p_c^2)^{-3/4}\int_{\mathbb{R}^3}\mathrm{d}\lambda^3(\mathbf{q})\ \mathrm{e}^{\frac{i}{\hbar}\alpha\mathbf{q}\cdot(\mathbf{y}-\hat{\mathbf{x}})}\mathrm{e}^{-(\hat{\mathbf{p}}-\mathbf{q})^2/(4p_c^2)} . \tag{7.14}$$

Now we assume that we have J different kinds of particle species with mass m_j and N_j particles of each species. The motion of the k-th particle of the j-th species is described by a pair of canonical variables $(\hat{\mathbf{x}}_{jk},\hat{\mathbf{p}}_{jk})$ with a corresponding Lindblad operator $\hat{L}^{(1)}_{jk}(\mathbf{y})$.

The question is now whether we can choose mass-dependent parameters α_j and p_{cj} such that the centre of mass motion follows the same master equation as the single particles. The sum of the general Lindblad operators weighted the sqaure root of the rates Γ_j is denoted by $\sqrt{\Gamma_M}\hat{L}^{(N)}(\mathbf{y})$, where $\Gamma^{(N)}$ is an effective rate, that we just use here for the right dimensions. We reshape the sum as

$$\sqrt{\Gamma^{(N)}}\hat{L}^{(N)}(\mathbf{y}) = \sum_{j=1}^{J}\sqrt{\Gamma_j}\sum_{k=1}^{N_j}\hat{L}^{(1)}_{jk}(\mathbf{y}) \tag{7.15}$$

$$= \sum_{j=1}^{J}\frac{\sqrt{\Gamma_j}\alpha_j^{3/2}}{\sqrt{2\pi\hbar}^3}(2\pi p_{cj}^2)^{-3/4}\sum_{k=1}^{N_j}\int_{\mathbb{R}^3}\mathrm{d}\lambda^3(\mathbf{q})\ \mathrm{e}^{\frac{i}{\hbar}\alpha_j\mathbf{q}\cdot\left(\mathbf{y}-\hat{\mathbf{x}}_{jk}\right)}\mathrm{e}^{-(\hat{\mathbf{p}}_{jk}-\mathbf{q})^2/(4p_{cj}^2)} . \tag{7.16}$$

Going in the rigid body approximation, we expresses everything in centre of mass coordinates $\hat{\mathbf{x}}_{c.m.}$ and $\hat{\mathbf{p}}_{c.m.}$ and constant body-fixed positions $\mathbf{r}_{jk}$

$$\hat{\mathbf{x}}_{jk} = \hat{\mathbf{x}}_{\mathrm{c.m.}} + \sum_{j'k'}\Xi_{(jk)(j'k')}\mathbf{r}_{j'k'} \tag{7.17}$$

$$\hat{\mathbf{p}}_{jk} = \frac{m_j}{M}\hat{\mathbf{p}}_{\mathrm{c.m.}} \tag{7.18}$$

with a matrix $\Xi_{(jk)(j'k')}$ and the total mass M. Plugging this into the momentum dis-

placement operator that appears under the integral in (7.14), we obtain

$$\exp\left(\frac{i}{\hbar}\alpha_j \mathbf{q}\cdot(\mathbf{y}-\hat{\mathbf{x}}_{jk})\right) \tag{7.19}$$

$$= \underbrace{\exp\left(-\frac{i}{\hbar}\alpha_j \sum_{j'k'} \Xi_{(jk)(j'k')}\mathbf{r}_{j'k'}\cdot\mathbf{q}\right)}_{=:\tilde{F}_{j,k}(\mathbf{q})} \exp\left(\frac{i}{\hbar}\alpha_j \mathbf{q}\cdot(\mathbf{y}-\hat{\mathbf{x}}_{\mathrm{c.m.}})\right) \tag{7.20}$$

$$= \tilde{F}_{j,k}(\mathbf{q})\ \exp\left(\frac{i}{\hbar}\alpha_j \mathbf{q}\cdot(\mathbf{y}-\hat{\mathbf{x}}_{\mathrm{c.m.}})\right)\ . \tag{7.21}$$

The newly defined form factor $\tilde{F}_{j,k}(\mathbf{q})$ will be discussed later. The Gaussian contribution to the Lindblad operator becomes

$$\exp\left(-\frac{(\hat{\mathbf{p}}_{jk}-\mathbf{q})^2}{4p_{cj}^2}\right) = \exp\left(-\frac{\left(\hat{\mathbf{p}}_{\mathrm{c.m.}}-\frac{M}{m_j}\mathbf{q}\right)^2}{4\left(\frac{M}{m_j}p_{cj}\right)^2}\right)\ . \tag{7.22}$$

For a universal, mass scale-invariant description, we must ensure that the centre-of-mass Gaussian on the right hand side is consistent with every single-particle operator for the masses m_j on the left hand side. We achieve this by defining a single universal model parameter p_c for an arbitrary reference mass m_0 and rescale

$$\boxed{p_{cj} := \frac{m_j}{m_0}p_c}\ . \tag{7.23}$$

Consistently this yields

$$p_{cM} := \frac{M}{m_0}p_c\ . \tag{7.24}$$

A (j-dependent) substitution of the integration variable $\mathbf{Q}(\mathbf{q}) := \frac{M}{m_j}\mathbf{q}$ fixes the prefactor of $\mathbf{q}$. This yields in total

$$\sqrt{\Gamma^{(N)}}\hat{L}^{(N)}(\mathbf{y}) = \sum_{j=1}^{J}\frac{\sqrt{\Gamma_j}\alpha_j^{3/2}}{\sqrt{2\pi\hbar}^3}(2\pi p_{cj}^2)^{-3/4}\left(\frac{m_j}{M}\right)^3 \tag{7.25}$$

$$\times\sum_{k=1}^{N_j}\int_{\mathbb{R}^3}\mathrm{d}\lambda^3(\mathbf{Q})\ \tilde{F}_{j,k}\left(\frac{m_j}{M}\mathbf{Q}\right)\mathrm{e}^{\frac{i}{\hbar}\left(\frac{m_j}{M}\alpha_j\right)\mathbf{q}\cdot(\mathbf{y}-\hat{\mathbf{x}}_{\mathrm{c.m.}})}\mathrm{e}^{-(\hat{\mathbf{p}}_{\mathrm{c.m.}}-\mathbf{Q})^2/(4p_{cM}^2)} \tag{7.26}$$

For universality we need to demand the kick operators in (7.25) to not depend on the single masses m_j. The only direct way to get the same M-dependent expression in every

exponential, is given by

$$\boxed{\alpha_j := \frac{m_0}{m_j}\alpha} \tag{7.27}$$

and consequently

$$\alpha_M := \frac{m_0}{M} \ . \tag{7.28}$$

The prefactor becomes

$$\frac{\sqrt{\Gamma_j}\alpha_j^{3/2}}{\sqrt{2\pi\hbar}^3}(2\pi p_{cj}^2)^{-3/4}\left(\frac{m_j}{M}\right)^3 = \frac{\sqrt{\Gamma_j}\alpha_M^{3/2}}{\sqrt{2\pi\hbar}^3}\left(2\pi p_{cM}^2\right)^{-3/4} \ . \tag{7.29}$$

Additionally, we define

$$\tilde{F}_{j,k}\left(\frac{m_j}{M}\mathbf{Q}\right) = \exp\left(-\frac{i}{\hbar}\alpha_M \sum_{j'k'} \Xi_{(jk)(j'k')}\mathbf{r}_{j'k'}\cdot\mathbf{Q}\right) =: F_{j,k}(\mathbf{Q}) \ , \tag{7.30}$$

which allows a m_j independent interpretation of the weighted sums of the form factors in appendix D.2. Since the Lindblad operator (7.25) only acts non-trivial on the centre of mass coordinates, taking the partial trace over the relative coordinates is a straightforward task: We set $\sqrt{\Gamma^{(N)}}\mathrm{Tr}_{\mathrm{rel}}\left(\hat{L}^{(N)}\right) = \sqrt{\Gamma_M}\hat{L}_{\mathrm{c.m.}}$. Note that we actually have to trace out on the level of the master equation. However, in this case the Lindblad operator is constant on the relative coordinates and we can build the partial trace of the Linblad operator. All things considered this yields

$$\sqrt{\Gamma_M}\hat{L}_{\mathrm{c.m.}}(\mathbf{y}) = \frac{\alpha_M^{3/2}}{\sqrt{2\pi\hbar}^3}(2\pi p_{cM}^2)^{-3/4}\int_{\mathbb{R}^3}\mathrm{d}\lambda^3(\mathbf{z}) \tag{7.31}$$

$$\left(\sum_{j=1}^{J}\sqrt{\Gamma_j}\sum_{k=1}^{N_j}F_{j,k}\left(\mathbf{Q}\right)\right)\mathrm{e}^{\frac{i}{\hbar}\alpha_M\mathbf{Q}\cdot(\mathbf{y}-\hat{\mathbf{x}}_{\mathrm{c.m.}})}\mathrm{e}^{-(\hat{\mathbf{p}}_{\mathrm{c.m.}}-\mathbf{Q})^2/(4p_{cM}^2)} \tag{7.32}$$

In appendix D.2 we find

$$\sum_{j=1}^{J}m_j\sum_{k=1}^{N_j}F_{j,k}(\mathbf{Q}) =: F(\mathbf{Q}) = \int_{\mathbb{R}^3}\mathrm{d}\lambda^3(\mathbf{Q})\mathrm{e}^{-i\frac{\alpha_M}{\hbar}\ \mathbf{z}\cdot\mathbf{Q}}\ \mu(\mathbf{z}) \tag{7.33}$$

to be the Fourier transform of the mass density $\mu(\mathbf{z})$. To find this expression in the bracket on the right hand side of equation (7.32), we choose the mass scaling of Γ_j to be

$$\boxed{\Gamma_j = \left(\frac{m_j}{m_0}\right)^2\Gamma} \ , \tag{7.34}$$

because this yields

$$\sum_{j=1}^{J}\sqrt{\Gamma_j}\sum_{k=1}^{N_j}F_{j,k}\left(\mathbf{Q}\right)=\frac{\sqrt{\Gamma_M}}{M}\sum_{j=1}^{J}m_j\sum_{k=1}^{N_j}F_{j,k}(\mathbf{Q}) \tag{7.35}$$

$$=\frac{\sqrt{\Gamma_M}}{M}F(\mathbf{Q})=\sqrt{\Gamma_M}F(\mathbf{Q})/F(\mathbf{0})\ . \tag{7.36}$$

In summary we found a mass scaling of our three parameters α, p_c and Γ such that the Lindblad operators behave like

$$\sum_{j=1}^{J}\sqrt{\Gamma_j}\sum_{k=1}^{N_j}\hat{L}_{jk}^{(1)}(\mathbf{y})=\sqrt{\Gamma_M}\ \hat{L}_{\mathrm{c.m.}}(\mathbf{y}), \tag{7.37}$$

with the effective cente-of-mass Lindblad operator

$$\hat{L}_{\mathrm{c.m.}}(\mathbf{y})=\frac{\alpha_M^{2/3}}{\sqrt{2\pi\hbar}^3}(2\pi p_{cM}^2)^{-3/4}\int_{\mathbb{R}^3}\mathrm{d}\lambda^3(\mathbf{Q})\ \frac{F(\mathbf{Q})}{F(\mathbf{0})}\mathrm{e}^{\frac{i}{\hbar}\alpha\mathbf{Q}\cdot(\mathbf{y}-\hat{\mathbf{x}}_{\mathrm{c.m.}})}\mathrm{e}^{-(\hat{\mathbf{p}}_{\mathrm{c.m.}}-\mathbf{Q})^2/(4p_{cM}^2)}\ . \tag{7.38}$$

This operator just depends on the total mass M and the Fourier transform $F(\mathbf{Q})$ of the mass density $\mu(\mathbf{z})$ of a compound particle. Consequently, a detailed description of the constituents is not necessary to describe the centre of mass motion correctly.

Point-particle limit That this description of compound objects is indeed consistent with the description of single particle gets clearer when we consider a homogeneous sphere of radius R. As can be seen in appendix D.3, the corresponding form factor can be written in terms of the spherical Bessel function of the first kind j_1

$$F(\mathbf{Q})/F(\mathbf{0})=3\frac{\hbar}{\alpha R|\mathbf{Q}|}\ \mathrm{j}_1\left(\alpha\frac{R|\mathbf{Q}|}{\hbar}\right) \tag{7.39}$$

and has the (point wise) property

$$F(\mathbf{Q})/F(\mathbf{0})\xrightarrow[R\to 0]{}1\ . \tag{7.40}$$

This shows that in the limit of point particles we retrieve the Lindblad operators of the single-particle master equation (7.14) we started with.

7.3. Comparison to dissipative CSL

In the last subsection (7.2) we learned how to generalize our model for Stokes friction to many particles with a consistent mass scaling for a certain choice of the Lindblad operators. It is noteworthy that the Lindblad operators after the transformation (7.13) are up to a substitution the ones from dissipative CSL since $u(\mathbf{y}, \mathbf{q})$ defines the same gauge transformation as in 4.3. Consequently, we can compare the parameters in the many-particle master equations. In 4.3 we learned how to translate the parameters. So we can check how our scaling from last subsection affects dissipative CSL.

Translation to CSL parameters In the single-particle case of Stokes friction 4.3 we found a way to express the parameters (α, p_c, Γ) by the dCSL parameters (r_c, k, γ). Expressing the dissipative CSL parameters with the stokes parameters yields

$$k = \frac{\alpha}{2 - \alpha} \tag{7.41}$$

and

$$r_c = \frac{\hbar}{\sqrt{2} p_c} \left(\frac{1}{\alpha} - \frac{1}{2} \right) \ . \tag{7.42}$$

Following from this, the scaling becomes

$$k_j = \frac{\alpha}{2\frac{m_j}{m_0} - \alpha} \tag{7.43}$$

and

$$r_{cj} = \frac{\hbar}{\sqrt{2} p_c} \left(\frac{1}{\alpha} - \frac{1}{2} \frac{m_0}{m_j} \right) \tag{7.44}$$

This is in strong contrast to the scaling in the actual dissipative CSL model, where r_c does not scale with the mass at all and k scales like $k_j \propto \frac{1}{m_j}$. Therefore, the mass consistent many-particle master equation, given by the Lindblad operators $\hat{L}^{(N)}$ in equation (7.14), does not coincide with the many-particle dCSL master equation. This questions the validity of consistent mass scaling in the dCSL model.

This has consequences for the effective equilibrium temperature T that was introduced as a parameter in [3] and calculated in subsection 2.3. In contrast to these aforementioned results, the effective temperature becomes mass dependent and scales like

$$T = \frac{\alpha p_c^2}{k_B m_0} \frac{1}{(2 - \frac{m_0}{m_j} \alpha)} \ . \tag{7.45}$$

We see that for decreasing mass m_j the temperature diverges at $\alpha_j = \frac{m_0}{m_j} \alpha = 2$ and flips its sign for smaller masses. This is compatible with our results from subsection 6.5, where we explained that the kinetic energy increases steadily for $\alpha > 2$. Conclusively, there is no equilibrium state in this parameter regime, which explains the behavior of T.

From this we can also conclude that the consistent mass scaling we found is not compatible with a mass independent temperature in the equilibrium of a free particle. We want to note that at this point it is not possible to tell, whether the scaling of dissipative CSL works. We can just state that the only correct scaling, we found, is not the one from dissipative CSL.

Only in the limit of big masses compared to the kick strength $\alpha \ll \frac{m_j}{m_0}$ we find approximately the scaling from dissipative CSL in $k_j \approx \frac{\alpha m_0}{2m_j}$ and $r_c \approx \frac{\hbar}{\sqrt{2}\alpha p_c}$. Consequently, the temperature also becomes mass independent as $T = \frac{\alpha p_c^2}{k_B m_0}$.

Summary and Conclusion

In this work we investigated the dissipative Continuous Spontaneous Localization (dCSL) model and its possible generalizations with special focus on the single-particle dynamics. We presented a way to interpret the single-particle dCSL model as a measurement feedback protocol based on the Gaussian position measurement

$$\hat{M}_{\mathbf{y}} = \sqrt{\hat{E}_{\mathbf{y}}} = \frac{1}{\pi^{3/4} r_c^{3/2} |1-k|^{3/2}} \exp\left(-\frac{(\hat{\mathbf{x}}-\mathbf{y})^2}{2(1-k)^2 r_c^2}\right)$$

in section 3. The unitary feedback operation $\hat{U}_y$ was found to be a phase-space scaling transformation followed by a measurement outcome-dependent translation,

$$\hat{U}_{\mathbf{y}} = \exp\left(\frac{i}{\hbar}\frac{2k}{1-k}\mathbf{y}\cdot\hat{\mathbf{p}}\right)\exp\left(\frac{i}{\hbar}\ln\left(\frac{1-k}{1+k}\right)\frac{\{\hat{\mathbf{x}},\hat{\mathbf{p}}\}}{2}\right) .$$

The full master equation has the form

$$\frac{\mathrm{d}}{\mathrm{d}t}\hat{\rho}_t = -\frac{i}{\hbar}\left[\hat{H},\hat{\rho}_t\right] + \Gamma\left(\int_{\mathbb{R}^3}\mathrm{d}\lambda^3(\mathbf{y})\ \hat{U}_{\mathbf{y}}\hat{M}_{\mathbf{y}}\hat{\rho}_t\hat{M}_{\mathbf{y}}\hat{U}_{\mathbf{y}}^\dagger - \hat{\rho}_t\right) .$$

In addition to providing an operational understanding of the dissipative collapse mechanism, this interpretation serves as an inspiration to introduce a broader class of measurement-based models of friction. To this end, we considered an arbitrary probability density $\mathcal{P}$ and promoted it to a momentum POVM with measurement operators

$$\left(\hat{N}_{\mathbf{q}}\right)_{\mathbf{q}} = \left(\sqrt{\mathcal{P}\left(\hat{\mathbf{p}}-\mathbf{q}\right)}\right)_{\mathbf{q}}$$

and measurement results $\mathbf{q}\in\mathbb{R}^3$ in section 4. Immediately upon the measurement, a kick operator $\hat{W}_{\mathbf{q}}$ is applied to shift the momentum towards the origin and thereby dissipate kinetic energy in a friction like manner. The strength of the kick is controlled by a function $\mathbf{f}(\mathbf{q})$ and a parameter α,

$$\hat{W}_{\mathbf{q}} = \exp\left(-i\frac{\alpha}{\hbar}\ \mathbf{f}(\mathbf{q})\cdot\hat{\mathbf{x}}\right) .$$

This results in an effective friction force $-\alpha\Gamma\left\langle\mathbb{E}_{\mathcal{P}(\mathbf{q})}\left[\mathbf{f}(\hat{\mathbf{p}}-\mathbf{q})\right]\right\rangle_{\hat{\rho}}$, which is the expectation value of the smeared our kick strength function. We have considered a constant Coulomb-like and a linear Stokes-like friction force explicitly, based on a Gaussian POVM with standard deviation p_c. It was shown that the Stokes friction model yields the same dynamics as the single-particle dCSL model.

After deriving the equations of motion for the first and second moments in $\hat{\mathbf{p}}$ for both models, we focused on the equilibration process under the Stokes friction model. The investigation can be divided into two parts: Firstly, we derived the time evolution of the characteristic function of the state under Stokes friction and proved that the equilibrium state cannot be a Gibbs state, except for singular cases like free, unconfined motion. In

any other case of motion in the presence of an external potential, the Stokes model may only yield a nonthermal equilibrium state.

Secondly, we focused our view on the equilibrium state in phase space for the case of one-dimensional harmonic motion in the presence of the Stokes (dCSL) model. The first moments in $\hat{\mathbf{x}}$ and $\hat{\mathbf{p}}$ were found to satisfy the equation of motion of a damped harmonic oscillator that can be solved analytically. The equations of motion for the second moments in position and momentum form a closed system of linear differential equations. An investigation of these differential equations showed that the harmonic oscillator relaxes to a mass- and frequency-dependent finite energy for a wide range of model parameters. However, a detailed comparison of this result to the equilibrium temperature parameter proposed for the dCSL model in [3] shows that such a temperature parameter cannot be universal, as claimed by the authors.

Finally, we presented a way to generalize the Stokes friction model to the many-particle case with consistent mass scaling. We found that this scaling does not coincide with the mass scaling of the dissipative CSL model.

This work provides an intuitive approach to collapse models that will help to deepen the understanding of this kind of dynamics. Based on the results in this work, one might investigate further on equlibrium state under dCSL. A remaining open question is whether the mass scaling in dCSL is consistent. If dCSL has an inconsistent mass scaling, it should be possible to find a counter example.

On the other hand, the implications on the proposed measurement based models are not fully understood. Further investigations could lead to more general collapse models or to applications in the control of open quantum systems.

A. Appendix for the preliminaries

A.1. Consequences of the canonical commutation relation

Here we derive useful identities and relations based on the canonical commutation relation (1.1), which are used throughout the main text. First we show that

$$[\hat{x}, \hat{p}^n] = i\hbar \; n\hat{p}^{n-1} \; , \tag{A.1}$$

which follows by induction over the natural numbers,

$$\left[\hat{x}, \hat{p}^{n+1}\right] = [\hat{x}, \hat{p}\hat{p}^n] = \hat{p}\,[\hat{x}, \hat{p}^n] + [\hat{x}, \hat{p}]\,\hat{p}^n = i\hbar \; n\hat{p}^n + i\hbar \; \hat{p}^n = i\hbar \; (n+1)\,\hat{p}^n. \tag{A.2}$$

Due to the linearity of the commutator, we can expand this formula on polynomials and even analytical functions. Employing the Taylor expansion for an analytic function $F\,\mathbb{R} \mapsto \mathbb{R}$, we obtain

$$[\hat{x}, F(\hat{p})] = i\hbar \; F'(\hat{p}) \; . \tag{A.3}$$

Following the same reasoning,

$$[G(\hat{x}), \hat{p})] = i\hbar \; G'(\hat{x}) \; . \tag{A.4}$$

With equations (A.3) and (A.4) we can obtain useful identities for the position and momentum translation operators:

$$\left[\hat{x}, \mathrm{e}^{\frac{i}{\hbar}y\hat{p}}\right] = -y \; \mathrm{e}^{\frac{i}{\hbar}y\hat{p}}, \quad \left[\mathrm{e}^{\frac{i}{\hbar}q\hat{x}}, \hat{p}\right] = -q \; \mathrm{e}^{\frac{i}{\hbar}q\hat{x}}. \tag{A.5}$$

Based on this commutators we can write

$$\mathrm{e}^{\frac{i}{\hbar}y\hat{p}} \; \hat{x} \; \mathrm{e}^{-\frac{i}{\hbar}y\hat{p}} = \mathrm{e}^{\frac{i}{\hbar}y\hat{p}} \; \left(\mathrm{e}^{-\frac{i}{\hbar}y\hat{p}}\hat{x} + \left[\hat{x}, \mathrm{e}^{-\frac{i}{\hbar}y\hat{p}}\right]\right) = \hat{x} + y, \tag{A.6}$$

and analogously

$$\mathrm{e}^{\frac{i}{\hbar}q\hat{x}} \; \hat{p} \; \mathrm{e}^{-\frac{i}{\hbar}q\hat{x}} = \hat{p} - q \; . \tag{A.7}$$

A.2. Norm conservation under stochastic evolution

Here we show that the stochastic Schrödinger equation (1.112) preserves the norm of the quantum state. This can be done by applying the stochastic calculus rules to show that the change in norm square $\mathrm{d}\left(||\psi_t||_2^2\right)$ vanishes.

$$\mathrm{d}\left(||\psi_t||_2^2\right) = \mathrm{d}\left(\langle\psi_t|\psi_t\rangle\right) = \langle \mathrm{d}\psi_t|\psi_t\rangle + \langle\psi_t|\mathrm{d}\psi_t\rangle + \langle \mathrm{d}\psi_t|\mathrm{d}\psi_t\rangle \ . \tag{A.8}$$

Due to the Ito rule (1.115) for multidimensional Wiener processes, the last term contributes to the linear order in $\mathrm{d}t$. The other two terms yield

$$\begin{aligned}
\langle\psi_t|\mathrm{d}\psi_t\rangle &= \left(-i\,\langle H\rangle - \frac{1}{2}\gamma\,\langle\hat{\mathbf{A}}^\dagger\cdot\hat{\mathbf{A}}\rangle + \gamma\mathbf{R}\cdot\langle\hat{\mathbf{A}}\rangle - \frac{1}{2}\gamma\mathbf{R}^2\right)\mathrm{d}t + (\langle\mathbf{A}\rangle - \mathbf{R})\cdot\mathrm{d}\mathbf{W}_t \ , \\
\langle\mathrm{d}\psi_t|\psi_t\rangle &= \left(+i\,\langle H\rangle - \frac{1}{2}\gamma\,\langle\hat{\mathbf{A}}^\dagger\cdot\hat{\mathbf{A}}\rangle + \gamma\mathbf{R}\cdot\langle\hat{\mathbf{A}}^\dagger\rangle - \frac{1}{2}\gamma\mathbf{R}^2\right)\mathrm{d}t + \left(\langle\mathbf{A}^\dagger\rangle - \mathbf{R}\right)\cdot\mathrm{d}\mathbf{W}_t \ .
\end{aligned}$$

Using the fact that $\langle\hat{\mathbf{A}}\rangle + \langle\mathbf{A}^\dagger\rangle = 2\mathbf{R}$ we get

$$\langle\psi_t|\mathrm{d}\psi_t\rangle + \langle\mathrm{d}\psi_t|\psi_t\rangle = \left(-\gamma\,\langle\hat{\mathbf{A}}^\dagger\cdot\hat{\mathbf{A}}\rangle + \gamma\mathbf{R}^2\right)\mathrm{d}t \ . \tag{A.9}$$

After neglecting terms of the form $\mathrm{d}t^2$, $\mathrm{d}t\mathrm{d}W_t^{(i)}$ the second order differential term in (A.8) yields

$$\begin{aligned}
\langle\mathrm{d}\psi_t|\mathrm{d}\psi_t\rangle &= \langle\psi_t|\left(\hat{\mathbf{A}}^\dagger - \mathbf{R}\right)\cdot\mathrm{d}\mathbf{W}_t\left(\hat{\mathbf{A}} - \mathbf{R}\right)\cdot\mathrm{d}\mathbf{W}_t\,|\psi_t\rangle && \text{(A.10)} \\
&= \sum_{ij}\langle\psi_t|\left(\hat{A}_i - R_i\right)\left(\hat{A}_j - R_j\right)|\psi_t\rangle\,\mathrm{d}W_t^{(i)}\mathrm{d}W_t^{(j)} && \text{(A.11)} \\
&= \sum_{ij}\langle\psi_t|\left(\hat{A}_i - R_i\right)\left(\hat{A}_j - R_j\right)|\psi_t\rangle\,\delta_{ij}\gamma\mathrm{d}t && \text{(A.12)} \\
&= \gamma\,\langle\psi_t|\left(\hat{\mathbf{A}}^\dagger - \mathbf{R}\right)\cdot\left(\hat{\mathbf{A}} - \mathbf{R}\right)|\psi_t\rangle\,\mathrm{d}t && \text{(A.13)} \\
&= \gamma\left(\langle\hat{\mathbf{A}}^\dagger\cdot\hat{\mathbf{A}}\rangle - \mathbf{R}^2\right)\mathrm{d}t \ . && \text{(A.14)}
\end{aligned}$$

Hence, the total change is given by

$$\mathrm{d}\left(||\psi_t||_2^2\right) = 0 \ . \tag{A.15}$$

A.3. Derivation of a Lindblad master equation from stochastic dynamics

In this part of the appendix we show how to obtain a Lindblad master equation by averaging over the trajectories given by the stochastic Schrödinger equation (1.112). For convenience, we set $\hat{H} = 0$ and consider only the terms coming from the stochastic process. We calculate an equation of motion for $\hat{\rho}_t := \mathbb{E}\left(|\psi_t\rangle\langle\psi_t|\right)$,

$$\mathrm{d}\hat{\rho}_t = \mathbb{E}\left(|\mathrm{d}\psi_t\rangle\langle\psi_t| + |\psi_t\rangle\langle\mathrm{d}\psi_t| + |\mathrm{d}\psi_t\rangle\langle\mathrm{d}\psi_t|\right) \ . \tag{A.16}$$

Once again, the second-order differential term must not be neglected because of the Ito rule (1.115). The first two terms in (A.16) are linear in $\mathrm{d}\mathbf{W}_t$ and therefore have zero expectation. The deterministic parts yield

$$\mathbb{E}\left(|\mathrm{d}\psi_t\rangle\langle\psi_t|\right) = \frac{\gamma}{2}\left[-\hat{\mathbf{A}}^\dagger\cdot\hat{\mathbf{A}} + 2\mathbf{R}\cdot\hat{\mathbf{A}} - \mathbf{R}^2\right]\hat{\rho}_t \tag{A.17}$$

$$\mathbb{E}\left(|\psi_t\rangle\langle\mathrm{d}\psi_t|\right) = \hat{\rho}_t\frac{\gamma}{2}\left[-\hat{\mathbf{A}}^\dagger\cdot\hat{\mathbf{A}} + 2\mathbf{R}\cdot\hat{\mathbf{A}}^\dagger - \mathbf{R}^2\right] \ . \tag{A.18}$$

In the third term in (A.16) most terms are of order $\mathrm{d}t^{\frac{3}{2}}$ or higher and can be neglected. The relevant part is

$$\mathbb{E}\left[|\mathrm{d}\psi_t\rangle\langle\mathrm{d}\psi_t|\right] = \mathbb{E}\left[\left(\hat{\mathbf{A}} - \mathbf{R}\right)\cdot\mathrm{d}\mathbf{W}_t\ \hat{\rho}_t\ \left(\hat{\mathbf{A}}^\dagger - \mathbf{R}\right)\cdot\mathrm{d}\mathbf{W}_t\right] \tag{A.19}$$

$$= \gamma\sum_{ij}\delta_{ij}\mathbb{E}\left[\left(\hat{A}_i - R_i\right)\ \hat{\rho}_t\ \left(\hat{A}_j - R_j\right)\right]\mathrm{d}t \tag{A.20}$$

$$= \gamma\left[\hat{\mathbf{A}}\hat{\rho}_t\hat{\mathbf{A}}^\dagger - \left(\mathbf{R}\cdot\hat{\mathbf{A}}\right)\hat{\rho}_t - \hat{\rho}_t\left(\mathbf{R}\cdot\hat{\mathbf{A}}^\dagger\right) + \mathbf{R}^2\hat{\rho}_t\right] \ . \tag{A.21}$$

All terms including $\mathbf{R}$ cancel and we obtain

$$\mathrm{d}\hat{\rho}_t = \gamma\left(\hat{\mathbf{A}}\hat{\rho}_t\hat{\mathbf{A}}^\dagger - \frac{1}{2}\left\{\hat{\mathbf{A}}^\dagger\cdot\hat{\mathbf{A}}, \hat{\rho}_t\right\}\right)\mathrm{d}t \tag{A.22}$$

$$= \gamma\sum_j\left(\hat{A}_j\hat{\rho}\hat{A}_j^\dagger - \frac{1}{2}\left\{\hat{A_j}^\dagger\hat{A}_j, \hat{\rho}_t\right\}\right)\mathrm{d}t \ . \tag{A.23}$$

If we had considered $\hat{H} \neq 0$ an additional term $-i\left[\hat{H}, \hat{\rho}_t\right]\mathrm{d}t$ would have occured on the right hand side. Now we can recognize the Lindblad master equation we have introduced in equation (1.85).

A.4. Gaussian integrals

Gaussian integrals appear on a regular basis throughout the thesis. We list here several useful identities:

$$\int_{\mathbb{R}} \mathrm{d}x \; \mathrm{e}^{-x^2} = \sqrt{\pi} \; . \tag{A.24}$$

Using the formula for variable change we immediately see for $a \in \mathbb{R}$

$$\int_{\mathbb{R}} \mathrm{d}x \; \mathrm{e}^{-ax^2} = \frac{1}{\sqrt{a}} \int_{\mathbb{R}} \mathrm{d}\left(\sqrt{a}x\right) \; \mathrm{e}^{-\left(\sqrt{a}x\right)^2} = \sqrt{\frac{\pi}{a}} \; . \tag{A.25}$$

Now we can use differentiation under the integral sign to obtain

$$\int_{\mathbb{R}} \mathrm{d}x \; x^2 \; \mathrm{e}^{-ax^2} = -\int_{\mathbb{R}} \mathrm{d}x \; \frac{\partial}{\partial a} \mathrm{e}^{-ax^2} = -\frac{\mathrm{d}}{\mathrm{d}a} \int_{\mathbb{R}} \mathrm{d}x \; \mathrm{e}^{-ax^2} = -\frac{\mathrm{d}}{\mathrm{d}a} \sqrt{\frac{\pi}{a}} = \frac{1}{2a} \sqrt{\frac{\pi}{a}} \; . \tag{A.26}$$

Most of the time we will use the three-dimensional case

$$\int_{\mathbb{R}^3} \mathrm{d}\lambda^3(\mathbf{x}) \; \mathbf{x}^2 \; \mathrm{e}^{-a\mathbf{x}^2} = 3 \left(\int_{\mathbb{R}} \mathrm{d}x_1 \; x_1^2 \; \mathrm{e}^{-ax_1^2} \right) \left(\int_{\mathbb{R}} \mathrm{d}x_2 \; \mathrm{e}^{-ax_2^2} \right)^2 = \frac{3}{2a} \sqrt{\frac{\pi}{a}}^3 \tag{A.27}$$

Finally we investigate on Gaussian integrals that can be used to evaluate Fourier transforms. To this end we introduce a complex vector $\mathbf{z} \in \mathbb{C}$ and calculate

$$\int_{\mathbb{R}^3} \mathrm{d}\lambda^3(\mathbf{x}) \; \mathrm{e}^{\mathbf{z}\cdot\mathbf{x}} \; \mathrm{e}^{-a\mathbf{x}^2} \tag{A.28}$$

by completing the square in the exponentials we get

$$\int_{\mathbb{R}^3} \mathrm{d}\lambda(\mathbf{x}) \; \mathrm{e}^{\mathbf{z}\cdot\mathbf{x}} \; \mathrm{e}^{-a\mathbf{x}^2} = \mathrm{e}^{\frac{\mathbf{z}^2}{4a}} \int_{\mathbb{R}^3} \mathrm{d}\lambda^3(\mathbf{x}) \mathrm{e}^{-a\left(\mathbf{x}-\frac{\mathbf{z}}{2a}\right)^2} = \mathrm{e}^{\frac{\mathbf{z}^2}{4a}} \int_{\mathbb{R}^3 - \mathbf{z}/(2a)} \mathrm{d}\lambda^3(\mathbf{y}) \mathrm{e}^{-a\mathbf{y}} \tag{A.29}$$

$$= \mathrm{e}^{\frac{\mathbf{z}^2}{4a}} \int_{\mathbb{R}^3} \mathrm{d}\lambda^3(\mathbf{y}) \mathrm{e}^{-a\mathbf{y}} = \sqrt{\frac{\pi}{a}}^3 \mathrm{e}^{\frac{\mathbf{z}^2}{4a}} \; . \tag{A.30}$$

Note that we substituted $\mathbf{y} = \mathbf{x} - \mathbf{z}/(2a)$ and then deformed the integration path to obtain again a real-valued Gaussian integral. This is possible because $\exp\left(-ay_j^2\right)$ is holomorphic for all components of $\mathbf{y}$.

A.5. Transforming the many particle Lindbladian into momentum space

Here we will explain the transformation of the position space Lindblad operators from equation (2.32) to momentum space. To this end, we plug in the relation between $\hat{\psi}(\mathbf{x})$ and $\hat{a}(\mathbf{p})$ as it is written in equation (1.80).

$$\hat{\mathbb{L}}(\mathbf{y}) = \sum_j \frac{m_j}{(1+k_j)^3} \int_{\mathbb{R}^3} \frac{\mathrm{d}\lambda^3(\mathbf{x})}{\left(\sqrt{2\pi} r_c\right)^3} \mathrm{e}^{-\frac{(\mathbf{x}-\mathbf{y})^2}{2r_c^2(1+k_j)^2}} \tag{A.31}$$

$$\times \int_{\mathbb{R}^6} \frac{\mathrm{d}\lambda^6(\mathbf{q},\mathbf{p})}{(2\pi\hbar)^3} \mathrm{e}^{-i\frac{\mathbf{q}\cdot\mathbf{x}}{\hbar}} \mathrm{e}^{i\frac{\mathbf{p}}{\hbar}\cdot\left(\frac{1-k_j}{1+k_j}\mathbf{x}+\frac{2k_j}{1+k_j}\mathbf{y}\right)} \hat{a}_j^\dagger(\mathbf{q})\hat{a}_j(\mathbf{p}) \ . \tag{A.32}$$

To carry out the $\mathbf{x}$-integration, we simplify the exponent as

$$-\frac{(\mathbf{x}-\mathbf{y})^2}{2r_c^2(1+k_j)^2} - i\frac{\mathbf{q}\cdot\mathbf{x}}{\hbar} + i\frac{\mathbf{p}}{\hbar}\cdot\left(\frac{1-k_j}{1+k_j}\mathbf{x} + \frac{2k_j}{1+k_j}\mathbf{y}\right) \tag{A.33}$$

$$= -\frac{\mathbf{x}^2}{2r_c^2(1+k_j)^2} + \mathbf{x}\cdot\left(\frac{\mathbf{y}}{r_c^2(1+k_j)^2} + \frac{i}{\hbar}\left(\frac{1-k_j}{1+k_j}\mathbf{p}-\mathbf{q}\right)\right) \tag{A.34}$$

$$+ i\frac{\mathbf{p}}{\hbar}\cdot\frac{2k_j}{1+k_j}\mathbf{y} - \frac{\mathbf{y}^2}{2r_c^2(1+k_j)^2} \ . \tag{A.35}$$

We see that this expression is just a second-order polynomial in $\mathbf{x}$ with complex numbers in the linear and constant term. The standard formula (A.29) for integration of exponentials of such expressions yields

$$\int_{\mathbb{R}^3} \mathrm{d}\lambda^3(\mathbf{x}) \mathrm{e}^{-\frac{(\mathbf{x}-\mathbf{y})^2}{2r_c^2(1+k_j)^2}} \mathrm{e}^{-i\frac{\mathbf{q}\cdot\mathbf{x}}{\hbar}} \mathrm{e}^{i\frac{\mathbf{p}}{\hbar}\cdot\left(\frac{1-k_j}{1+k_j}\mathbf{x}+\frac{2k_j}{1+k_j}\mathbf{y}\right)} \tag{A.36}$$

$$= (2\pi)^{\frac{3}{2}} r_c^3 (1+k_j)^3 \mathrm{e}^{i\frac{\mathbf{p}}{\hbar}\cdot\frac{2k_j}{1+k_j}} \mathrm{e}^{\frac{i}{\hbar}\mathbf{y}\cdot\left(\frac{1-k_j}{1+k_j}\mathbf{p}-\mathbf{q}\right)} \mathrm{e}^{-\frac{r_c^2(1+k_j)^2}{2\hbar^2}\left(\frac{1-k_j}{1+k_j}\mathbf{p}-\mathbf{q}\right)^2} \tag{A.37}$$

$$= (2\pi)^{\frac{3}{2}} r_c^3 (1+k_j)^3 \mathrm{e}^{\frac{i}{\hbar}\mathbf{y}\cdot(\mathbf{p}-\mathbf{q})} \mathrm{e}^{-\frac{r_c^2(1+k_j)^2}{2\hbar^2}\left((\mathbf{p}-\mathbf{q})-\frac{2k_j}{1+k_j}\mathbf{p}\right)^2} \tag{A.38}$$

$$= (2\pi)^{\frac{3}{2}} r_c^3 (1+k_j)^3 \mathrm{e}^{-\frac{i}{\hbar}\mathbf{y}\cdot\mathbf{Q}} \mathrm{e}^{-\frac{r_c^2(1+k_j)^2}{2\hbar^2}\left(\mathbf{Q}+\frac{2k_j}{1+k_j}\mathbf{P}\right)^2} \tag{A.39}$$

$$= (2\pi)^{\frac{3}{2}} r_c^3 (1+k_j)^3 \mathrm{e}^{-\frac{i}{\hbar}\mathbf{y}\cdot\mathbf{Q}} \mathrm{e}^{-\frac{r_c^2}{2\hbar^2}((1+k_j)\mathbf{Q}+2k_j\mathbf{P})^2} \ , \tag{A.40}$$

where we introduced the change of variable $\mathbf{Q}(\mathbf{q},\mathbf{p}) = \mathbf{q}-\mathbf{p}$, $\mathbf{P}(\mathbf{q},\mathbf{p}) = \mathbf{p}$ with Jacobian 1. Plugging this back into our expression for $\hat{\mathbb{L}}(\mathbf{y})$ yields the momentum representation

$$\hat{\mathbb{L}}(\mathbf{y}) = \sum_j m_j \int_{\mathbb{R}^6} \frac{\mathrm{d}\lambda^6(\mathbf{Q},\mathbf{P})}{(2\pi\hbar)^3} \mathrm{e}^{-i\frac{\mathbf{y}\cdot\mathbf{Q}}{\hbar}} \mathrm{e}^{-\frac{r_c^2}{2\hbar^2}((1+k_j)\mathbf{Q}+2k_j\mathbf{P})^2} \hat{a}_j^\dagger(\mathbf{P}+\mathbf{Q})\hat{a}_j(\mathbf{P}) \ . \tag{A.41}$$

B. Appendix for Coulomb friction

B.1. Integrals for Coulomb friction (Force)

In subsection 4.4 we encountered the two integrals

$$\int_{\epsilon/(\sqrt{2}p_c)}^{+\infty} \mathrm{d}s\ s\cosh(2\xi s)\mathrm{e}^{-s^2}, \tag{B.1}$$

$$\int_{\epsilon/(\sqrt{2}p_c)}^{+\infty} \mathrm{d}s \sinh(2\xi s)\mathrm{e}^{-s^2}\ . \tag{B.2}$$

We start with the solution of the second integral by splitting up sinh in two exponentials and then completing the square. With

$$\mathrm{e}^{-\left(s^2 \mp 2\xi s\right)} = \mathrm{e}^{-(s\mp\xi)^2}\mathrm{e}^{\xi^2} \tag{B.3}$$

and the substitution $a = s \mp \xi$, the second integral yields

$$\int_{\epsilon/(\sqrt{2}p_c)}^{+\infty} \mathrm{d}s \sinh(2\xi s)\mathrm{e}^{-s^2} = \frac{1}{2}\int_{\epsilon/(\sqrt{2}p_c)}^{+\infty} \mathrm{d}s \left(e^{2\xi s} - e^{-2\xi s}\right)\mathrm{e}^{-s^2} \tag{B.4}$$

$$= \frac{1}{2}\mathrm{e}^{\xi^2}\left(\int_{\epsilon/(\sqrt{2}p_c)-\xi}^{+\infty} \mathrm{d}a\mathrm{e}^{-a^2} - \int_{\epsilon/(\sqrt{2}p_c)+\xi}^{+\infty} \mathrm{d}a\ \mathrm{e}^{-a^2}\right) \tag{B.5}$$

$$= \frac{\sqrt{\pi}}{4}\mathrm{e}^{\xi^2}\frac{2}{\sqrt{\pi}}\int_{\epsilon/(\sqrt{2}p_c)-\xi}^{\epsilon/(\sqrt{2}p_c)+\xi} \mathrm{d}a\ \mathrm{e}^{-a^2} \tag{B.6}$$

$$= \frac{\sqrt{\pi}}{4}e^{\xi^2}\left(\mathrm{erf}\left(\frac{\epsilon}{\sqrt{2}p_c} + \xi\right) - \mathrm{erf}\left(\frac{\epsilon}{\sqrt{2}p_c} - \xi\right)\right) \tag{B.7}$$

$$=: \frac{\sqrt{\pi}}{4}\mathrm{e}^{\xi^2}\Delta\mathrm{erf}(\xi,\epsilon) \tag{B.8}$$

where we introduced the short-hand notation Δerf in the last step. For the evaluation of the first integral (B.1) we use differentiation under the integral sign ,

$$\int_{\epsilon/(\sqrt{2}p_c)}^{+\infty} \mathrm{d}s\ s\cosh(2\xi s)\mathrm{e}^{-s^2} = \int_{\epsilon/(\sqrt{2}p_c)}^{+\infty} \mathrm{d}s\ \mathrm{e}^{-s^2}\frac{1}{2}\frac{\partial}{\partial\xi}\sinh(2\xi s) \tag{B.9}$$

$$= \frac{1}{2}\frac{\mathrm{d}}{\mathrm{d}\xi}\int_{\epsilon/(\sqrt{2}p_c)}^{+\infty} \mathrm{d}s \sinh(2\xi s)\mathrm{e}^{-s^2} = \frac{\sqrt{\pi}}{8}\frac{\mathrm{d}}{\mathrm{d}\xi}\Delta\mathrm{erf}(\xi,\epsilon) \tag{B.10}$$

$$= \frac{\sqrt{\pi}}{4}\left[\xi\mathrm{e}^{\xi^2}\Delta\mathrm{erf}(\xi,\epsilon) + \frac{2}{\sqrt{\pi}}\mathrm{e}^{-\frac{\epsilon^2}{2p_c^2}}\cosh\left(2\xi\frac{\epsilon}{\sqrt{\pi}p_c}\right).\right] \tag{B.11}$$

B.2. Integral for Coulomb friction (Energy)

In subsection 4.4 we encountered the integral (4.82) we will solve by starting with the change of variable $\mathbf{u}(\mathbf{q}) = \mathbf{q} - \mathbf{p}$. Followed by expressing $\mathbf{u}$ in spherical coordinates, where u_z is aligned parallel to $\mathbf{p}$. This yields

$$\Pi_\epsilon(\mathbf{p}) = \mathbb{E}_{\mathcal{P}}\left(\mathbf{f}^2(\mathbf{p}-\cdot)\right) \tag{B.12}$$

$$= \left(2\pi p_c^2\right)^{-3/2} \int_{\mathbb{R}^3} \mathrm{d}\lambda^3(\mathbf{q}) \left(\frac{\mathbf{p}-\mathbf{q}}{|\mathbf{p}-\mathbf{q}|} 1_{\{|\mathbf{p}-\mathbf{q}|\geq\epsilon\}}\right)^2 \mathrm{e}^{-\frac{\mathbf{q}^2}{2p_c^2}} \tag{B.13}$$

$$= \left(2\pi p_c^2\right)^{-3/2} \int_{\mathbb{R}^3} \mathrm{d}\lambda^3(\mathbf{u}) \left(\frac{\mathbf{u}}{|\mathbf{u}|} 1_{\{|\mathbf{u}|\geq\epsilon\}}\right)^2 \mathrm{e}^{-\frac{(\mathbf{u}+\mathbf{p})^2}{2p_c^2}} \tag{B.14}$$

$$= \left(2\pi p_c^2\right)^{-3/2} \int_\epsilon^{+\infty} \mathrm{d}u\ u^2 \int_{-1}^{+1} \mathrm{d}\cos(\vartheta) \int_0^{2\pi} \mathrm{d}\varphi\ \mathrm{e}^{-\frac{u^2 2\mathbf{u}\cdot\mathbf{p}+p^2}{2p_c^2}} \tag{B.15}$$

$$= 2\pi \left(2\pi p_c^2\right)^{-3/2} \mathrm{e}^{-\frac{p^2}{2p_c^2}} \int_\epsilon^{+\infty} \mathrm{d}u\ u^2 \mathrm{e}^{-\frac{u^2}{2p_c^2}} \int_{-1}^{+1} \mathrm{d}\cos(\vartheta)\ \mathrm{e}^{-\frac{-up\cos(\vartheta)}{p_c^2}} \tag{B.16}$$

$$= 4\pi \left(2\pi p_c^2\right)^{-3/2} \mathrm{e}^{-\frac{p^2}{2p_c^2}} \int_\epsilon^{+\infty} \mathrm{d}u\ u^2 \mathrm{e}^{-\frac{u^2}{2p_c^2}} \frac{p_c^2}{up} \sinh\left(\frac{up}{p_c^2}\right) \tag{B.17}$$

$$= 2\sqrt{\frac{2}{\pi}} \left(\frac{p_c}{p}\right) \mathrm{e}^{-\frac{p^2}{2p_c^2}} \int_{\tilde\epsilon}^{+\infty} \mathrm{d}s\ s \sinh(2\xi s)\, \mathrm{e}^{-s^2} \tag{B.18}$$

$$= \sqrt{\frac{2}{\pi}} \left(\frac{p_c}{p}\right) \mathrm{e}^{-\frac{p^2}{2p_c^2}} \frac{\mathrm{d}}{\mathrm{d}\xi} \int_{\tilde\epsilon}^{+\infty} \mathrm{d}s\ \cosh(2\xi s)\, \mathrm{e}^{-s^2}\ . \tag{B.19}$$

Here we introduced the dimensionless variables $s := u/(\sqrt{2}p_c)$, $\xi := p/(\sqrt{2}p_c)$, and $\tilde\epsilon := \epsilon/(\sqrt{2}p_c)$, and we rephrased in the last line by exchanging the order of derivative and integral. Analogous to appendix B.1 we can integrate by completing the square and identifying the Gaussian error function

$$\int_{\tilde\epsilon}^{+\infty} \mathrm{d}s\ \cosh(2\xi s) e^{-s^2} = \frac{\sqrt{\pi}}{4} \mathrm{e}^{\xi^2} \left[2 - (\mathrm{erf}(\tilde\epsilon+\xi) + \mathrm{erf}(\tilde\epsilon-\xi))\right]\ . \tag{B.20}$$

It follows that

$$\frac{\mathrm{d}}{\mathrm{d}\xi} \int_{\tilde\epsilon}^{+\infty} \mathrm{d}s\ \cosh(2\xi s) e^{-s^2} \tag{B.21}$$

$$= \frac{\sqrt{\pi}}{4} \frac{\mathrm{d}}{\mathrm{d}\xi} \mathrm{e}^{\xi^2} \left[2 - (\mathrm{erf}(\tilde\epsilon+\xi) + \mathrm{erf}(\tilde\epsilon-\xi))\right] \tag{B.22}$$

$$= \frac{\sqrt{\pi}}{2} \xi \mathrm{e}^{\xi^2} \left[2 - \mathrm{erf}(\tilde\epsilon+\xi) - \mathrm{erf}(\tilde\epsilon-\xi)\right] + \mathrm{e}^{-\tilde\epsilon^2} \sinh(2\tilde\epsilon\xi) \tag{B.23}$$

$$= \sqrt{\frac{\pi}{2}} \left(\frac{p}{p_c}\right) \mathrm{e}^{\frac{p^2}{2p_c^2}} \left[1 - \frac{1}{2}\left(\mathrm{erf}\left(\frac{\epsilon+p}{\sqrt{2}p_c}\right) + \left(\frac{\epsilon-p}{\sqrt{2}p_c}\right)\right)\right] + \mathrm{e}^{-\frac{\epsilon^2}{2p_c^2}} \sinh\left(\frac{\epsilon p}{p_c^2}\right). \tag{B.24}$$

Putting everything together we have

$$\Pi_\epsilon(\mathbf{p}) = 1 - \frac{1}{2}\left[\mathrm{erf}\left(\frac{\epsilon + p}{\sqrt{2}p_c}\right) + \mathrm{erf}\left(\frac{\epsilon - p}{\sqrt{2}p_c}\right)\right] + \sqrt{\frac{2}{\pi}}\mathrm{e}^{-\frac{\epsilon^2+p^2}{2p_c^2}}\left(\frac{p_c}{p}\right)\sinh\left(\frac{\epsilon p}{p_c^2}\right) \ . \quad \text{(B.25)}$$

From the fact that the error function and sinh are odd, we can immediately deduce that for vanishing cutoff $\epsilon = 0$, $\Pi(\mathbf{p}) := \Pi_{\epsilon=0}(\mathbf{p}) = 1$.

C. Appendix for equilibration

C.1. Partition function of a free particle

The Gibbs state for a free particle with Hamiltonian $\hat{H} = \hat{\mathbf{p}}^2/(2m)$ has an infinite partition function and is thus not normalizable. To tame this infinity, consider confining the particle in a box of volume $V = L^3$ with periodic boundary conditions. The confinement makes the momentum spectrum discrete. So for $\mathbf{n} \in \mathbb{Z}^3$ we have a proper orthonormal momentum basis $(|\mathbf{n}\rangle)_{\mathbf{n}}$ with eigenvalues

$$\mathbf{p}_{\mathbf{n}} = \left(\frac{2\pi\hbar}{L}\right)\mathbf{n} \ . \tag{C.1}$$

Tracing out in this discrete basis yields the regularized partition function

$$Z = \sum_{\mathbf{n}\in\mathbb{Z}^3} \langle\mathbf{n}|\, \mathrm{e}^{-\beta\hat{H}}\, |\mathbf{n}\rangle = \sum_{\mathbf{n}\in\mathbb{Z}^3} \mathrm{e}^{-\beta\frac{\mathbf{p}_n^2}{2m}} = \left(\sum_{n\in\mathbb{Z}} \mathrm{e}^{-\beta\frac{p_n^2}{2m}}\right)^3 \ . \tag{C.2}$$

Making the box asymptotically big, the sum approaches a Riemann integral as

$$\sum_{n\in\mathbb{Z}} \mathrm{e}^{-\beta\frac{p_n^2}{2m}} = \frac{L}{2\pi\hbar}\sum_{n\in\mathbb{Z}} \underbrace{\frac{2\pi\hbar}{L}}_{=\Delta p}\, e^{-\beta\frac{p_n}{2m}} \longmapsto \frac{L}{2\pi\hbar}\int_{\mathbb{R}^3} \mathrm{d}p\ e^{-\beta\frac{p^2}{2m}} = \frac{L}{\hbar}\sqrt{\frac{mk_BT}{2\pi}} = \frac{L}{\lambda_{th}} \ . \tag{C.3}$$

Here we introduced the thermal wavelength

$$\lambda_{th} := \hbar\sqrt{\frac{mk_BT}{2\pi}} \ . \tag{C.4}$$

Putting everything together, we get the partition function

$$Z = \frac{V}{\lambda_{th}^3} \ . \tag{C.5}$$

For practical purposes, we can always assume a sufficiently large box volume and have a finite partition function with the right asymptotics.

C.2. Coherent evolution of a harmonic oscillator

For the Ehrenfest equations of motion of a harmonic oscillator in subsection 6.5, must also compute the coherent contribution to the time evolution of the observables, as determined by the respective commutators with the Hamiltonian $\hat{H} = (\hat{\mathbf{p}}^2 + \hat{\mathbf{x}}^2)/2$. Here we list these commutator terms for all first and second moments of $\hat{\mathbf{x}}$ and $\hat{\mathbf{p}}$; they follow from the product rule $\left[\hat{A}\hat{B}, \hat{C}\right] = \hat{A}\left[\hat{B}, \hat{C}\right] + \left[\hat{A}, \hat{C}\right]\hat{B}$ and from (A.3).

$$\left[\hat{x}, \hat{H}\right] = \frac{i}{2}\frac{\mathrm{d}}{\mathrm{d}\hat{p}}\hat{p}^2 = i\hat{p} \ , \quad \left[\hat{p}, \hat{H}\right] = -\frac{i}{2}\frac{\mathrm{d}}{\mathrm{d}\hat{x}}\hat{x}^2 = -i\hat{x} \ , \tag{C.6}$$

$$\left[\hat{x}^2, \hat{H}\right] = \frac{1}{2}\left\{\hat{x}, \left[\hat{x}, \hat{p}^2\right]\right\} = i\left\{\hat{x}, \hat{p}\right\} \ , \tag{C.7}$$

$$\left[\hat{p}^2, \hat{H}\right] = \frac{1}{2}\left\{\hat{p}, \left[\hat{p}, \hat{x}^2\right]\right\} = -i\left\{\hat{x}, \hat{p}\right\} \tag{C.8}$$

$$\left[\hat{x}\hat{p}, \hat{H}\right] = \hat{x}\left[\hat{p}, \hat{H}\right] + \left[\hat{x}, \hat{H}\right]\hat{p} = i\left(\hat{p}^2 - \hat{x}^2\right) \tag{C.9}$$

$$\left[\hat{p}\hat{x}, \hat{H}\right] = \hat{p}\left[\hat{x}, \hat{H}\right] + \left[\hat{p}, \hat{H}\right]\hat{x} = i\left(\hat{p}^2 - \hat{x}^2\right) \tag{C.10}$$

$$\left[\left\{\hat{x}, \hat{p}\right\}, \hat{H}\right] = 2i\left(\hat{p}^2 - \hat{x}^2\right) \tag{C.11}$$

C.3. Properties of the system matrix

In subsection 6.6, we introduced the system matrix M in (6.73), which describes the linear time evolution of second moments in position and momentum under harmonic motion and Stokes friction (dCSL). Here we examine the properties of this matrix. We start with the determinant

$$\det(\tilde{M}) = \begin{vmatrix} 0 & 1 & 0 \\ -2 & -\alpha\Gamma & 2 \\ 0 & -1 & -\alpha\Gamma(2-\alpha) \end{vmatrix} = -1 \begin{vmatrix} -2 & 2 \\ 0 & -\alpha\Gamma(2-\alpha) \end{vmatrix} = -\alpha\Gamma 2(2-\alpha) \ , \quad \text{(C.12)}$$

where we used the Laplace expansion along the first row. Next we assess the spectral properties of the matrix. This is surprisingly hard in the general case. Assuming that α is a small parameter, we can neglect the α^2-term on the bottom right of M, which simplifies the problem drastically. The so approximated matrix depends only on one parameter $\chi := \alpha\Gamma$,

$$\tilde{M} = \begin{pmatrix} 0 & 1 & 0 \\ -2 & -\chi & 2 \\ 0 & -1 & -2\chi \end{pmatrix} \ . \quad \text{(C.13)}$$

The characteristic polynomial then becomes

$$\det\left(\tilde{M} - \lambda\mathbb{1}\right) = \begin{vmatrix} -\lambda & 1 & 0 \\ -2 & -\chi-\lambda & 2 \\ 0 & -1 & -2\chi-\lambda \end{vmatrix} \quad \text{(C.14)}$$

$$= -\lambda \begin{vmatrix} -\chi-\lambda & 2 \\ -1 & -2\chi-\lambda \end{vmatrix} - 1 \begin{vmatrix} -2 & 2 \\ 0 & -2\chi-\lambda \end{vmatrix} \quad \text{(C.15)}$$

$$= -\lambda\left[(\chi+\lambda)(2\chi+\lambda)+2\right] - 2(2\chi+\lambda) \quad \text{(C.16)}$$

$$= -\lambda(\chi+\lambda)(2\chi+\lambda) \underbrace{-2\lambda - 2(2\chi+\lambda)}_{=-4(\chi+\lambda)} \quad \text{(C.17)}$$

$$= -(\chi+\lambda)\left[\lambda(2\chi+\lambda)+4\right], \quad \text{(C.18)}$$

with the roots

$$\lambda_1 = -\chi \quad \text{(C.19)}$$

$$\lambda_{2,3} = -\chi \pm i\sqrt{4-\chi^2} \ . \quad \text{(C.20)}$$

Eigenvector to λ_1 We need to find the kernel of

$$\tilde{M} - \lambda_1\mathbb{1} = \begin{pmatrix} \chi & 1 & 0 \\ -2 & 0 & 2 \\ 0 & -1 & -\chi \end{pmatrix} \ . \quad \text{(C.21)}$$

To this end we simplify by dividing the second row by 2 and adding it χ times to the first row

$$\begin{pmatrix} 0 & 1 & \chi \\ -1 & 0 & 1 \\ 0 & -1 & -\chi \end{pmatrix} . \tag{C.22}$$

From this we can see that the first and last row are linearly dependent. It is easy to check that the two remaining conditions are fulfilled by

$$\mathbf{v}_1 = \frac{1}{\sqrt{2+\chi^2}} \begin{pmatrix} 1 \\ -\chi \\ 1 \end{pmatrix} \tag{C.23}$$

Eigenvectors to $\lambda_{2,3}$ For compact notation we introduce $\eta := \sqrt{4-\chi^2}$ and note that for $\chi \leq 2$ we have $|\chi \pm i\eta|^2 = 4$.

$$\tilde{M} - \lambda_3 \mathbb{1} = \begin{pmatrix} \chi + i\eta & 1 & 0 \\ -2 & i\eta & 2 \\ 0 & -1 & -(\chi - i\eta) \end{pmatrix} . \tag{C.24}$$

We multiply the first row by $\chi - i\eta$ and the third row by $\chi + i\eta$ followed by adding the third row to the first one

$$\begin{pmatrix} 4 & -2i\eta & -4 \\ -2 & i\eta & 2 \\ 0 & -(\chi + i\eta) & -4 \end{pmatrix} . \tag{C.25}$$

This shows that the first two rows are linearly dependent. We add the third row to the second one and go on without the first row

$$\begin{pmatrix} -2 & -\chi & -2 \\ 0 & -(\chi + i\eta) & -4 \end{pmatrix} . \tag{C.26}$$

Setting $\mathbf{v}_3 = (a, b, c)^T$ the second line reads

$$b = -(\chi - i\eta)c = \left(\chi - i\sqrt{2-\chi^2}\right) c . \tag{C.27}$$

Plugged into the first line this yields

$$a = \frac{1}{2}\left(\chi^2 - i\chi\eta - 2\right) c = \frac{1}{2}\left(\chi^2 - i\chi\sqrt{2-\chi^2} - 2\right) c . \tag{C.28}$$

So c just depends on the normalization. We get

$$\mathbf{v}_3 = \frac{1}{\sqrt{\chi^2/2+6}} \begin{pmatrix} \frac{1}{2}\left(\chi^2 - i\chi\sqrt{4-\chi^2} - 2\right) \\ -\chi + i\sqrt{4-\chi^2} \\ 1 \end{pmatrix} . \tag{C.29}$$

From this we immediately find $\mathbf{v}_2$ by noting that M only has real entries so

$$M\mathbf{v}_3 = \lambda_3 \mathbf{v}_3 \tag{C.30}$$

can be conjugated on both sides to obtain

$$M\mathbf{v}_3^* = \underbrace{\lambda_3^*}_{\lambda_2} \mathbf{v}_3^* \ . \tag{C.31}$$

So $\mathbf{v}_3$ is the eigenvector to eigenvalue λ_2

$$\mathbf{v}_2 = \frac{1}{\sqrt{\chi^2/2+6}} \begin{pmatrix} \frac{1}{2}\left(\chi^2 + i\chi\sqrt{4-\chi^2} - 2\right) \\ -\chi - i\sqrt{4-\chi^2} \\ 1 \end{pmatrix} \ . \tag{C.32}$$

D. Appendix for consistency properties

D.1. The rigid body approximation

In subsection 7.2 we derived an effective master equation for the centre-of-mass state of a compound particle in the rigid-body approximation. To this end, we made use of need to perform the so called rigid body approximation. To this end, we made use of centre-of-mass and relative coordinates. We chose the so-called heliocentric coordinates, which are related to the original phase-space coordinates of the constituent masses by a canonical transformation, as we will show explicitly here. For simplicity, and in contrast to subsection 7.2 we label the individual constituents with a single index j, $(m_j, \hat{\mathbf{x}}_j, \hat{\mathbf{p}}_j)_j$.

Heliocentric coordinates The heliocentric coordinates are defined as [29]

$$\hat{\mathbf{x}}_{cm} := \frac{1}{M}\sum_{j=1}^{N} m_j \hat{\mathbf{x}}_j \tag{D.1}$$

$$\hat{\mathbf{r}}_j := \hat{\mathbf{x}}_j - \hat{\mathbf{x}}_1 \quad (j \geq 2). \tag{D.2}$$

The corresponding momenta are

$$\hat{\mathbf{p}}_{\text{c.m.}} := \sum_{j=1}^{N} \hat{\mathbf{p}}_j \tag{D.3}$$

$$\hat{\mathbf{q}}_j := \hat{\mathbf{p}}_j - \frac{m_j}{M}\sum_{k=1}^{N} \hat{\mathbf{p}}_k \ , \tag{D.4}$$

with $M = \sum_j m_j$ the total mass. Th heliocentric transformation is in fact canonical, as we can verify by the commutators

$$[\hat{\mathbf{x}}_{c.m}, \hat{\mathbf{q}}_j] = [\hat{\mathbf{x}}_{c.m}, \hat{\mathbf{p}}_j] - \frac{m_j}{M}\left[\hat{\mathbf{x}}_{c.m}, \sum_{k=1}^{N}\hat{\mathbf{p}}_k\right] = i\hbar\mathbb{1}\frac{m_j}{M}\left(1 - \frac{1}{M}\sum_{l=1}^{N} m_l\right) = 0 \tag{D.5}$$

$$[\hat{\mathbf{r}}_j, \hat{\mathbf{q}}_k] = i\hbar\mathbb{1}\delta_{jk} - \frac{m_k}{M}\left[\hat{\mathbf{x}}_j - \hat{\mathbf{x}}_1, \sum_{l=1}^{N}\hat{\mathbf{p}}_l\right] = i\hbar\mathbb{1}\delta_{jk} - \frac{m_k}{M}\left(i\hbar\mathbb{1} - i\hbar\mathbb{1}\right) = i\hbar\mathbb{1}\delta_{jk} \tag{D.6}$$

$$[\hat{\mathbf{r}}_j, \hat{\mathbf{p}}_{c.m.}] = \left[\hat{\mathbf{x}}_j - \hat{\mathbf{x}}_1, \sum_{k=1}^{N}\hat{\mathbf{p}}_k\right] = 0 \tag{D.7}$$

$$[\hat{\mathbf{x}}_{c.m.}, \hat{\mathbf{p}}_{c.m}] = \frac{1}{M}\left[\sum_{j=1}^{N} m_j\hat{\mathbf{x}}_j, \sum_{k=1}^{N}\hat{\mathbf{p}}_k\right] = \frac{1}{M}\sum_{j,k=1}^{N} i\hbar\mathbb{1}\ m_j\delta_{jk} = i\hbar\mathbb{1}\ . \tag{D.8}$$

Note that the transformation is also linear and does not mix different spatial directions. This justifies considering only the vector-valued commutators above.

Inverting the transformation, we can rephrase the individual constituents´ coordinates as

$$\hat{\mathbf{x}}_1 = \hat{\mathbf{x}}_{c.m.} - \frac{1}{M}\sum_{j=2}^{N} m_j \hat{\mathrm{r}}_j \tag{D.9}$$

$$\hat{\mathbf{x}}_k = \hat{\mathbf{x}}_{c.m.} + \left(\hat{\mathbf{r}}_k - \frac{1}{M}\sum_{j=2}^{N} m_j \hat{\mathbf{r}}_j\right) \quad (k \geq 2) \ . \tag{D.10}$$

More abstractly, we can express the linear equations in terms of the masses m_j

$$\hat{\mathbf{p}}_j = \frac{m_j}{M}\hat{\mathbf{p}}_{c.m.} + \hat{\mathbf{q}}_j \ . \tag{D.11}$$

and a matrix Ξ_{jk} such that

$$\hat{\mathbf{x}}_j = \hat{\mathbf{x}}_{c.m} + \sum_{k=2}^{N} \Xi_{jk}\hat{\mathbf{r}}_k \ . \tag{D.12}$$

D.2. Interpretation of the form factor

In Subsection 7.2, we encountered the form factor $F(\mathbf{Q})$ consisting of the individual summands

$$F_{j,k}(\mathbf{Q}) = \exp\left(-\frac{i}{\hbar}\alpha_M \sum_{j'k'} \Xi_{(j,k)(j'k')}\mathbf{r}_{j'k'} \cdot \mathbf{Q}\right) , \tag{D.13}$$

whose physical meaning as a Fourier-transformed particle density we are about to explore. We first note that the complicated expression in the exponent is just the relative coordinate of the jk- particle with respect to the centre of mass

$$\sum_{j'k'} \Xi_{(jk)(j'k')}\mathbf{r}_{j'k'} = \mathbf{x}_{jk} - \mathbf{x}_{c.m.} =: \mathbf{x}_{jk}^{rel} , \tag{D.14}$$

see appendix D.1. A Fourier transform yields

$$\int_{\mathbb{R}^3} \frac{\mathrm{d}\lambda(\mathbf{Q})}{(2\pi\hbar)^3} \mathrm{e}^{i\alpha_M \frac{\mathbf{z}\cdot\mathbf{Q}}{\hbar}} F_{j,k}(\mathbf{Q}) = \int_{\mathbb{R}^3} \frac{\mathrm{d}\lambda(\mathbf{Q})}{(2\pi\hbar)^3} \mathrm{e}^{\frac{i\alpha_M}{\hbar}\mathbf{Q}\cdot\left(\mathbf{z}-\mathbf{x}_{j,k}^{rel}\right)} = \frac{1}{\alpha_M^3}\delta^{(3)}\left(\mathbf{z} - \mathbf{x}_{j,k}^{rel}\right) , \tag{D.15}$$

which is the particle density of the single particle j, k. Due to the linearity of the Fourier transform, we find

$$\alpha_M^3 \sum_{j=1}^{J} m_j \sum_{k=1}^{N_j} F_{j,k}(\mathbf{Q}) =: \alpha_M^3 F(\mathbf{Q}) \tag{D.16}$$

to be the Fourier transform of the mass-density of the rigid body in consideration. In most practical cases, it is often allowed to describe the rigid body by a continous mass density $\mu(\mathbf{z})$, which results in

$$F(\mathbf{Q}) = \int_{\mathbb{R}^3} \mathrm{d}\lambda^3(\mathbf{Q}) \mathrm{e}^{-i\frac{\alpha_M}{\hbar}\ \mathbf{z}\cdot\mathbf{Q}}\ \mu(\mathbf{z}). \tag{D.17}$$

It is normalized to $F(0) = M$.

D.3. Form factor for a homogeneous ball

Here we consider the Fourier-transformed mass density, i.e. the formfactor $F(\mathbf{Q})$, for a homogeneous ball of radius R. With the Heaviside function, we can express the mass density distribution as

$$\mu(\mathbf{z}) := \mu_0 \; \Theta(|\mathbf{z}| - R) \tag{D.18}$$

with the constant factor $\mu_0 := \frac{3M}{4\pi R^3}$ such that the total mass is M. We carry out the Fourier integral in spherical coordinates,

$$\begin{aligned}
\frac{1}{\mu_0} F(\mathbf{Q}) &= \int_{\mathbb{R}^3} \mathrm{d}\lambda^3(\mathbf{z}) \; \mathrm{e}^{-i\frac{\alpha}{\hbar}\mathbf{z}\cdot\mathbf{Q}} \; \Theta(|\mathbf{z}| - R) && \text{(D.19)}\\
&= \int_0^R \mathrm{d}r \; r^2 \int_0^{2\pi} \mathrm{d}\varphi \int_{-1}^{+1} \mathrm{d}\cos(\vartheta) \; \mathrm{e}^{-i\frac{\alpha}{\hbar}|\mathbf{Q}|r\cos(\vartheta)} && \text{(D.20)}\\
&= 2\pi \int_0^R \mathrm{d}r \; r^2 \frac{\hbar}{-i\alpha|\mathbf{Q}|r} \left(\mathrm{e}^{-i\frac{\alpha}{\hbar}|\mathbf{Q}|r} - \mathrm{e}^{i\frac{\alpha}{\hbar}|\mathbf{Q}|r}\right) && \text{(D.21)}\\
&= 4\pi \frac{\hbar}{\alpha|\mathbf{Q}|} \int_0^R \mathrm{d}r \; r \sin\left(\alpha \frac{|\mathbf{Q}|r}{\hbar}\right) && \text{(D.22)}\\
&= 4\pi \frac{\hbar}{\alpha|\mathbf{Q}|} \left(-r \frac{\hbar}{\alpha|\mathbf{Q}|} \cos\left(\frac{\alpha|\mathbf{Q}|r}{\hbar}\right)\Big|_0^R + \frac{\hbar}{\alpha|\mathbf{Q}|} \int_0^R \mathrm{d}r \cos\left(\frac{\alpha|\mathbf{Q}r|}{\hbar}\right)\right) && \text{(D.23)}\\
&= 4\pi \frac{\hbar R^2}{\alpha|\mathbf{Q}|} \left(\frac{\sin\left(\alpha\frac{R|\mathbf{Q}|}{\hbar}\right)}{\left(\alpha\frac{R|\mathbf{Q}|}{\hbar}\right)^2} - \frac{\cos\left(\alpha\frac{R|\mathbf{Q}|}{\hbar}\right)}{\left(\alpha\frac{R|\mathbf{Q}|}{\hbar}\right)}\right) && \text{(D.24)}\\
&= 4\pi R^3 \frac{\hbar}{\alpha R|\mathbf{Q}|} \; \mathrm{j}_1\left(\alpha\frac{R|\mathbf{Q}|}{\hbar}\right) \; , && \text{(D.25)}
\end{aligned}$$

After integration by parts in r, we indentify the spherical Bessel function of the first kind. This yields

$$F(\mathbf{Q}) = 3M \frac{\hbar}{\alpha R|\mathbf{Q}|} \; \mathrm{j}_1\left(\alpha\frac{R|\mathbf{Q}|}{\hbar}\right) \; . \tag{D.26}$$

The Taylor expansion tells us that

$$F(\mathbf{Q})/F(\mathbf{0}) = 1 - \frac{1}{10}\frac{\alpha R|\mathbf{Q}|}{\hbar} + \frac{1}{280}\left(\frac{\alpha R|\mathbf{Q}|}{\hbar}\right)^4 + \mathcal{O}\left(\left(\frac{\alpha R|\mathbf{Q}|}{\hbar}\right)^5\right) \tag{D.27}$$

converges point wise towards the constant 1-function.

E. Appendix for numerical treatment

Here we summarize the numerical methods we employed to compute the dynamics of one dimensional harmonic motion under the Stokes friction model. All our simulations

were carried out using the Quantum Optics package for the Julia language [30].

In this subsection we want to check our analytical results for a harmonic oscillator from section 6.

Setup The one dimensionsional equation (6.26) in oscillator units is perfectly suited for numerical treatment. Suppressing all irrelevant indices, we have

$$\frac{\mathrm{d}}{\mathrm{d}t}\hat{\rho} = -i\left[\hat{H},\hat{\rho}\right] + \Gamma\int_{\mathbb{R}}\mathrm{d}q\ \left(\hat{L}(q)\hat{\rho}\hat{L}^{\dagger}(q) - \frac{1}{2}\left\{\hat{L}^{\dagger}(q)\hat{L}(q),\hat{\rho}\right\}\right) \tag{E.1}$$

with

$$\hat{H} = \frac{1}{2}\left(\hat{p}^2+\hat{x}^2\right) = \hat{a}^{\dagger}\hat{a} + \frac{1}{2} \tag{E.2}$$

and

$$\hat{L}(q) := \left(2\pi p_c^2\right)^{(-1/4)}\, e^{-i\alpha q\hat{x}}\ \mathrm{e}^{-(\hat{p}-q)^2/\left(4p_c^2\right)}\ . \tag{E.3}$$

For a numerical integration of the master equation with the Quantum Optics package, we are required to provide a discretized state basis and discrete list of Lindblad operators. Our choice is the Fock basis up to a cutt-off excitation number N_{points}. The discretized version of the integral over the Lindbald operators needs to be evaluated at discrete momentum points. To this end, we start with a resolution in position and choose a momentum discretization accordingly. With the position parametersx_{max}, x_{min} we define the spatial resolution

$$\Delta x = \frac{x_{max}-x_{min}}{N_{\text{points}}} \tag{E.4}$$

from which the corresponding momentum basis can be derived with

$$p_{max/min} = \pm\frac{\pi}{\Delta x}\ , \qquad \Delta p = \frac{p_{max}-p_{min}}{N_{\text{points}}}\ . \tag{E.5}$$

With the momentum resolution Δp we approximate the continuous q integral and obtain the dissipator with $q_n := q_{min} + n\ \Delta q$

$$\mathcal{D}\hat{\rho} \approx \Gamma\sum_n \Delta q\left(\hat{L}(q_n)\hat{\rho}\hat{L}^{\dagger}(q_n) - \frac{1}{2}\left\{\hat{L}^{\dagger}(q_n)\hat{L}(q_n),\hat{\rho}\right\}\right)\ . \tag{E.6}$$

To be explicit, we generate a list of Lindblad operators $\hat{L}_n := \sqrt{\Delta q\ \Gamma}\ \hat{L}(q_n)$ as input for the master equation solver provided by the package.

References

[1] David Bohm and Jeffrey Bub. A proposed solution of the measurement problem in quantum mechanics by a hidden variable theory. *Reviews of Modern Physics*, 38(3):453, 1966.

[2] Philip Pearle. Combining stochastic dynamical state-vector reduction with spontaneous localization. *Phys. Rev. A*, 39:2277–2289, Mar 1989.

[3] Andrea Smirne and Angelo Bassi. Dissipative continuous spontaneous localization (csl) model. *Scientific reports*, 5:12518, August 2015.

[4] Peter A Jackson and John S Minkowski. The measurement problem, an ontological solution. *Foundations of Physics*, 51(4):1–16, 2021.

[5] Angelo Bassi and GianCarlo Ghirardi. A general argument against the universal validity of the superposition principle. *Physics Letters A*, 275(5):373–381, 2000.

[6] Paul G Federbush. Philosophical problems: The many-worlds interpretation of quantum mechanics. a fundamental exposition. bryce s. dewitt and neill graham, eds. princeton university press, princeton, nj, 1973. viii, 253 pp. cloth, 12.50;paper, 5.50. princeton series in physics. *Science*, 183(4130):1189–1190, 1974.

[7] G. C. Ghirardi, A. Rimini, and T. Weber. Unified dynamics for microscopic and macroscopic systems. *Phys. Rev. D*, 34:470–491, Jul 1986.

[8] L. Diósi. A universal master equation for the gravitational violation of quantum mechanics. *Physics Letters A*, 120(8):377–381, 1987.

[9] Angelo Bassi, Kinjalk Lochan, Seema Satin, Tejinder P. Singh, and Hendrik Ulbricht. Models of wave-function collapse, underlying theories, and experimental tests. *Rev. Mod. Phys.*, 85:471–527, Apr 2013.

[10] Andrea Smirne, Bassano Vacchini, and Angelo Bassi. Dissipative extension of the ghirardi-rimini-weber model. *Physical Review A*, 90(6), Dec 2014.

[11] Rainer Kaltenbaek, Markus Arndt, Markus Aspelmeyer, Peter Barker, Angelo Bassi, James Bateman, Alessio Belenchia, Joel Bergé, Claus Braxmaier, Sougato Bose, et al. Research campaign: Macroscopic quantum resonators (maqro). 2022.

[12] Bassano Vacchini and Klaus Hornberger. Quantum linear boltzmann equation, 2009.

[13] Markus Aspelmeyer, Tobias J. Kippenberg, and Florian Marquardt. *Cavity Optomechanics - Nano- and Micromechanical Resonators Interacting with Light*. Springer, Berlin, Heidelberg, 2014.

[14] D. Möhl, G. Petrucci, L. Thorndahl, and S. van der Meer. Physics and technique of stochastic cooling. *Physics Reports*, 58(2):73–102, 1980.

[15] J. Sakurai and Jim Napolitano. *Modern Quantum Mechanics*. 09 2017.

[16] Teiko Heinosaari and Mário Ziman. *The Mathematical Language of Quantum Theory: From Uncertainty to Entanglement*. Cambridge University Press, 2011.

[17] Christopher C. Gerry and Peter L. Knight. *Introductory Quantum Optics*. Cambridge University Press, 2008.

[18] Heinz-Peter Breuer and F. Petruccione. *The theory of Open Quantum Systems*. Clarendon Press, 2010.

[19] Thomas L. Curtright and Cosmas K. Zachos. Quantum mechanics in phase space. *Asia Pacific Physics Newsletter*, 01(01):37–46, May 2012.

[20] Wolfgang Nolting. *Grundkurs Theoretische Physik 7 - Viel-Teilchen-Theorie*. Springer Berlin Heidelberg, Wiesbaden, 2016.

[21] W. Pauli. On the Connection between Spin and Statistics. *Progress of Theoretical Physics*, 5(4):526–543, 07 1950.

[22] Gian Carlo Ghirardi, Philip Pearle, and Alberto Rimini. Markov processes in hilbert space and continuous spontaneous localization of systems of identical particles. *Phys. Rev. A*, 42:78–89, Jul 1990.

[23] Niels Bohr. The quantum postulate and the recent development of atomic theory. *Nature*, 121:580–590, 1928.

[24] Joseph Polchinski. Weinberg's nonlinear quantum mechanics and the einstein-podolsky-rosen paradox. *Phys. Rev. Lett.*, 66:397–400, Jan 1991.

[25] G. J. Milburn. Intrinsic decoherence in quantum mechanics. *Phys. Rev. A*, 44:5401–5406, Nov 1991.

[26] K Hornberger. Monitoring approach to open quantum dynamics using scattering theory. *Europhysics Letters (EPL)*, 77(5):50007, Feb 2007.

[27] Raúl Naulin and Carlos Pabst. The roots of a polynomial depend continuously on its coefficients. 1994.

[28] Stefan Nimmrichter. *Macroscopic Matter Wave Interferometry* -. Springer, Berlin, Heidelberg, 2014.

[29] Jack Wisdom. Symplectic correctors for canonical heliocentric n-body maps. *Astronomical Journal - ASTRON J*, 131:2294–2298, 04 2006.

[30] Sebastian Krämer, David Plankensteiner, Laurin Ostermann, and Helmut Ritsch. Quantumoptics.jl: A julia framework for simulating open quantum systems. *Computer Physics Communications*, 227:109–116, Jun 2018.